

DEA DEGRADATION IN HEAT EXCHANGER TUBES

by

AMITABHA CHAKMA

Dipl.Ing., Algerian Petroleum Institute, 1982

A THESIS SUBMITTED IN PARTIAL FULFILMENT OF  
THE REQUIREMENTS FOR THE DEGREE OF  
MASTER OF APPLIED SCIENCE

in

THE FACULTY OF GRADUATE STUDIES  
Department Of Chemical Engineering

We accept this thesis as conforming  
to the required standard

THE UNIVERSITY OF BRITISH COLUMBIA

June 1984

© Amitabha Chakma, 1984

In presenting this thesis in partial fulfilment of the requirements for an advanced degree at the University of British Columbia, I agree that the Library shall make it freely available for reference and study. I further agree that permission for extensive copying of this thesis for scholarly purposes may be granted by the head of my department or by his or her representatives. It is understood that copying or publication of this thesis for financial gain shall not be allowed without my written permission.

Department of CHEMICAL ENGINEERING

The University of British Columbia  
1956 Main Mall  
Vancouver, Canada  
V6T 1Y3

Date JUNE 27, 1984

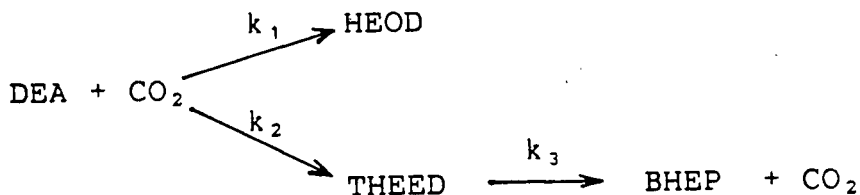
## ABSTRACT

Aqueous diethanolamine ("DEA") is widely used for the removal of acid gases such as  $\text{CO}_2$  and  $\text{H}_2\text{S}$  from natural gas as well as refinery gases. In addition to the desired absorption and desorption reactions, some side reactions occur between  $\text{CO}_2$  and DEA resulting in the formation of degradation compounds. Degradation not only represents a loss of valuable DEA, but may also lead to operational problems such as corrosion, foaming and fouling. DEA degradation is a complex process and depends on solution concentration, raw gas composition, solution flow rate and (most importantly) temperature.

Carefully controlled DEA degradation experiments were carried out in a coiled heat exchanger tube (2.032 mm ID, 3.175 mm OD and 4.8 m long) heated by means of a constant temperature heat transfer fluid. The operating conditions covered are: 1379 to 4137 kPa  $\text{CO}_2$  partial pressure, 60 to 200 °C, 20 to 40 wt% DEA solutions and 0.011 L/s to 0.0172 L/s (3.4 m/s to 5.3 m/s) solution flow rate measured at 60 °C.

The DEA degradation rate was found to increase with temperature,  $\text{CO}_2$  partial pressure and DEA concentration and decrease with solution flow rate. Degradation resulted in severe fouling of the heat exchanger tube. The viscosity as well as foaming tendency of the solutions were found to increase with the concentration of degradation products.

The following simple mathematical model for the prediction of DEA degradation in heat exchangers was developed :



The rate constants  $k_1$ ,  $k_2$  and  $k_3$  are given by :

$$\ln(k_1) = 11.924 - 6421/T$$

$$\ln(k_2) = 8.450 - 5580/T$$

$$\ln(k_3) = 39.813 - 15160/T$$

Potentiodynamic corrosion studies as well as conventional weight loss tests were carried out and degraded DEA solutions were found to be corrosive towards AISI-SAE 1020 carbon steel. 3-(hydroxyethyl)-2-oxazolidone ("HEOD") was identified as one of the corrosive components. Severe pitting of AISI-SAE 1020 carbon steel by HEOD was detected by electron micrographic analysis. Minor pitting was also noticed in the case of BHEP and DEA.

Use of activated carbon filters and soda ash treatment were both found to be incapable of removing major degradation products. A purification method consisting of NaOH injection was developed and found to be effective in converting HEOD and N,N,N-tris-(hydroxyethyl)ethylenediamine ("THEED") back to DEA. However, conversion of HEOD to DEA apparently depends on the presence of other degradation compounds.



## TABLE OF CONTENTS

ABSTRACT .....	ii
LIST OF TABLES .....	viii
LIST OF FIGURES .....	x
ACKNOWLEDGEMENTS .....	xiv

### Chapter

1	INTRODUCTION .....	1
	1.1 The DEA process .....	2
	1.2 DEA degradation .....	5
	1.3 Objectives of present study .....	7
2	LITERATURE REVIEW .....	8
	2.1 Absorption of CO <sub>2</sub> in DEA .....	8
	2.2 DEA degradation .....	10
	2.2.1 Other degradation products .....	14
	2.3 Corrosion in DEA solutions .....	15
	2.3.1 Corrosivity of DEA degradation products .....	17
	2.4 Role of heat exchanger variables .....	22
	2.5 Fouling of heat exchangers .....	23
	2.6 Analysis of DEA solutions .....	24
3	EXPERIMENTAL EQUIPMENT AND PROCESS DESCRIPTION .....	28
	3.1 Equipment design .....	28
	3.2 Process description .....	38
	3.3 Equipment description .....	32
	3.3.1 Autoclave .....	32
	3.3.2 Heat exchanger .....	33

	3.3.3 Solution pump .....	34
	3.3.4 Water cooler .....	34
	3.3.5 Flow meter .....	34
	3.3.6 Temperature controller .....	36
	3.3.7 Temperature measurements .....	36
	3.3.8 Vapor recovery system .....	36
	3.4 System preparation .....	37
	3.5 System loading .....	37
	3.6 Start up .....	39
4	ANALYTICAL PROCEDURE .....	42
	4.1 Calibration of Gas Chromatograph .....	42
	4.2 Operating conditions .....	42
	4.3 Errors .....	46
5	CORROSION STUDIES .....	47
	5.1 Principles of potentiodynamic technique .....	47
	5.2 Calculation of corrosion current .....	51
	5.3 Experimental procedure .....	54
6	MISCELLANEOUS TESTS .....	55
	6.1 Viscosity measurements .....	55
	6.2 Foaming tests .....	57
7	MODEL DEVELOPMENT .....	59
	7.1 Heat exchanger model .....	59
	7.1.1 Temperature profile determination .....	59
	7.1.2 DEA transport properties .....	67
	7.1.3 Heat transfer fluid properties .....	68
	7.1.4 Thermal conductivity of 316 stainless steel .....	72
	7.1.5 Pressure drop determination .....	73
	7.1.6 Film thickness determination .....	74
	7.1.7 Heat exchanger model performance .....	75

7.2	Kinetic model .....	77
7.2.1	Determination of rate constants .....	81
7.2.2	Determination of inlet conditions .....	83
8	RESULTS AND DISCUSSION OF DEGRADATION EXPERIMENTS .....	84
8.1	Comparison of experimental data with model prediction .....	84
8.2	Effects of operating variables on degradation .....	90
8.2.1	Effect of flow rate .....	90
8.2.2	Effect of temperature .....	97
8.2.3	Effect of solution concentration .....	97
8.2.4	Effect of CO <sub>2</sub> partial pressure .....	101
8.3	Effect of degradation on solution viscosity .....	103
8.4	Effect of degradation on solution foaming .....	103
8.5	Effect of degradation on solution pH .....	105
8.6	Heat exchanger fouling .....	108
8.6.1	Effect of temperature .....	108
8.6.2	Electron microprobe analysis .....	110
8.6.3	Apparent deposit thickness .....	110
8.7	Experiment with a new tube .....	111
9	RESULTS AND DISCUSSION OF CORROSION STUDIES .....	116
9.1	Corrosion rate in undegraded DEA solutions .....	116
9.2	Corrosion rate in degraded DEA solutions ....	116
9.3	Effect of CO <sub>2</sub> dissolved in DEA solutions on corrosion .....	119
9.4	Effect of solution concentration on corrosion .....	120
9.5	Effect of solution pH on corrosion .....	120
9.6	Effect of individual degradation products on corrosion .....	121

9.7	Effect of metal complexing .....	123
9.8	Passivity .....	124
9.9	Pitting .....	125
10	PURIFICATION OF DEGRADED DEA SOLUTIONS .....	131
10.1	Use of activated carbon filters .....	131
10.2	Use of chemicals .....	133
10.3	Removal of HEOD .....	133
10.4	Removal of THEED .....	133
10.5	Purification of industrial sample .....	135
10.6	NaOH treatment of a mixture of DEA, HEOD and THEED .....	138
10.7	Soda ash treatment .....	138
11	CONCLUSION AND RECOMMENDATIONS .....	142
11.1	Conclusions .....	142
11.2	Recommendations .....	145
11.3	Recommendations for further work .....	148
	NOMENCLATURE .....	149
	REFERENCES .....	153
	APPENDIX	
A	Listing of the computer program for the calculation of DEA degradation rate in the heat transfer tube .....	162

## LIST OF TABLES

### Table

4.1	Operating conditions of the gas chromatograph .....	43
4.2	G.C. retention time of major degradation compounds .....	44
7.1	Density of Shell Thermia Oil-C .....	69
7.2	Viscosity of Shell Thermia Oil-C .....	70
7.3	Comparison of outlet temperature and initial pressure drop data for different runs .....	76
8.1	Comparison of DEA, HEOD, THEED and BHEP concentrations of run 1 with the theoretical model prediction (30 wt% DEA, inlet temp.60°C, outlet temp.190°C, heating fluid temp.250°C, flow rate 0.0124 L/s, CO <sub>2</sub> partial pressure 4137 kPa) .....	85
8.2	Comparison of DEA, HEOD, THEED and BHEP concentrations of run 2 with the theoretical model prediction (30 wt% DEA, inlet temp.60°C, outlet temp.170°C heating fluid temp.250°C, flow rate 0.0124 L/s, CO <sub>2</sub> partial pressure 4137 kPa) .....	85
8.3	Comparison of DEA, HEOD, THEED and BHEP concentrations of run 3 with the theoretical model prediction (30 wt% DEA, inlet temp.60°C, outlet temp.195°C, heating fluid temp.250°C, flow rate 0.011 L/s, CO <sub>2</sub> partial pressure 4137 kPa) .....	86
8.4	Comparison of DEA, HEOD, THEED and BHEP concentrations of run 4 with the theoretical model prediction (30 wt% DEA, inlet temp.60°C, outlet temp.165°C, heating fluid temp.250°C, flow rate 0.0172 L/s, CO <sub>2</sub> partial pressure 4137 kPa) .....	86
8.5	Comparison of DEA, HEOD, THEED and BHEP concentrations of run 5 with the theoretical model prediction (30 wt% DEA, inlet temp.60°C, outlet temp.165°C, heating fluid temp.250°C, flow rate 0.011 L/s, CO <sub>2</sub> partial pressure 4137 kPa) .....	87

8.6	Comparison of DEA, HEOD, THEED and BHEP concentrations of run 6 with the theoretical model prediction (30 wt% DEA, inlet temp.60°C, outlet temp.140°C, heating fluid temp.190°C, flow rate 0.011 L/s, CO <sub>2</sub> partial pressure 4137 kPa) .....	87
8.7	Comparison of DEA, HEOD, THEED and BHEP concentrations of run 7 with the theoretical model prediction (30 wt% DEA, inlet temp.60°C, outlet temp.195°C, heating fluid temp.250°C, flow rate 0.011 L/s, CO <sub>2</sub> partial pressure 2758 kPa) .....	88
8.8	Comparison of DEA, HEOD, THEED and BHEP concentrations of run 8 with the theoretical model prediction (30 wt% DEA, inlet temp.60°C, outlet temp.195°C, heating fluid temp.250°C, flow rate 0.011 L/s, CO <sub>2</sub> partial pressure 1379 kPa) .....	88
8.9	Comparison of DEA, HEOD, THEED and BHEP concentrations of run 9 with the theoretical model prediction (40 wt% DEA, inlet temp.60°C, outlet temp.195°C, heating fluid temp.250°C, flow rate 0.011 L/s, CO <sub>2</sub> partial pressure 4137 kPa) .....	89
8.10	Comparison of DEA, HEOD, THEED and BHEP concentrations of run 10 with the theoretical model prediction (20 wt% DEA, inlet temp.60°C, outlet temp.195°C, heating fluid temp.250°C, flow rate 0.011 L/s, CO <sub>2</sub> partial pressure 4137 kPa) .....	89
8.11	Average DEA degradation rates. (Inlet temp.60°C, outlet temp.195°C, heating fluid temp.250°C, flow rate 0.011 L/s) .....	101
9.1	Effect of CO <sub>2</sub> on corrosion rates .....	119
9.2	Effect of DEA concentration on corrosion rates .....	121

## LIST OF FIGURES

### Figure

1.1	Typical flowsheet of a DEA plant .....	3
1.2	Typical flowsheet of a DEA plant showing areas where corrosion usually occurs .....	16
2.2	Pourbaix potential-pH diagram for the iron-water system .....	19
3.1	Flowsheet of the equipment for the study of DEA degradation in heat exchangers .....	29
3.2	Photograph of overall view of the equipment .....	30
3.3	Photograph showing main components of the equipment .....	31
3.4	Calibration curve for the capillary flow meter .....	35
3.5	Schematic diagram of the feed tank system .....	38
4.1	Chromatogram of a degraded DEA sample from run 3 after 192 hr. ....	45
5.1	Typical anodic polarization plot showing important zones and transition points .....	49
5.2	Typical anodic polarization curve showing the effect of environment and inhibitor addition upon the curve .....	50
5.3	Cathodic polarization diagram for a corroding metal .....	52
6.1	Schematic diagram of the viscosimeter .....	56
6.2	Schematic diagram of the foam testing apparatus .....	58
7.1	Schematic diagram of the temperature profile across a segment of the heat exchanger tube .....	62
7.2	Schematic diagram of temperature profile across the metal tube wall .....	65

8.1	DEA concentration as a function of and flow rate. (30 wt% DEA, inlet temp.60°C, heating oil temp.250°C, CO <sub>2</sub> partial pressure 4.14 MPa) .....	91
8.2	Temperature of the DEA solution as a function of the distance from the tube entrance and flow rate. (30 wt% DEA, inlet temp.60°C, outlet temp.170°C, heating oil temp. 250°C, CO <sub>2</sub> partial pressure 4.14 MPa) .....	94
8.3	DEA concentration as a function of time and flow rate. (30 wt% DEA, inlet temp.60°C, outlet temp.170°C, CO <sub>2</sub> partial pressure 4.14 MPa) .....	95
8.4	Theoretical model prediction of DEA concentration as a function of time and flow rate (single pass). (30 wt% DEA, inlet temp.60°C, outlet temp.170°C, CO <sub>2</sub> partial pressure 4.14 MPa) .....	96
8.5	Theoretical model prediction of the film thickness as a function of the distance from the tube entrance and flow rate. (30 wt% DEA, inlet temp.60°C, outlet temp.170°C, CO <sub>2</sub> partial pressure 4.14 MPa) .....	97
8.6	DEA concentration as a function of time and heating fluid temperature. (30 wt% DEA, inlet temp.60°C, flow rate 0.011 L/s, CO <sub>2</sub> partial pressure 4.14 MPa) .....	99
8.7	DEA concentration as a function of time and initial DEA concentration. (Inlet temp.60°C, outlet temp.195°C, flow rate 0.011 L/s, CO <sub>2</sub> partial pressure 4.14 MPa) .....	100
8.8	DEA concentration as a function of time and CO <sub>2</sub> partial pressure (30 wt% DEA, inlet temp.60°C, outlet temp.195°C, heating fluid temp.250°C,) .....	102
8.9	Solution viscosity as a function of time and degradation product concentration .....	104
8.10	Typical pH change of partially degraded DEA solution as a function of time (30 wt% DEA, inlet temp.60°C, outlet temp.195°C, heating fluid temp.250°C, flow rate 0.011 L/s) .....	107



8.11	Pressure drop as a function of time and heating fluid temp. (30 wt% DEA, inlet temp. 60°C, flow rate 0.011 L/s) .....	109
8.12	Electron micrographic photos of the uncontaminated and contaminated surfaces of the heat exchanger tube (20 x) .....	112
8.13	Electron micrographic photos of the fouled surface of the heat exchanger tube (20 x) and a magnified view (400 x) of the same surface .....	113
8.14	Electron microprobe plots of the uncontaminated and contaminated surfaces of the heat exchanger tube .....	114
8.15	Apparent deposit thickness as a function of time and heating fluid temperature (30 wt% DEA, inlet temp. 60°C, flow rate 0.011 L/s) .....	115
9.1	Potentiodynamic anodic polarization curve of 30 wt% undegraded DEA solution (temp. 25°C) ....	117
9.2	Potentiodynamic anodic polarization curve of 30 wt% partially degraded DEA solution containing 8.7 wt% degradation products (temp. 25°C) .....	118
9.3	Electron micrographic photo of an uncorroded AISI 1020 carbon steel test coupon (400 x) .....	126
9.4	Electron micrographic photo of AISI 1020 carbon steel test coupon after 120 hr. immersion in 15 wt% DEA solution at 100°C (400x) .....	127
9.5	Electron micrographic photo of AISI 1020 carbon steel test coupon after 120 hr. immersion in 15 wt% BHEP solution at 100°C (400x) .....	128
9.6	Electron micrographic photo of AISI 1020 carbon steel test coupon after 120 hr. immersion in 15 wt% HEOD solution at 100°C (400x) .....	129

9.7	Electron micrographic photo of a pit area of AISI 1020 carbon steel coupon after 120 hr. immersion in 15 wt% HEOD solution at 100°C (2000x) .....	130
10.1	Chromatograms of partially degraded DEA samples taken upstream and downstream of an activated carbon filter located in a gas plant in Alberta .....	132
10.2	Chromatograms of a partially degraded DEA sample of run 3 before and after NaOH treatment .....	136
10.3	Chromatograms of a partially degraded DEA sample from a gas processing plant before and after NaOH treatment .....	137
10.4	Chromatograms of laboratory made mixture of 30 wt% DEA, 12 wt% HEOD and 8 wt% THEED before and after NaOH treatment .....	139
10.5	Chromatograms of a partially degraded DEA sample from a gas processing plant before and after soda ash treatment .....	141

## CHAPTER 1

### INTRODUCTION

Natural gas produced from geological formations is usually saturated with water vapor and frequently contains carbon dioxide and/or hydrogen sulphide. Water vapor and acid gases must be removed from the natural gas prior to its transportation and subsequent use in order to avoid hydrate formation, prevent corrosion in pipelines and to minimise health and pollution problems upon subsequent use. The degree of removal of these constituents varies according to end use.

The aqueous diethanolamine (DEA) process, which belongs to the amine process group, was developed by Bottoms [1,2] in 1930 to remove acid gases ( $\text{CO}_2$  and  $\text{H}_2\text{S}$ ) from high volume, high pressure natural gas streams. For many years, the amine processes were virtually the only choice available to gas processors for the sweetening of (removal of acid gases from) natural gas using chemical solvents. Although numerous new sweetening processes have been developed since the nineteen thirties, the majority of the gas processing plants use amines of one kind or another.

The DEA sweetening process has long been favoured for the sweetening of refinery or manufactured gases because DEA reacts only very slowly with carbon disulphide and carbonyl sulphide,

i.e. typical contaminants of refinery or manufactured gases.

However, in recent years, DEA has also become increasingly popular with natural gas processors and many MEA plants have been converted to DEA [3-9]. DEA's popularity can be attributed to the following factors :

1. Low energy requirement for regeneration compared with most other solvents; this is due to DEA's lower specific heat and heat of reaction with  $\text{CO}_2$  and  $\text{H}_2\text{S}$ .
2. Low solvent loss due to lower vapor pressure of DEA.
3. Less corrosion.
4. Low rate of degradation as a result of irreversible side reactions with  $\text{CO}_2$ .

Although difficulties are sometimes encountered with reducing hydrogen sulphide concentration to pipeline specifications, the SNPA modification of the DEA process is claimed to be able to reduce hydrogen sulphide concentration to about 1.15 to 3.45 mg/std  $\text{m}^3$  (0.05 to 0.15 grains per 100 SCF) [10].

### 1.1 The DEA Process

A typical flow sheet of an industrial DEA sweetening unit is shown in Figure 1.1. The raw sour gas enters the unit through an inlet separator where entrained hydrocarbon liquids and solid particulates are removed.

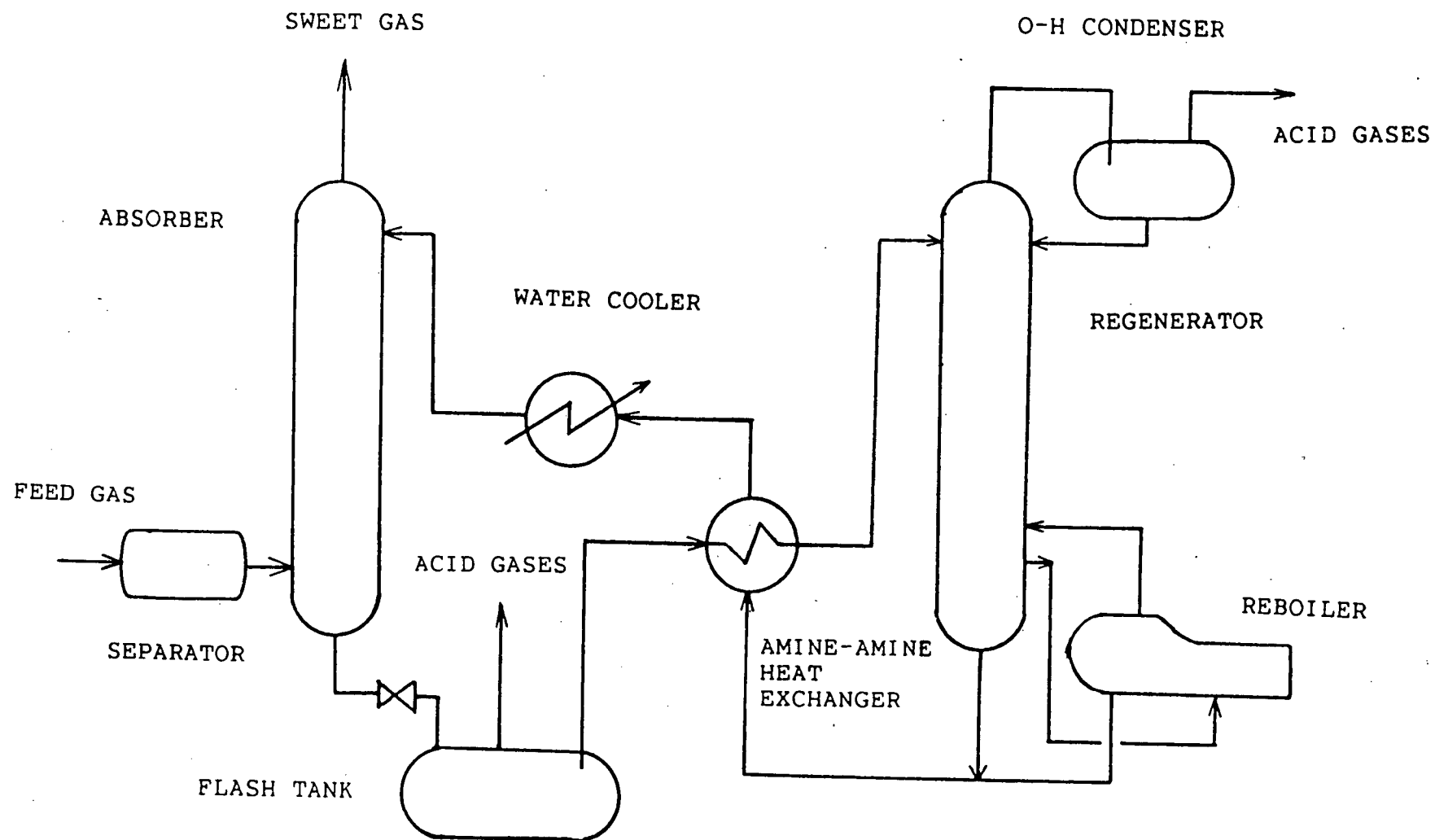


Figure 1.1 Typical flow sheet of a DEA plant.

The gas then enters the bottom of the absorber and flows upward against a counter-current stream of aqueous DEA. The acid gases are absorbed by the DEA solution. The sweetened gas, which is saturated with water vapour, leaves the top of the absorber and is usually sent to a dehydration unit.

The rich DEA solution containing  $\text{CO}_2$  and  $\text{H}_2\text{S}$  flows from the bottom of the absorber and passes through the lean-rich heat exchanger where it is heated by the hot, lean DEA solution. It then enters the top of the stripper column. In some cases a flash tank is installed upstream of the lean-rich heat exchanger, where the absorbed hydrocarbons are desorbed from the solution by letting down the pressure of the rich DEA stream.

Upon entry into the stripper, some of the absorbed acid gases are flashed on the top tray of the column. The solution then flows downward against a counter current flow of stripping vapor generated in the reboiler. The stripping vapor, which consists mainly of steam, removes the acid gases from the rich DEA solution.

The overhead products pass through a condenser where most of the steam is condensed. The acid gases are separated from the condensate in a separator and the condensate is returned to the top of the stripper as reflux.

The lean DEA solution leaving the bottom of the stripper, exchanges heat with the rich solution in the lean-rich heat exchanger and then passes through a cooler, where it is cooled

to the operating temperature of the absorber. A small side stream of lean DEA solution is usually passed through an activated carbon filter to prevent the build-up of contaminants.

## 1.2 DEA Degradation

In spite of DEA's supposed resistance to degradation, DEA can react with carbon dioxide to form some undesirable products. Most plant operators experience some loss of DEA due to degradation but the severity of degradation varies depending on raw gas composition and plant operation.

Degradation of DEA is undesirable not only because it represents a loss of valuable DEA, but also because accumulation of degradation compounds results in fouling of process equipment and increases the foaming tendency of the solution in the absorber and stripper. Furthermore, some of the degradation compounds are believed to be corrosive [11-14].

Plant operators usually try to minimise degradation of DEA solutions by changing operating variables such as solution concentration, temperature, pressure etc. Unlike monoethanolamine, DEA can not be reclaimed economically. Activated carbon filters are installed in most DEA sweetening plants and are believed to be able to absorb some degradation compounds along with other contaminants [13,15,16]. However, limited laboratory tests have indicated that activated carbon filters are not capable of removing any major degradation compounds from partially degraded solutions [17].

The strong temperature dependence of DEA degradation has been observed in industrial operations and has been confirmed by laboratory studies [17]. Therefore, degradation of DEA is expected to occur mostly in equipment operated at elevated temperatures such as the lean-rich heat exchanger and the stripper-reboiler. In order to minimise degradation in heat exchangers, temperature is considered to be the most important variable in the design and operation of DEA units. Usually, bulk solution temperatures are measured and used for process control. However, from the point of view of degradation as well as corrosion, the skin temperature is of greatest importance. The fluid adjacent to the heat transfer surface experiences the greatest temperature increase and is therefore most susceptible to degradation. The skin temperature depends not only on the temperature of the heating medium but also on the flow rate of the DEA solution. In addition, the flow rate determines the temperature profile in the DEA solution.

No information concerning the effect of flow rate on DEA degradation is presently available. Since flow rate is an important operating variable over which designers as well as the operators have some control, the study of the effect of flow rate on DEA degradation is of considerable industrial interest.



### 1.3 Objectives of present study

The objectives of this study may be summarized as follows:

1. Perform carefully controlled DEA degradation experiments which simulate the conditions in industrial heat exchangers and reboilers;
2. Develop a simple mathematical model which predicts the rate of degradation of DEA in heat exchangers using kinetic data obtained in previous batch-wise experiments;
3. Study the effect of DEA and its degradation products on the corrosion of mild steel.

The present work is restricted to  $\text{CO}_2$  as the acid gas.

## CHAPTER 2

### LITERATURE REVIEW

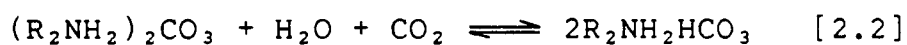
Several papers on the performance of DEA sweetening units have been published [18-21]. The SNPA modification of the DEA sweetening process, which uses higher concentrations of DEA than conventional DEA sweetening processes, has been reported by Wendt and Dailey [10].

In addition, there are several text books and handbooks available which review natural gas processing in general [22 - 25]. Various analytical methods for routine analysis of gas treating solutions are described in the "Gas Conditioning Fact Book" [26].

#### 2.1 ABSORPTION OF CARBON DIOXIDE IN DEA

The chemistry of  $\text{CO}_2$  reactions with aqueous DEA solutions is fairly complex and not yet fully understood. The literature on  $\text{CO}_2$ -DEA reactions is extensive [27-39], with Blauwhoff et al. [40] providing an excellent recent review.

The overall CO<sub>2</sub>-DEA reactions can be represented by the following equations [3] :



Where, R stands for - C<sub>2</sub>H<sub>4</sub>OH.

The equilibrium of the above reactions lies to the right at low temperature and high pressure and left at high temperature and low pressure. For this reason, industrial absorbers are operated at low temperature and high pressure.

## 2.2 DEA DEGRADATION

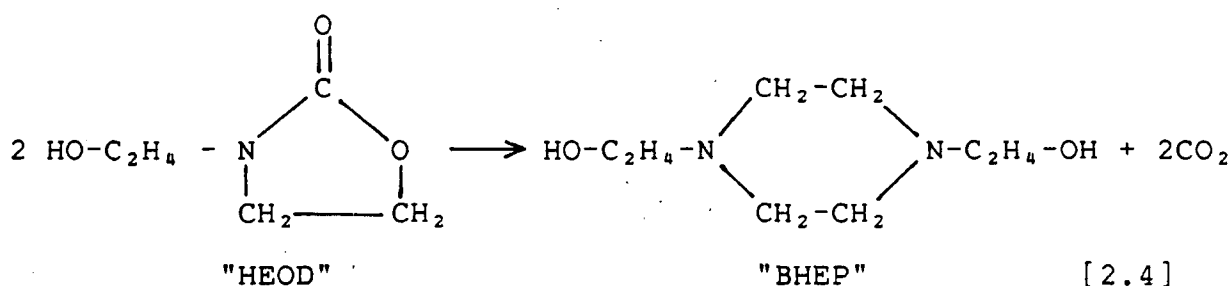
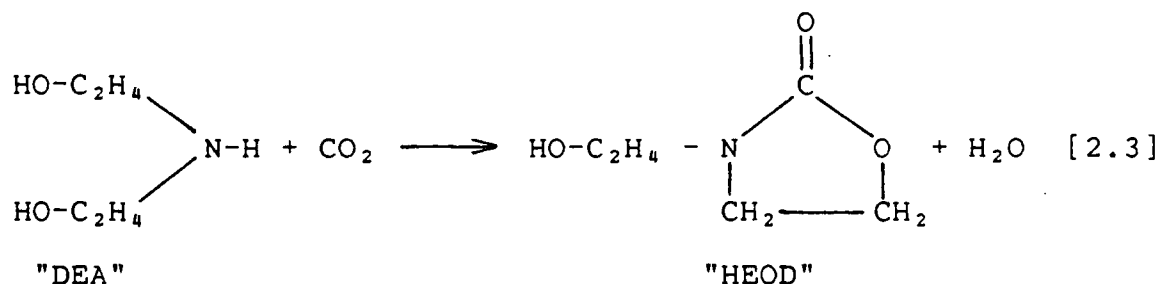
Besides the main  $\text{CO}_2$  absorption reactions, certain irreversible side reactions may occur and result in undesirable compounds; the latter are termed "degradation compounds."

In his exploratory work on organic nitrogen bases for gas sweetening, which led to the discovery of amine processes, Bottoms [2] observed that ethanolamines (including DEA), were stable at low temperatures. However, when the pure compounds or their aqueous solutions were heated above  $150^\circ\text{C}$ , some decomposition was noticed. This was probably the first reported indication of amine degradation.

DEA degradation is a complex phenomenon. Smith and Younger [7,13,18] as well as Nonhebel [14] have reported that degradation apparently depends on temperature, pressure, gas composition, amine concentration, solution pH and the presence of metal ions.

The first comprehensive work on DEA degradation was published by Polderman and Steele [12] in 1956. Their work consisted of saturating a 25 wt% DEA solution with  $\text{CO}_2$  at  $25^\circ\text{C}$  inside a stainless steel autoclave, sealing and heating the autoclave to a temperature ranging from 100 to  $175^\circ\text{C}$ . The pressure inside the vessel varied from 1257 to 4137 kPa (180 to 600 psi). After 8 hr the autoclave was cooled to  $25^\circ\text{C}$  and the partially degraded solutions were analysed by fractional distillation and crystallization.

DEA losses ranged from 0% at 100°C and 1257 kPa to 97% at 175°C and 4137 kPa. They identified N,N-bis (hydroxyethyl) piperazine ("BHEP") as a degradation compound and postulated the following reaction scheme for its formation:



The authors however, did not identify other degradation compounds due to the lack of suitable analytical techniques.

In a follow-up study, Hakka et al.[41] were able to detect N,N,N'-tris (2-hydroxyethyl) ethylenediamine ("THEED") in degraded DEA solutions by using more sophisticated analytical procedures. According to the authors, THEED occurred frequently at concentrations of 0.5 to 2 wt% in the DEA solution and should be regarded as a major degradation compound.

These authors and others [8,9,12] found that both BHEP and THEED can absorb acid gases and that their basicity is similar to that of triethanolamine ("TEA"). However, under normal industrial operating conditions, only one of the nitrogen atoms in the BHEP or THEED molecule is likely to react with acid gases. Hence, on a molecular basis, the acid gas removal capacity of the DEA solution falls with increasing solution degradation.

Smith and Younger [13] and others [42] have discussed DEA degradation and mentioned several other degradation compounds reported by gas plant operators. One of these degradation compounds was found to have the same retention time as triethanolamine ("TEA") in gas chromatographic analysis.

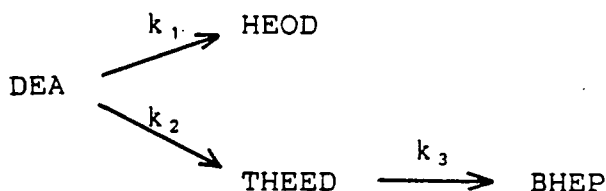
Choy [42,43] performed several carefully controlled degradation experiments and found that DEA degradation appears to be governed by a first order reaction at temperatures and CO<sub>2</sub> partial pressures ranging from 165 - 185°C and 1207 to 4137 kPa (175 to 600 psi), respectively. He also found that the rate of degradation was affected by the initial DEA concentration. This clearly contradicts the simple first order reaction concept. Furthermore, several unidentifiable degradation compounds were detected and their concentration changes with time suggested a series of simultaneous and consecutive degradation reactions.

Kennard and Meisen, [17,44] undertook a comprehensive study on the reaction mechanisms and kinetics of DEA degradation. Their work consisted of reacting  $\text{CO}_2$  with DEA in a 600 mL stirred autoclave. The temperature was varied from 90 to 250°C, the pressure from 413.7 to 6895 kPa and the initial DEA concentration from 5 to 100 wt%.

They found the reactions between  $\text{CO}_2$  and DEA to be complex and consisting of a combination of equilibrium, parallel, series and ionic steps. They proposed a pseudo-first order equation to describe the overall degradation reaction of DEA.

Among 12 detectable degradation compounds Kennard [51] found HEOD, THEED and BHEP to be the main ones. He also found that  $\text{CO}_2$  is neither consumed nor produced during the degradation of DEA to THEED and BHEP; this suggested that  $\text{CO}_2$  acts as a catalyst. HEOD, although produced from DEA and  $\text{CO}_2$ , was shown to be unstable and could be converted back to DEA.

Kennard [51] proposed the following simplified reaction scheme which is valid for DEA concentrations of 0 to 100 wt%, temperatures of 90 to 175°C and  $\text{CO}_2$  loading greater than 0.2 g $\text{CO}_2$ /gDEA.



In a recent study, Blanc et al. [45] reacted  $\text{CO}_2$  separately with DEA and HEOD solutions in a sealed autoclave. The temperature of the autoclave was varied from 90 to 130°C. They proposed various mechanisms for the formation of HEOD, THEED, BHEP and other degradation compounds. However, no quantitative data were presented in support of these reaction mechanisms.

### 2.2.1 Other degradation products

Other types of degradation products known as "heat stable salts" may also form in the presence of any acidic constituents stronger than  $\text{H}_2\text{S}$  and  $\text{CO}_2$ . Such strong acids, reported by Henry and Grennert [46,47] in 1955, were later identified by Blanc et al. [45] as formic, acetic, propionic and oxalic acids. These acids react with DEA by proton transfer. However, the anions of these acids are not capable of accepting the proton back from the protonated DEA molecule during the regeneration process. The DEA molecule which has been protonated by a strong acid thus becomes neutralized. Formation of these acids has been attributed to the presence of oxygen, but the mechanism of their formation is not clearly understood. Waterman et al. [50] reported the presence of heat stable anions such as acetate, chloride, formate, oxalate and thiosulphate in gas treating DEA solutions.



Industrial-grade DEA solutions usually contain small amounts of monoethanolamine ("MEA"). MEA can also degrade [48,49] to form oxazolidone ("OZD"), 1-(2-hydroxyethyl)imidazolidone ("HEI"), N,N'-bis hydroxyethyl)urea (BHEU), and N-(hydroxyethyl) ethylenediamine (HEED) [48,49].

Degradation compounds of high molecular weight have also been suggested but not identified [4,12]. These compounds are believed to be linear-polycarbamides containing polyalkylene amine structures.

### 2.3 CORROSION IN DEA SOLUTIONS

Corrosion in DEA treating plants have been widely reported in the literature [11-14]. Corrosion problems in some industrial DEA treating units in Western Canada have been reported by Fitzgerald and Richardson [52]. Hall and Barron [53] presented a detailed analysis of corrosion problems at the Ram River Gas Plant operated by the Aquitaine Company of Canada. The effects of acid gas loading and high temperature on corrosion are well recognised [3,54]. The higher the acid gas loading and the temperature, the higher the rate of corrosion. The equipment processing rich DEA at high temperatures, such as the rich side of the lean-rich amine heat exchanger, the reboiler and the top trays of the regenerator are most prone to corrosion. Figure 2.1 shows the areas of a DEA unit where corrosion is most likely to occur.

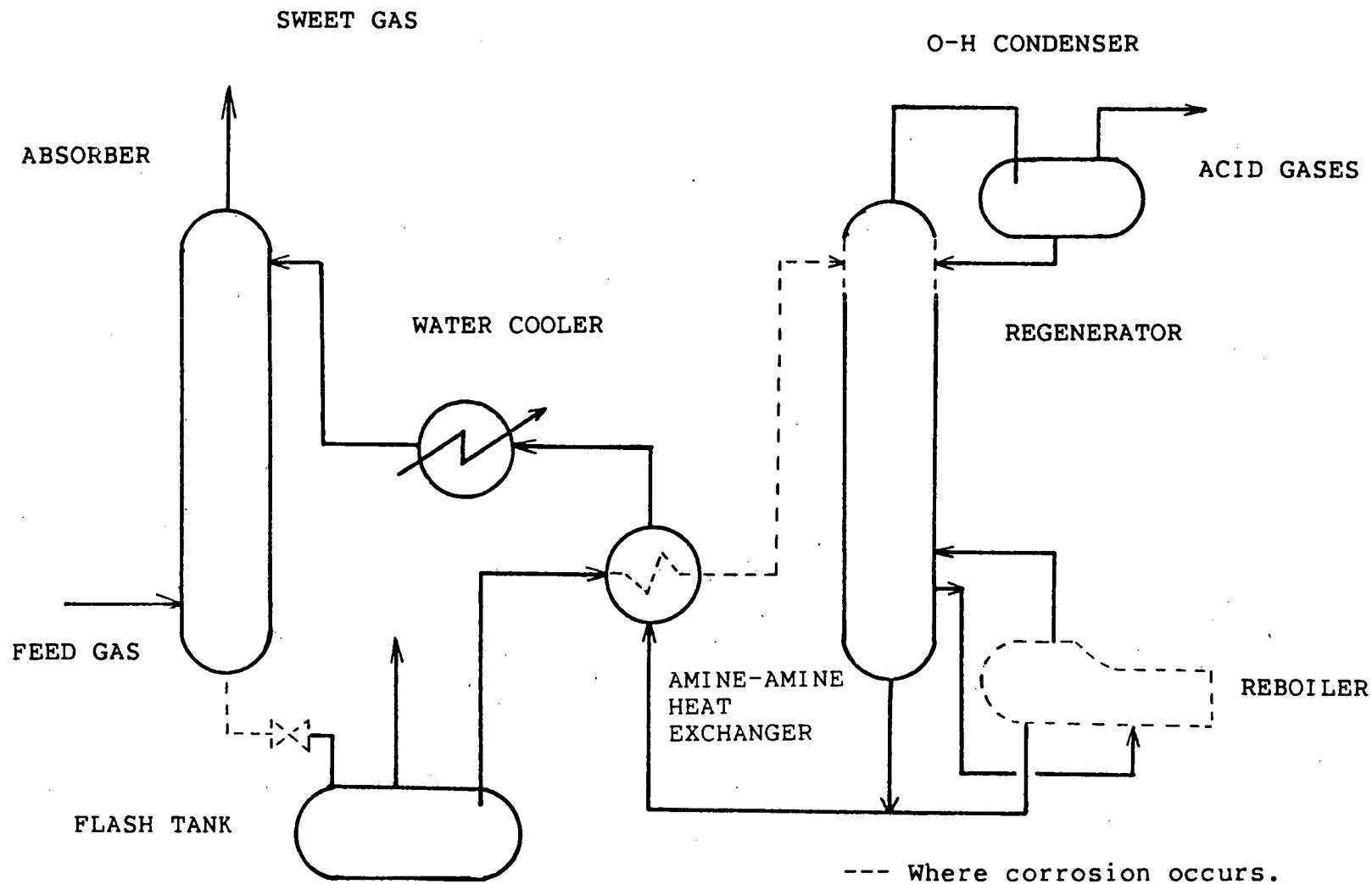


Figure 2.1 Typical flow sheet of a DEA plant showing areas where corrosion usually occurs.

### 2.3.1 Corrosivity of DEA degradation products

Polderman et al. [48] have reported that the major MEA degradation products (i.e. 1-(2-hydroxyethyl)imidazolidone ("HEI") and N-(hydroxyethyl)ethylenediamine ("HEED") are corrosive. Their findings were later confirmed by Lang and Mason [55]. Corrosiveness of MEA degradation products has generally been accepted to date [56-59]. However, in the case of DEA, the corrosiveness of the degradation products is still a matter of controversy.

Polderman et al. [12] reported in 1956 that DEA degradation products were corrosive. Moore [11] in 1960 was probably the first to publish some industrial data on corrosion in DEA systems. The author reported a substantial increase in the rate of corrosion with the concentration of degradation products, reaching 1 mm/year (40 mpy). Since then, the corrosive nature of the degradation products has been described in various publications [13,14].

However, Blanc et al. [45] recently published data in support of the claim that DEA degradation products are not corrosive. They suggest that, within the operating temperature range of 20 to 100°C, the pH of 30 wt% DEA solution lies between 11.5 and 10 depending on the concentration of degradation products.

They proposed that, under these conditions, iron and carbon steel are either non-corrosive or passive according to the Pourbaix potential-pH diagram [60]. A schematic Pourbaix potential-pH diagram for the iron water system is given in Figure 2.2.

Although Pourbaix potential-pH diagrams can provide some indication on the feasibility of corrosion under certain conditions, they do not prove that it actually occurs. To obtain an accurate picture of what actually takes place, one has to resort to experimental kinetic studies, such as plotting potentiodynamic polarization curves for the system under consideration [60].

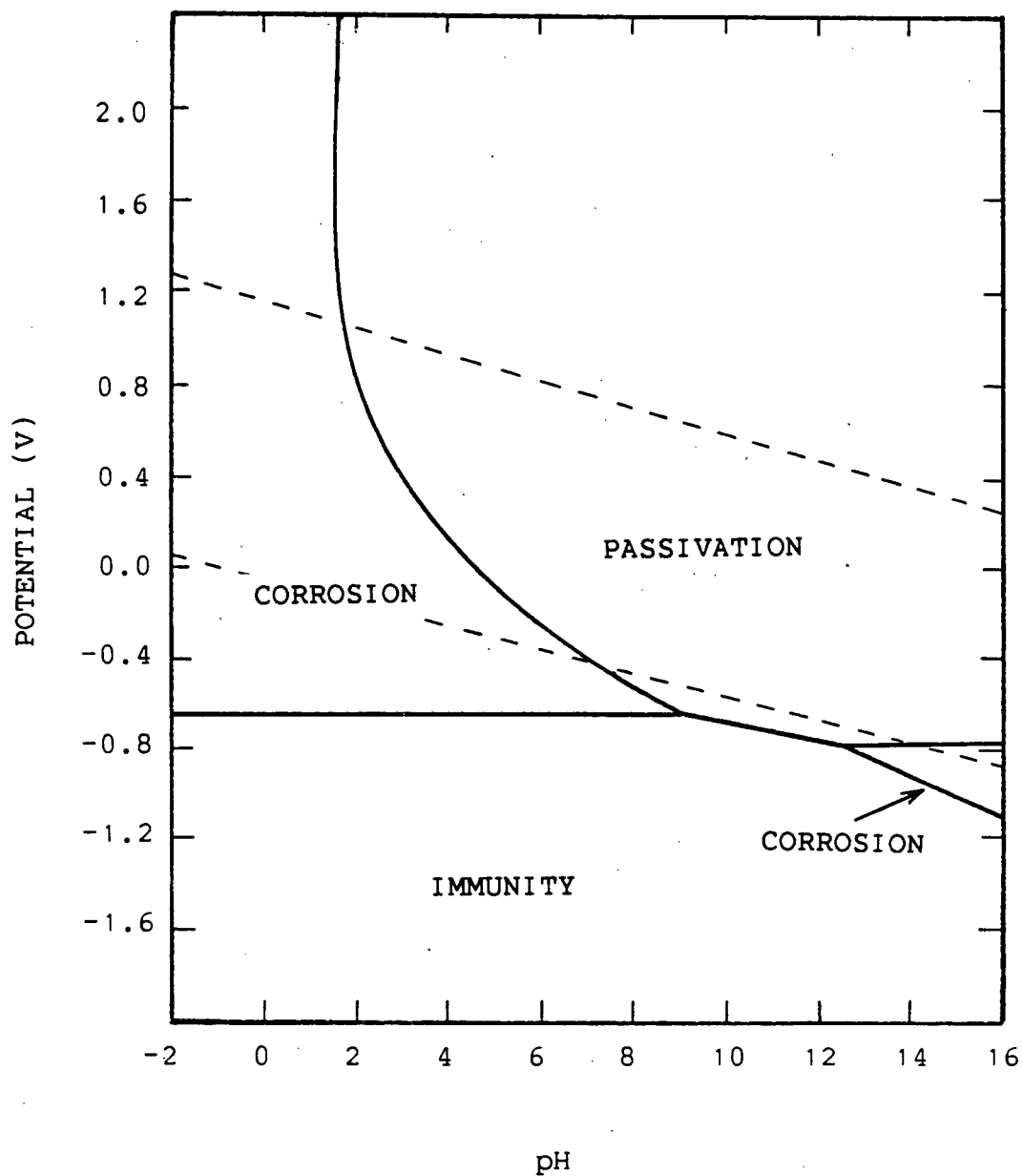


Figure 2.2 Pourbaix potential-pH diagram for the iron-water system.

The potential-pH diagram to which Blanc et al.[44] referred (see Figure 2.2) is representative of the iron-water system. However, the DEA system, in general, is far more complex due to the following reasons :

1. The system consists of iron, carbon dioxide, hydrogen sulphide, water and DEA.
2. The shape of the potential-pH curve changes substantially with temperature; in the case of the iron-water system, the region of corrosion widens and the region of passivity narrows.
3. Degraded industrial DEA solutions usually contain heat stable salts. These salts (such as cyanides) may form complexes with the metal thus invalidating the use of Pourbaix potential-pH diagram [60].

Blanc et al. [45] carried out their corrosion experiment by immersing mild steel coupons in 3N (30 wt%) aqueous DEA solutions at 80°C with a H<sub>2</sub>S partial pressure of 2000 kPa (290 psi). After 500 hours of immersion, the weight loss measurement of the coupons yielded a corrosion rate of 0.05 mm/year (2 mpy).

Choy [43], in his work on DEA degradation, found hydrogen sulphide to inhibit DEA degradation. In light of Choy's work, the results of Blanc et al. [45] are understandable, as the DEA solution did not degrade noticeably.

In another corrosion test, Blanc et al. [45] used an aqueous mixture of DEA and BHEP and obtained a corrosion rate of 0.02 mm/year (0.8 mpy), less than that obtained for the DEA-H<sub>2</sub>S-Fe system. They attributed the lower corrosion rate to the presence of BHEP, which is also basic in nature. However, this is in contradiction to the findings of Hakka et al. [41]. The latter conducted corrosion tests with SAE1010 low carbon steel immersed in boiling, aqueous solutions of 6 wt.% DEA, BHEP, THEED and HEED. They reported a weight loss of 1.8 mg in the case of BHEP compared to a weight loss of 0.4 mg in the case of DEA.

Recent extensive work on DEA degradation by Meisen and Kennard [10] revealed that HEOD, THEED and BHEP are the major DEA degradation products. The statement by Blanc et al. [45] that DEA degradation products are not corrosive can not be regarded as proven since not all the major DEA degradation products were examined in their corrosion tests.

## 2.4 ROLE OF HEAT EXCHANGER VARIABLES

To date, no research has been directed towards the role of the heat exchanger operation regarding degradation of DEA. However, it is recognised that the DEA solution is particularly susceptible to degradation in the rich solution side of lean-rich heat exchanger and in the reboiler. This may be due to the elevated temperature and dissolved acid gas level in the solution.

Ballard [61] published comprehensive guidelines for the proper design and operation of amine reboilers. He emphasized corrosion problems and suggested that :

- \* steam temperatures above  $140^{\circ}\text{C}$  ( $285^{\circ}\text{F}$ ) be avoided to prevent excessive skin temperatures on the tubes;
- \* the maximum allowable reboiler temperature be kept at  $127^{\circ}\text{C}$  ( $260^{\circ}\text{F}$ ) to prevent amine degradation;
- \* partial flooding of the reboiler tubes be avoided to prevent high heat loads in the top section of the tube bundle;
- \* the reboiler bundle always be kept covered with 0.15 - 0.20 m (6 - 8 inches) of liquid to prevent localised drying and overheating.

These guidelines should minimise not only corrosion but also degradation by preventing local hot spots (or high skin temperatures).



McMin and Farmer [54] also emphasize the importance of metal skin temperatures in connection with corrosion.

Amines are known to act as corrosion inhibitors by forming films on metal surfaces [61]. For this reason, there is a general tendency to keep solution velocities in heat exchangers and pipes low. In addition, higher solution velocities may lead to breakout of acid gases from the solution and thus cause corrosion [53,62,63]. Ballard [61] recommends maximum solution velocities of 0.6 m/sec (2 ft/sec) in heat exchangers, 3 - 6 m/sec (10-20 ft/sec) in pipes and 4.5 - 6 m/sec (15 -20 ft/sec) in valves.

## 2.5 FOULING OF HEAT EXCHANGERS

Although the accumulation of impurities usually increases the fouling resistance in heat exchangers, no particular attention has been focused on DEA heat exchangers. Hall and Barron [53] reported fouling of such heat exchangers but did not identify its cause. However, they did mention the existence of corrosion and degradation products.

Fouling in DEA heat exchangers is most likely caused by chemical reaction fouling. Temperature effects tend to dominate chemical reaction rates and fouling therefore increases exponentially with absolute temperature [64]. Watkinson and Epstein [65] reported exponential increases in fouling rates with wall temperatures and heat flux. They also reported a decrease in fouling rate with increasing flow rate. Shah et.

al. [66] reported that fouling rates were higher in tubes of small diameter. These findings may also have important implications in the fouling of DEA heat exchangers.

## 2.6 ANALYSIS OF DEA SOLUTIONS

Quantitative analysis of partially degraded DEA solutions has proven to be rather difficult due to the fact that the degradation compounds have fairly low vapor pressures, decompose at elevated temperatures, are highly polar and occur in low concentrations.

Henry and Grennert [46,47] were among the first researchers interested in the detection and measurements of heat stable salts in refinery samples. They investigated four types of acidic materials: organic acids; chlorides; cyanides and thiocyanates; sulphites, sulphates, and thiosulphates. They used potentiometric titration for the detection of organic acids. They also discussed conventional wet chemical methods (such as titration and Kjeldahl total nitrogen determination) as well as other methods for the determination of total sulphur, sulphide, mercaptide, sulphate, thiocyanate, cyanide, chloride, carbonate, alkalinity and sodium. However, their study failed to detect the presence of DEA degradation compounds.

Conventional wet chemical methods for analysing DEA solution are also described in reference [26]. Again these methods are not capable of identifying DEA degradation compounds.

Polderman and Steele [12] attempted to analyse the DEA degradation compounds by fractional distillation and crystallization and were able to isolate and identify N,N'-bis(hydroxyethyl)piperazine ("BHEP"). Hakka et al. [41] used infrared spectroscopy, mass spectroscopy, gas chromatography and thin layer chromatography to detect THEED.

Gough [67] provided a comprehensive study on the analysis of DEA solutions. He described two analytical schemes:

- a) a comprehensive scheme for component analysis, to obtain detailed information on composition,
- b) a simple scheme for quality evaluation, appropriate for routine analysis.

However, these procedures were not suitable for detecting or identifying individual degradation compounds.

Brydia and Persinger [68] described a chromatographic technique, using derivatization for the analysis of ethanolamine solutions. Trifluoroacetyl anhydride was used to convert non-volatile amines into volatile amine trifluoroacetyl derivatives prior to chromatographic separation. Although the method was fairly simple and rapid, the authors reported difficulties with reproducibility, precision, and the presence of water.

Piekos et al. [69] eliminated the shortcomings experienced by Brydia et al. [68] by converting the alkanolamines to trimethylsilyl derivatives. N,O-bis(trimethylsilyl) acetamide was used as a silylation reagent, which reacts with both the amino and hydroxyl groups of the alkanolamines. This method produces fairly stable compounds which are more easily separated and identified by gas chromatography. The addition of a trimethylsilyl group also decreases the polarity of the alkanolamines and reduces hydrogen bonding. Silylated compounds are more volatile and more stable due to reduction of reactive sites. The authors were able to separate MEA, DEA and TEA derivatives and found that the presence of up to 5% water could be tolerated provided the silylation agent is present in excess.

Saha et al. [70] described the problems of derivatization of amines prior to gas chromatographic analysis. Among the inconveniences mentioned were: time consuming process of derivative preparation, probability of incomplete derivatization and instability of the derivatives for long periods. Consequently, they investigated the use of organic polymer beads as column packing and found that Tenax G.C., a porous polymer based on 2,6-diphenyl paraphenylene oxide, was able to separate alkanolamines with excellent results. They were able to separate an aqueous mixture of MEA, DEA and TEA in less than eight minutes using a 3.175 mm O.D., 1.2192 m long (1/8" O.D., 4 ft long) stainless steel column. No sample preparation was required and the column was not affected by water.

Choy and Meisen [42] were the first to investigate specifically the analysis of DEA and its degradation products. They adopted a technique which consisted of first drying the degraded DEA sample by air stripping, then dissolving it in dimethyl formamide and finally silylating it with N,O-bis(trimethylsilyl)acetamide. The silylated compounds were then separated using a 3.175 mm O.D., 1.8288 m long (1/8", 6 ft long) stainless steel column packed with 8% OV17 on 80/100 mesh chromosorb followed by flame ionization detection. Nitrogen was used as the carrier gas. Although the method was accurate and reliable, it was time consuming, required considerable care during silylation particularly with regard to removal of water. Consequently, it was not suitable for plant use.

Kennard [51] developed a simple, reliable and direct gas chromatographic technique for the analysis of DEA and its degradation compounds. He used Tenax G.C. as the column packing. He was able to detect 14 compounds in degraded DEA solutions and later identified them by using combined gas chromatography and mass spectrometry. He was able to detect DEA and known degradation products at concentrations as low as about 0.5 wt%. The reproducibility was typically  $\pm 5\%$ .

## CHAPTER 3

### EXPERIMENTAL EQUIPMENT AND PROCESS DESCRIPTION

#### 3.1 EQUIPMENT DESIGN

A principal objective of the present work was to perform carefully controlled DEA degradation experiments under flow conditions typically encountered in industrial heat transfer equipment such as lean-rich heat exchangers and reboilers. The flowsheet of the equipment developed for this purpose is shown in Figure 3.1. The equipment essentially consists of a heat exchanger tube, a high pressure autoclave, a pump, a water cooler and associated instrumentation. Figure 3.2 is a photograph of the entire equipment whereas Figure 3.3 shows the main components of the equipment.

#### 3.2 PROCESS DESCRIPTION

The aqueous DEA solution is first saturated with  $\text{CO}_2$  in the high pressure autoclave. It is then filtered and pumped under high pressure through the heat exchanger tube. The heat exchanger tube is the heart of the equipment where DEA is heated to the desired temperature by means of a heat transfer fluid in an aluminum tank. The heat transfer fluid itself is heated by an immersion heater. The temperature of the heat transfer fluid is kept uniform by means of a stirrer.

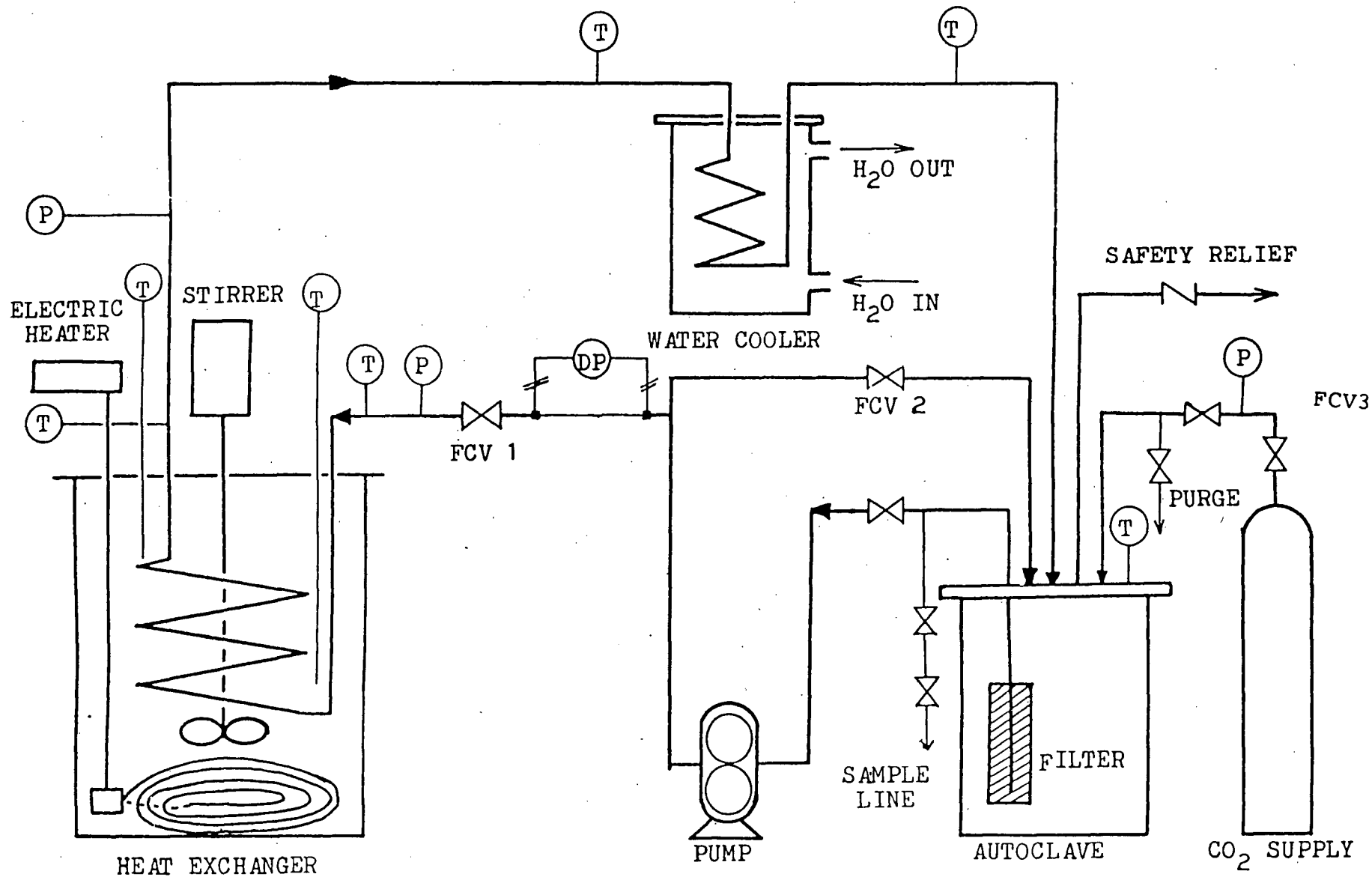


Figure 3.1 Flow sheet of the equipment for the study of DEA degradation in heat exchangers.

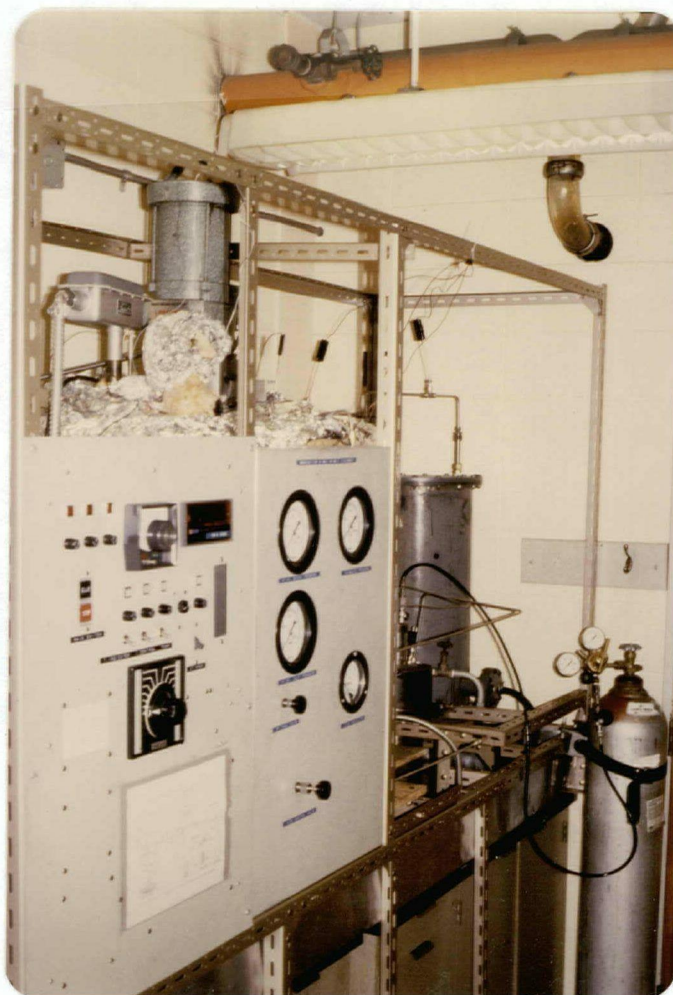


Figure 3.2 Photograph of overall view of the equipment.





Figure 3.3 Photograph showing main components of the equipment.

Degradation reactions take place inside the heat transfer tube. The temperature of the DEA solution is then lowered again to the autoclave temperature by heat exchange in a water cooler. The autoclave temperature, heat exchanger inlet and outlet temperatures, and water cooler inlet and outlet temperatures are measured by thermocouples. The autoclave pressure, heat exchanger inlet and outlet pressures are monitored by means of Bourdon pressure gauges. This process of heating and cooling of the DEA solution is carried out continuously for a long period of time (typically about 120 to 240 hr). 10 mL samples are withdrawn at least every 24 hours and analyzed for degradation compounds by gas chromatography.

### 3.3 EQUIPMENT DESCRIPTION

#### 3.3.1 Autoclave

The autoclave is a 4 L, 316 stainless steel vessel (Autoclave Engineers, Erie, PA. ) capable of withstanding pressures up to 34.5 MPa (5000 psi). It is used as the solution container as well as to saturate the solution with carbon dioxide at the desired pressure and temperature. It is provided with 6 ports, which can be used as inlet and outlet ports for incoming and outgoing streams. To prevent excessive pressure build up, one of the autoclave ports is connected to an adjustable pressure relief valve.

### 3.3.2 Heat exchanger

The heat exchanger set-up consists of a single heat exchanger tube, an aluminum tank containing heat transfer fluid, a stirrer and an immersion heater. The heat exchanger tube is a helical coil 4.80 m long, 3.175 mm OD, and 2.032 mm ID. The turning radius of the tube is 0.4064 m (16 inch). The tube, which was made of 316 stainless steel, was immersed in the aluminum tank (0.7 m ID, 0.75 m high). The tank was filled with approximately 150 L commercial Shell Thermia Oil-C, a petroleum-based heat transfer fluid. The tank was fitted with 1/3 HP variable speed (100 - 1625 rpm) Lightnin Stirrer (Greedy Mixing Equipment, Toronto, Model NS-1 (EVS)). The tank was connected to a vapor recovery system (see Section 3.3.8). The stirrer was attached to a 0.914 m long, 12.7 mm dia., 304 stainless steel shaft which was connected to a single 0.1016 m diameter marine propeller type blade.

A 10 kw over-the-side immersion heater (Chromalox Canada, Rexdale, Ontario, Model KTLO-310-1) was used to heat the heat transfer fluid. The heater is made up of 3 steel-sheathed tubular heating elements welded into a junction box. The heater was fitted with three 0.1016 m long sludge legs and was placed inside the aluminum tank. A 3 phase, 240 volts power line provided the required electricity.

### 3.3.3 Solution pump

The solution pump is a magnetically driven gear pump (Micropump, Concord, CT., Model 210-513 ) driven by a 1/6 HP explosion-proof motor. The wetted parts were made of 316 stainless steel. The pump is capable of operating under high pressure and is rated up to 10.3 MPa (1500 psi) at a temperature of 135°C (275 °F).

### 3.3.4 Water cooler

The water cooler is a 12.19 m (40 ft) long helical coil, 12.7 mm (0.5 inch) OD, 10.92 mm (0.430 inch) ID, 316 stainless steel tube, placed inside a 0.508 m (20 inch) diameter, 0.9144 m (3 ft) high PVC shell. The hot DEA solution passes downwards in the coil and is cooled by an upward flow of water flowing through the PVC shell.

### 3.3.5 Flow meter

The meter used to measure the DEA flow rate consists of a 1.75 mm (0.069 inch) ID, 3.17 mm (0.125 inch) OD, 50.8 mm (2 inches) long capillary tube connected to a differential pressure gauge (Orange Research Inc., Milford, CT., Model 1502 DG). Flow rate was measured at 60 °C at the inlet of the the heat transfer tube. The pressure gauge was calibrated to give flow rate as a function of pressure drop. The calibration curve is shown in Figure 3.4.

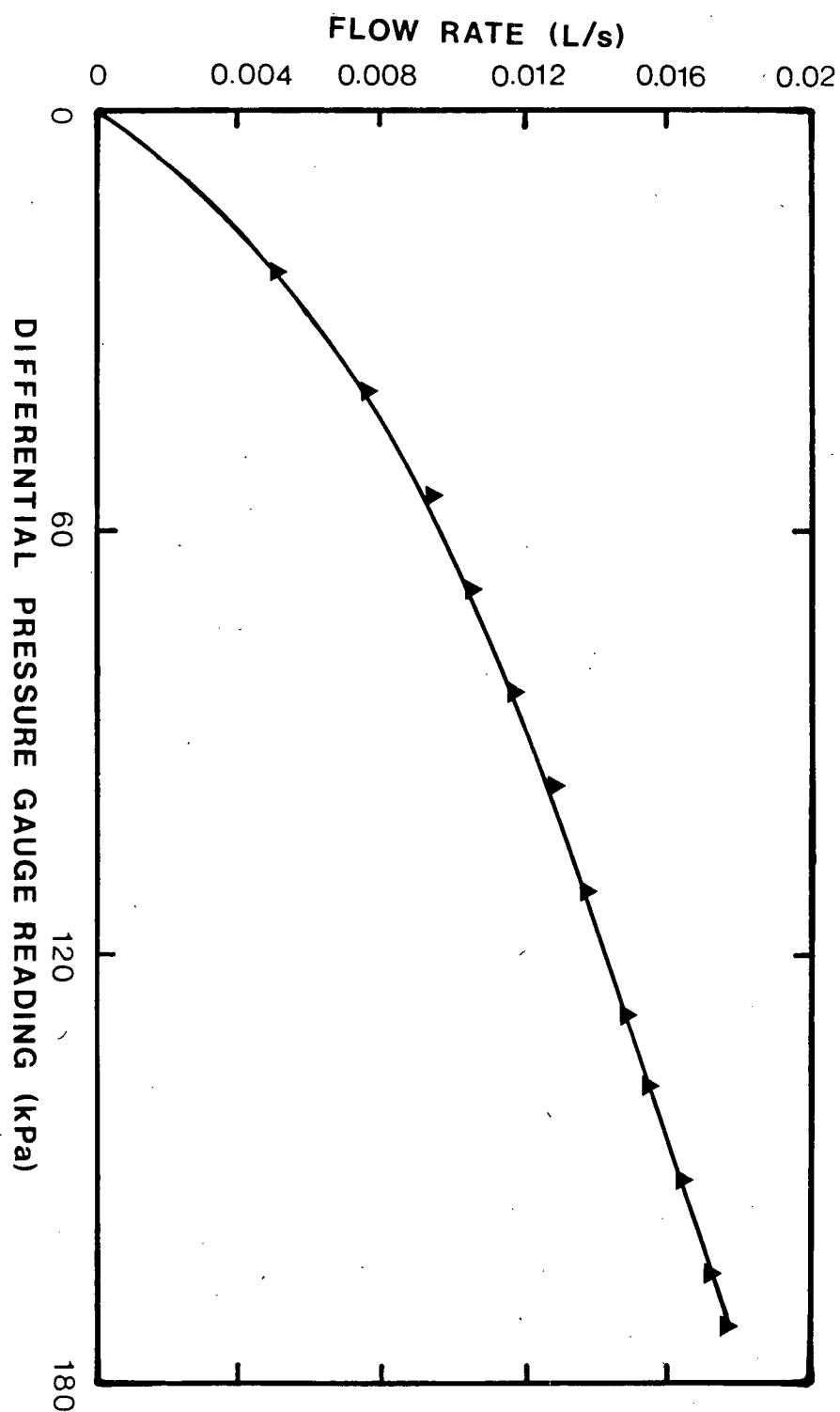


Figure 3.4 Calibration curve for the capillary flow meter.

The calibration was done by measuring the flow of 30 wt% DEA solution for a given time at a particular meter reading by means of a stop watch and a graduated cylinder. The average of at least 10 readings were taken for each flow rate in order to minimise the error.

### 3.3.6 Temperature controller

The temperature controller is a proportional controller (Omega, Stamford, CT., Model 49). It was connected to a thermocouple placed about 10 mm from the heating elements to measure the temperature of the heat transfer fluid. The controller then compares the measured temperature with the set point and takes corrective proportional action by controlling the electricity supply to the heater.

### 3.3.7 Temperature measurements

Temperatures were measured by thermocouples (J-type, Iron-constantan) connected to a digital temperature indicator (Doric, Trendicator 410A) by means of a multiple rotary switch.

### 3.3.8 Vapor recovery system

The vapor recovery system consisted of a condenser, a 2L collection tank and a water ejector. Vapor generated in the heat transfer fluid tank was condensed in a water condenser

placed at the top of the tank. The other end of the condenser was connected to a collector tank, where the condensed heat transfer fluid is collected. In order to prevent leakage of vapor from the tank, the vapor recovery system was connected to a water ejector, which ensured that all the vapor generated in the tank passed through the condenser.

### 3.4 SYSTEM PREPARATION

In order to prevent oxygen from coming in contact with the DEA solution, the heat transfer tube is purged with carbon dioxide for about 2 min before each run. After purging, a slight positive pressure 205 to 239 kPa (15 - 20 psig) is maintained in order to exclude the possibility of air re-entering the system.

### 3.5 SYSTEM LOADING

A feed tank of 4L capacity, shown in Figure 3.5 was used for loading the system. The feed tank, usually filled with 2.5 L of aqueous DEA solution of the desired concentration was put under positive pressure, slightly higher than that of the system 170 kPa (10 psig) by introducing carbon dioxide. The outlet port of the feed tank was then connected to the inlet port of the autoclave. The system then could be loaded simply by opening valves VA01 and VA02 (see Figure 3.5).

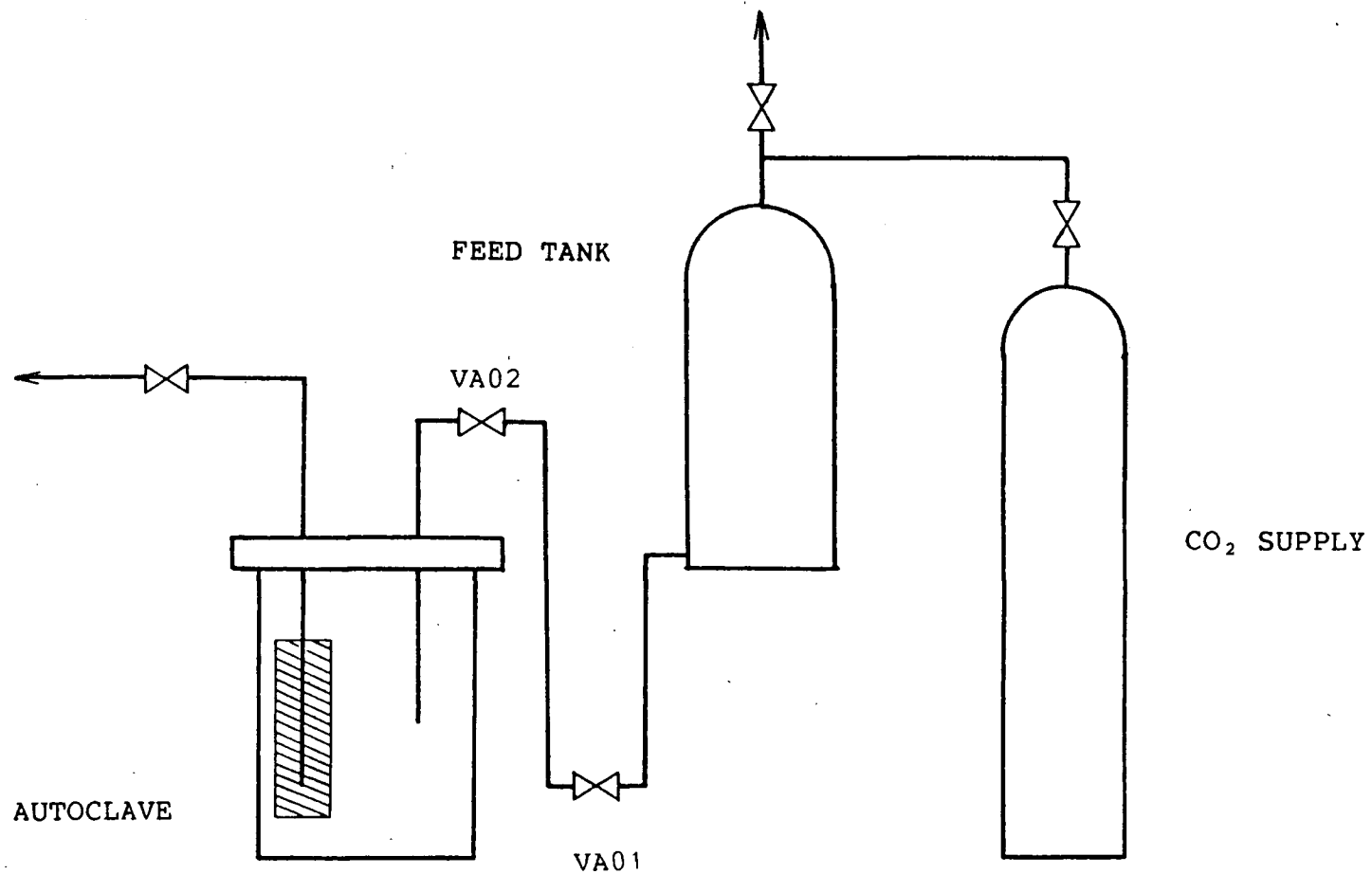


Figure 3.5 Schematic diagram of the feed tank system.



This method allowed loading of the solution without introducing air into the system. Loading usually required about 10 - 15 min. After solution loading was completed, the autoclave inlet valve was shut off, and the feed tank disconnected from the system.

The total liquid inventory was kept small to minimise the total time required for each run. However, enough liquid inventory was provided for adequate circulation throughout the system as well as for solution sampling. The minimum liquid inventory was found to be about 2.5 L.

### 3.6 START UP

After loading the system with DEA solution, the following steps were taken :

1. The water inlet valve to the heat exchanger tank overhead condenser was opened.
2. The stirrer speed was raised to about 200 rpm.
3. The temperature controller set point was set to 50 °C and the electric heater was switched on.

4. The temperature of the heat transfer fluid was gradually raised to the desired temperature (typically about 250°C) by gradually increasing the temperature controller set point and the stirrer speed.
5. The solution by-pass valve FCV2 was fully opened.
6. The system pressure was raised to 791 kPa (100psig) by opening the carbon dioxide supply valve FCV3.
7. The pump was started with the by pass valve FCV2 fully open. This is not only required for the startup of the pump, but also helps in saturating the DEA solution with carbon dioxide.
8. The system pressure was gradually increased by opening the carbon dioxide supply valve FCV3 to the desired value, i.e. typically 4238 kPa (600 psig).
9. The flow through the heat exchanger tube was started and gradually increased to its maximum to bring the autoclave temperature up to the desired temperature (typically 60 °C), by opening the flow control valve FCV1 and closing the by-pass valve FCV2.

10. Maximum flow was continued until the solution temperature in the autoclave reached the desired temperature (typically 60 °C). Usually this was achievable within 5 min.
11. The solution flow rate was reduced to the desired value by adjusting the by-pass valve. The water inlet valve to the water cooler was opened and set to obtain a DEA outlet temperature of 60°C.
12. The operating variables were carefully monitored and regulated in order to achieve steady state operation of the equipment. Usually, steady state was reached in about 15 min. The experiment was then continued for extended periods (about 150 - 200 hr) while monitoring all variables as required.
13. A 10mL sample of the DEA solution was withdrawn every 24 hr (or more frequently) and analysed by gas chromatography.
14. At the end of each run, the system was flushed with distilled water in order to prepare it for the next run.

## CHAPTER 4

ANALYTICAL PROCEDURE

The gas chromatographic technique developed by Kennard [51] was adopted for the analysis of DEA and its degradation products in this work.

4.1 CALIBRATION OF GAS CHROMATOGRAPH

Calibration curves for DEA, HEOD, THEED and BHEP were obtained from Kennard's thesis [51] and checked from time to time to ensure that the calibration curves were still applicable.

4.2 OPERATING CONDITIONS

The operating conditions of the Gas Chromatograph are summarized in Table 4.1.

Table 4.1 Operating conditions of the gas chromatograph.Gas Chromatograph

Manufacturer	Hewlett Packard
Model	5830A
Detector	Hydrogen flame ionization

Chromatographic Column

Material	Stainless steel
Dimensions	1/8" O.D., 6' long
Packing	Tenax G.C., 60/80 mesh

Operating conditions

Carrier gas	Nitrogen
Carrier gas flow	25ml/min
Injection port temp.	300°C
Detector port temp.	300°C
Column temp.	Isothermal at 150°C for 0.5 min., then temperature raised at 8°C/min to 300°C.

Syringe

Manufacturer	Hamilton Co., Reno, Nevada.
Model	701, 10 $\mu$ l, with fixed needle and Chaney adapter
Injected sample size	1 $\mu$ L

Typically 1  $\mu$ L samples of degraded DEA solution were injected directly into the column with a precision syringe fitted with a Chaney adapter. The adapter helped in ensuring that a constant volume of sample was injected into the column. A needle guide was used at the injection port, which not only protected the fragile syringe needle but also served as a spacer for needle penetration and helped lengthen the septum life.

The major degradation products could be detected in about 20 min. However, the analysis was carried out for about 30 min. in order to ensure the elution of heavy compounds. After each run the column had to be cooled from 300°C to 150°C which took about 5 min.

A chromatogram of a degraded DEA solution from run 3 is shown in Figure 4.1. Table 4.2 gives the GC retention times of compounds in degraded DEA solutions.

Table 4.2 Retention time of major degradation compounds.

Compound	Retention time (min)
DEA	7.80 - 7.95
BHEP	14.30 - 14.40
HEOD	14.90 - 15.10
THEED	17.80 - 18.00

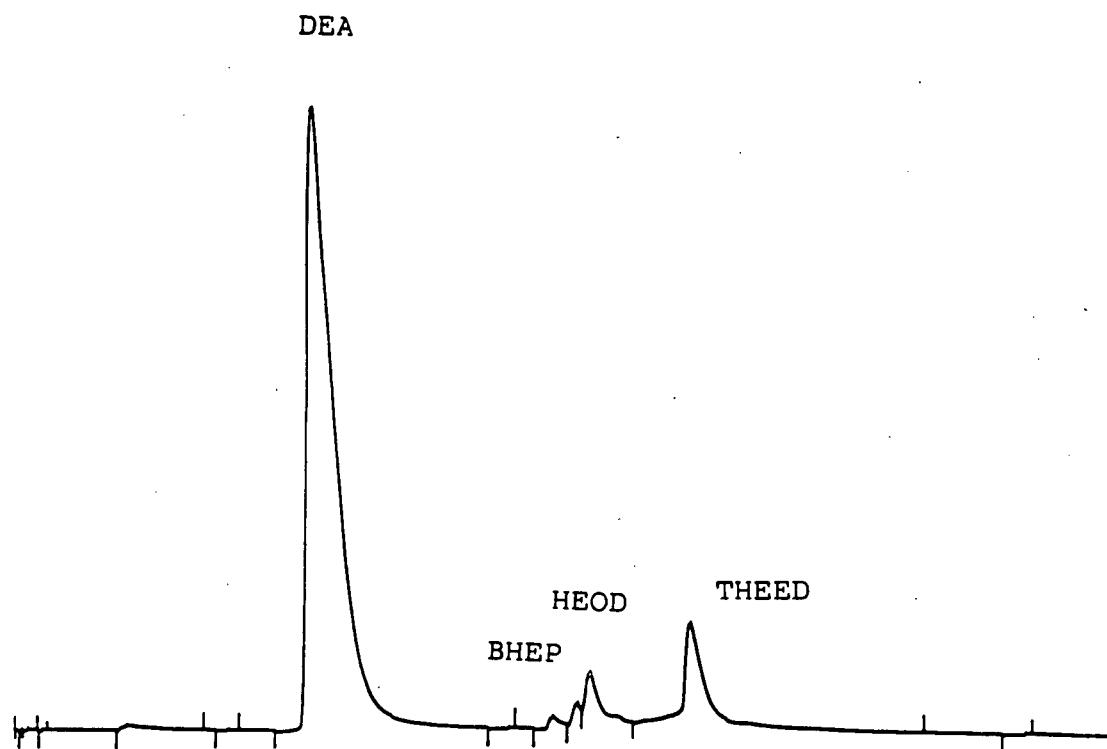


Figure 4.1 Chromatogram of a degraded DEA sample from run 3 after 192 hr.

### 4.3 ERRORS

The major source of error in the G.C. analysis is the injection time of the sample (i.e. the time spent by the needle inside the column port during injection). Slight increases in injection time result in larger peak areas due to the vaporization of the small amount of liquid normally held in the needle. The extent of this error depends on the skill of the operator. To minimise this error, at least six injections of the same sample were made and the average areas were then used for the determination of concentrations by means of the calibration charts. Another source of error was the change in the flow rate of carrier gas. As the column became clogged, the flow rate fell. This problem was overcome by checking the carrier gas flow rate and making the necessary adjustments on a daily basis.

Another error was associated with the automatic integration of peak areas by the chromatograph. If the peaks tend to tail or bunch, the automatic integrator may make small errors in deciding where to begin and end integration. Finally, there is some error associated with establishing and reading the calibration curves. However, this form of error is minor compared to that produced by the variation in sample injection time.



## CHAPTER 5

CORROSION STUDIES5.1 PRINCIPLES OF POTENTIODYNAMIC TECHNIQUE

When a metal specimen is immersed in a corrosive medium, both oxidation and reduction reactions occur on its surface. Typically, the metal corrodes due to oxidation and the medium is reduced with the liberation of hydrogen. The metal acts as both anode and cathode. Corrosion usually is a result of anodic currents.

To get a better understanding of corrosion processes, it is advantageous to make the metal specimen act either as an anode or as a cathode (but not both). When a metal is immersed in a corrosive liquid, it assumes a potential  $E_{corr}$ , known as the "free corrosion potential" relative to a reference electrode [71]. At this free corrosion potential, both anodic and cathodic currents have exactly the same magnitude and there is no net current. The metal can be made more anodic by use of an external voltage and the anodic current then predominates over the cathodic current. Similarly, the cathodic current can be made to predominate by shifting the potential in the negative direction.

The corrosion characteristics of a metal specimen in a given environment can be studied by plotting the current

response as a function of applied potential. This plot is known as "Potentiodynamic Polarization Plot." A potentiodynamic anodic polarization plot can yield important information such as:

1. The ability of the material to spontaneously passivate in the particular medium; (Passivation is defined as the transformation of an active metal in the Emf series in electrochemical behaviour to that of an appreciably less active or noble metal)
2. The potential region over which the specimen remains passive;
3. The corrosion rate in the passive region.

A typical anodic polarization plot is shown in Figure 5.1. Important zones and transition points are labelled. The metal corrodes increasingly from A to B. At point B the corrosion current reaches a maximum and formation of a passive film begins. From B to C, the corrosion current decreases rapidly due to the formation of a protective metal oxide layer. There is no change in corrosion current from C to D and the metal remains passive. At point E, the protective film starts to break down as the potential is increased.

Figure 5.2 shows the effect of environment upon the polarization curve. As can be seen from Figure 5.2, raising the temperature, acidity of the solution and the formation of metal complexes increase the corrosion current. By contrast, alloying and inhibitor addition decrease the corrosion current.

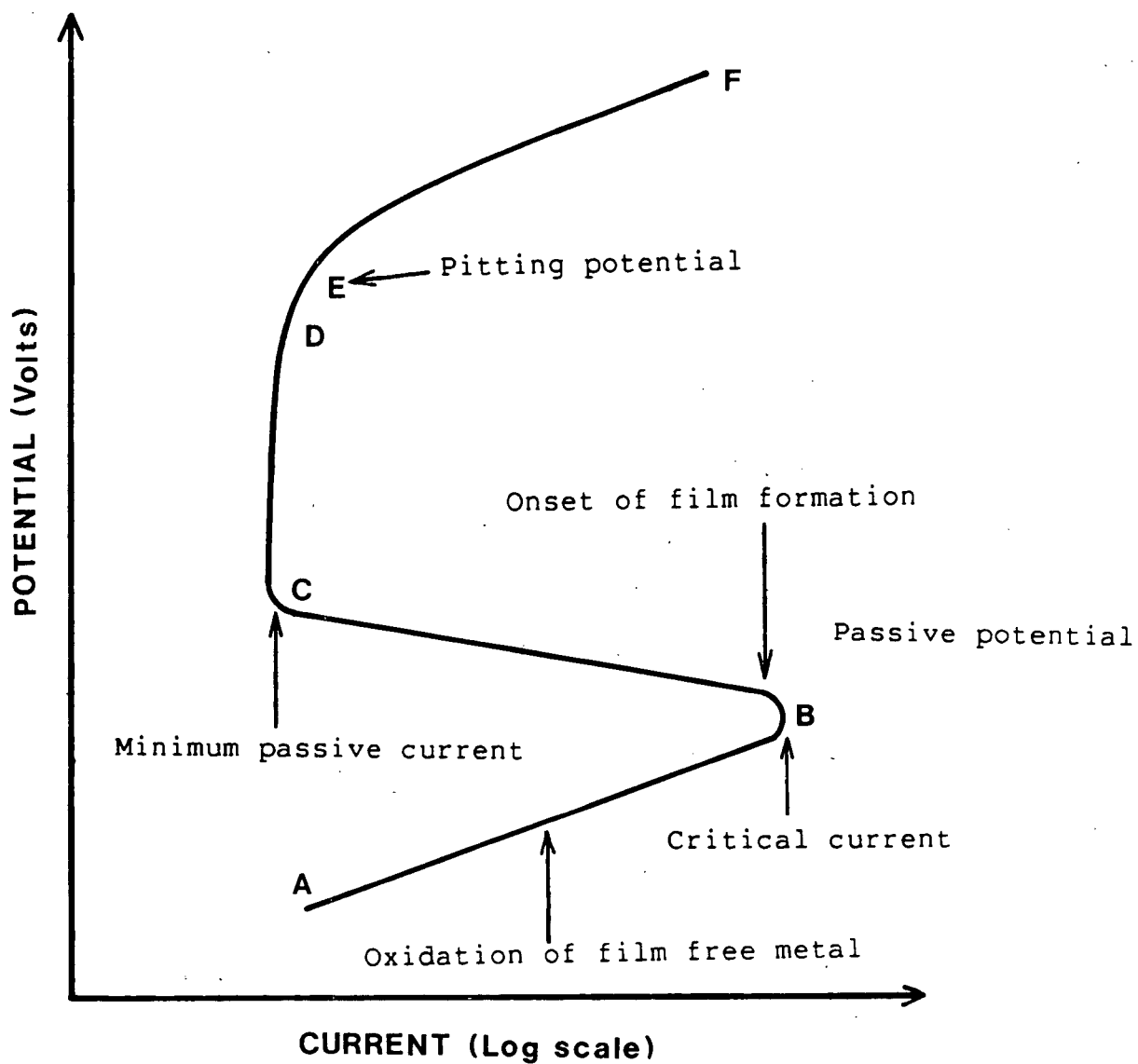


Figure 5.1 Typical anodic polarization plot showing important zones and transition points.

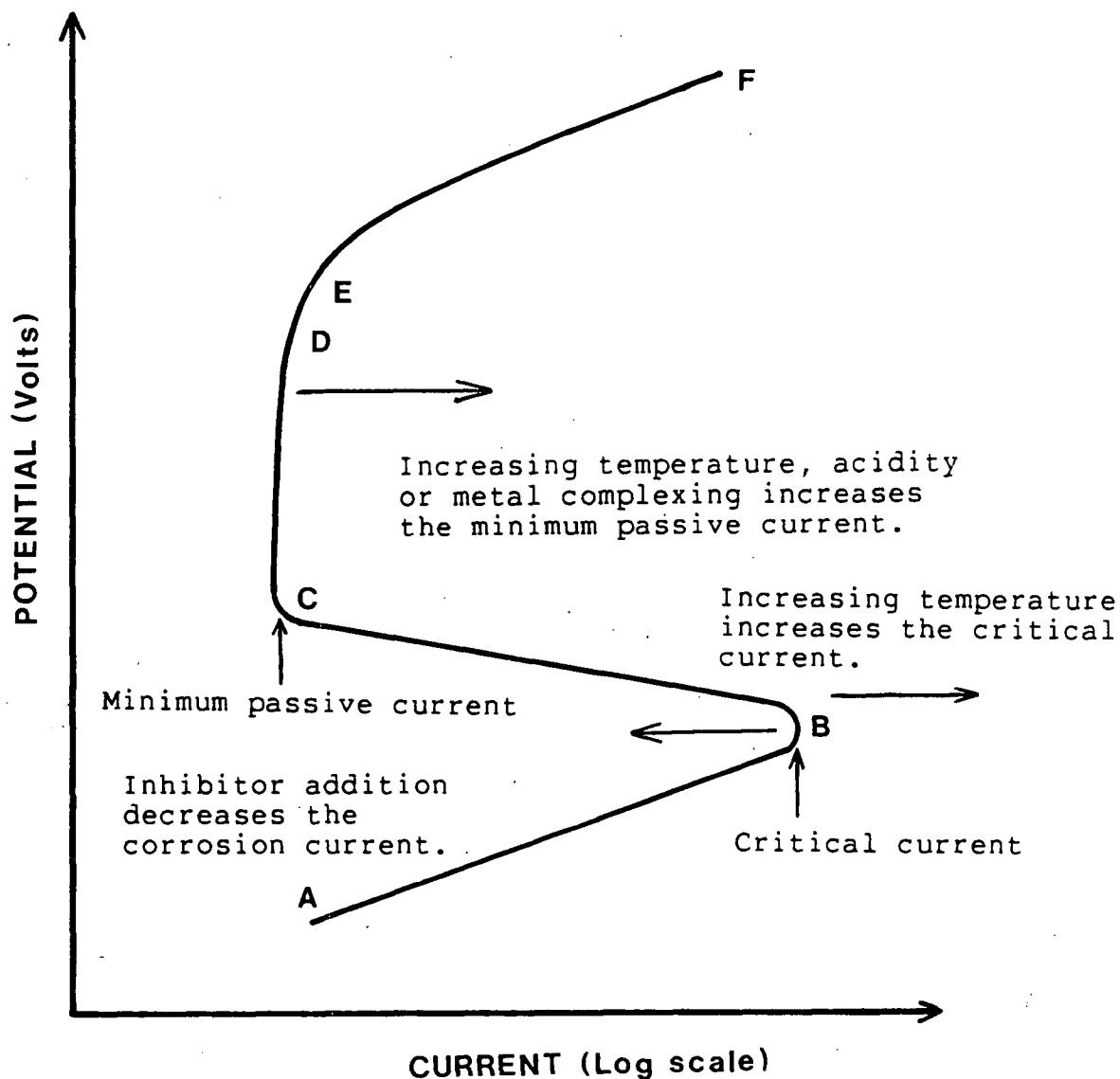


Figure 5.2 Typical anodic polarization curve showing the effect of environment and inhibitor addition upon the curve.

## 5.2 CALCULATION OF CORROSION CURRENT

The corrosion current can be calculated from polarization data by using the Stern-Geary equation [71].

As seen from Figure 5.3, if a corroding metal is polarized cathodically by raising an externally applied potential from  $\phi_{cor}$  to  $\phi'$ , the cathodic current ( $I_c$ ) increases according to the following relationship :

$$I_c = I_a + I_{\text{applied}} \dots\dots [5.1]$$

Similarly, for anodic polarization;

$$I_a = I_c - I_{\text{applied}} \dots\dots [5.2]$$

where

$I_a$  - Anodic current

$I_c$  - cathodic current

$I_{\text{applied}}$  - applied current.

The change in potential due to polarization can be expressed as follows :

For cathodic polarization;

$$\phi_{cor} - \phi' = \Delta\phi = \beta_c \log \frac{I_c}{I_{cor}} \quad [5.3]$$

Similarly for anodic polarization;

$$\Delta\phi = - \beta_a \log \frac{I_a}{I_{cor}} \quad [5.4]$$

Where

$\beta_a$  - anodic Tafel constant,

$\beta_c$  - cathodic Tafel constant,

$I_{cor}$  - corrosion current.

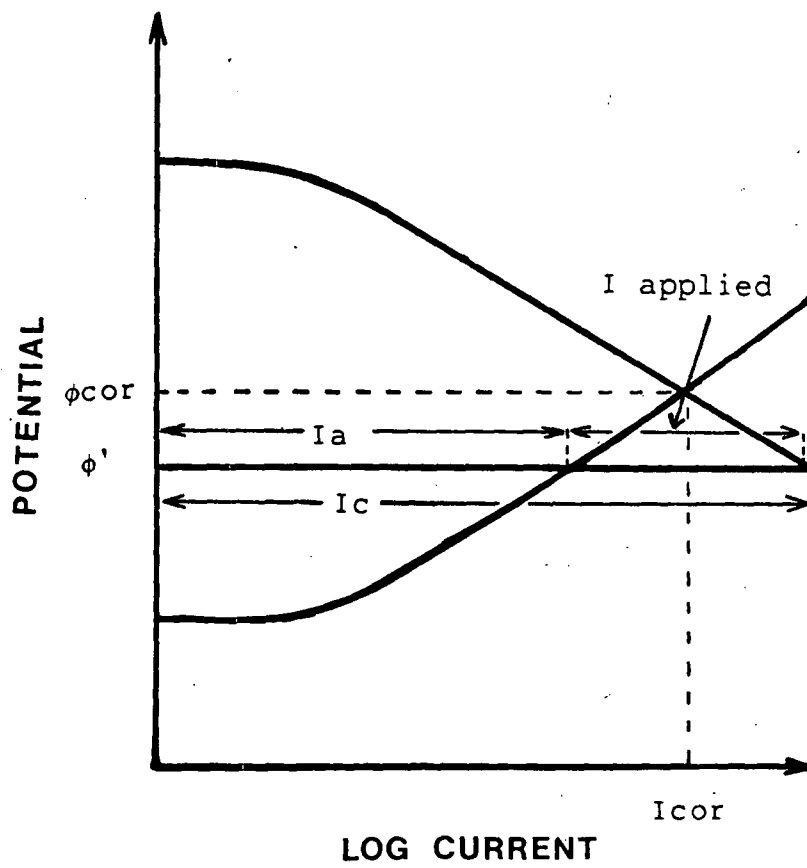


Figure 5.3 Cathodic polarization diagram for a corroding metal.

From equations 5.1 and 5.2;

$$I_{\text{applied}} = I_c - I_a$$

Therefore,

$$I_{\text{applied}} = I_{\text{cor}} \left[ 10^{\frac{(\Delta\phi/\beta_c)}{10}} - 10^{\frac{(\Delta\phi/\beta_a)}{10}} \right] \quad [5.5]$$

$10^{\frac{(\Delta\phi/\beta_c)}{10}}$  and  $10^{\frac{(\Delta\phi/\beta_a)}{10}}$  can be expressed as series as follows

$$10^{\frac{(\Delta\phi/\beta_c)}{10}} = 1 + 2.3 \frac{(\Delta\phi/\beta_c)}{10} + \frac{(-2.3(\Delta\phi/\beta_c))^2}{2!} + \dots \quad [5.6]$$

and

$$10^{\frac{-(\Delta\phi/\beta_a)}{10}} = 1 - 2.3 \frac{(\Delta\phi/\beta_a)}{10} + \frac{(-2.3(\Delta\phi/\beta_a))^2}{2!} - \dots \quad [5.7]$$

Assuming  $\Delta\phi/\beta_c$  and  $\Delta\phi/\beta_a$  to be small, the higher terms can be neglected and equation 5.5 can be approximated by :

$$I_{\text{applied}} = 2.3 I_{\text{cor}} \Delta\phi \left( \frac{1}{\beta_c} + \frac{1}{\beta_a} \right)$$

or,

$$I_{\text{cor}} = \frac{1}{2.3} \frac{I_{\text{applied}}}{\Delta\phi} \left( \frac{\beta_a \beta_b}{\beta_a + \beta_c} \right) \quad [5.8]$$

Equation 5.8 is the Stern Geary equation.

### 5.3 EXPERIMENTAL PROCEDURE

Polished mild steel specimens, each with a surface area of 6.44 cm<sup>2</sup> were immersed in a corrosion cell containing aqueous DEA solution. A calomel electrode with saturated KCl solution was used as the reference electrode. The corrosion cell was then connected to a corrosion measurement system (Princeton Applied Research, Princeton, NJ, Model 350A), equipped with a microcomputer. Potentiodynamic polarization curves were obtained at 1 mv/sec scanning rate and the free corrosion rate was determined via Tafel slope determination and extrapolation. The experiments were conducted at 25°C.



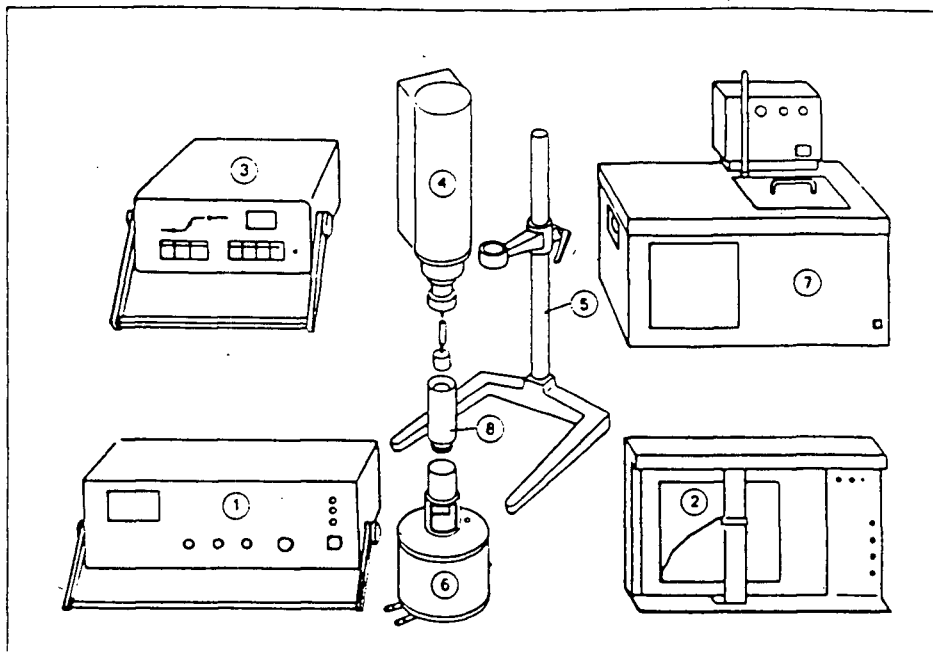
## CHAPTER 6

MISCELLANEOUS TESTS6.1 VISCOSITY MEASUREMENTS

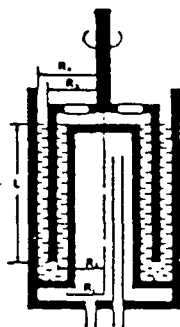
The viscosity of partially degraded DEA solutions were measured by means of a rotoviscometer (Haake Rotovisco, Berlin, West Germany, Model RV12) using a small-gap-clearance bob and cup combination(NV). A schematic diagram of the viscosimeter is given in Figure 6.1. The temperature of the solution was maintained at the desired value by circulating water from a constant temperature water bath through the tempering. bath and the cup's inner core.

At least three readings at various rotational speeds were taken and the average of the three readings was used to minimise the instrumental and experimental errors.

The minimum viscosity which could be determined accurately was 2 cp. Since the viscosity decreases with increasing temperature, all viscosity measurements were carried out at 25°C in order to keep the viscosity of the degraded DEA solutions above the minimum readable limit of the Rotoviscometer.



- ① Basic instrument ROTOVISCO RV 12
- ② Recorder: xy/t
- ③ Speed programmer PG 142
- ④ Measuring-drive-units: M 150, M 500, M 1500 – choose one or more to cover the full range of your samples.
- ⑤ Stand
- ⑥ Temperature vessel
- ⑦ Thermal liquid constant temperature circulator. A refrigerated circulator model is best suited for viscosity measurements at or below room temperature.
- ⑧ Sensor system: 40 alternatives to choose from for optimal test conditions and results.



SENSOR SYSTEM	NV
Rotor (BOB) radius $R_2$ ; $R_3$ (mm) height $L$ (mm)	17,85; 20,1 60
STATOR (CUP) radius $R_1$ ; $R_4$ (mm)	17,5 ; 20,5
RADII RATIO $R_2/R_1$	1,02
SAMPLE VOLUME $V$ (cm <sup>3</sup> )	9
TEMPERATURE: max. (°C) min. (°C)	150 -30
CALCULATION FACTORS $A'$ (Pa/scale grad.) $M$ (min/s) $G$ (mPa·s/scale grad.·min)	0,5336 5,41 98,63

Figure 6.1 Schematic diagram of the viscosimeter.

## 6.2 FOAMING TEST

A standard industrial technique [26] was used for the determination of foaming characteristics of degraded DEA solutions.

The foaming apparatus (see Figure 6.2) consisted of a 1000 mL graduated cylinder, an extra coarse fritted glass gas dispersion tube (8 mm diameter, 20 mm long) and a wet gas meter. The gas dispersion tube was placed inside the graduated cylinder and passed through a stopper.

200mL of degraded DEA sample was poured into the cylinder. An air supply tube was connected to the gas dispersion tube and oil-free air at a rate of 4 L/min was passed for 5 min. The air supply was then stopped and the foam height and the time for the foam to break completely were noted.

Although this method does not provide a quantitative relationship between foaming tendency and the concentration of degradation products in the solution, it does indicate whether the accumulation of degradation products has a significant effect on foaming.

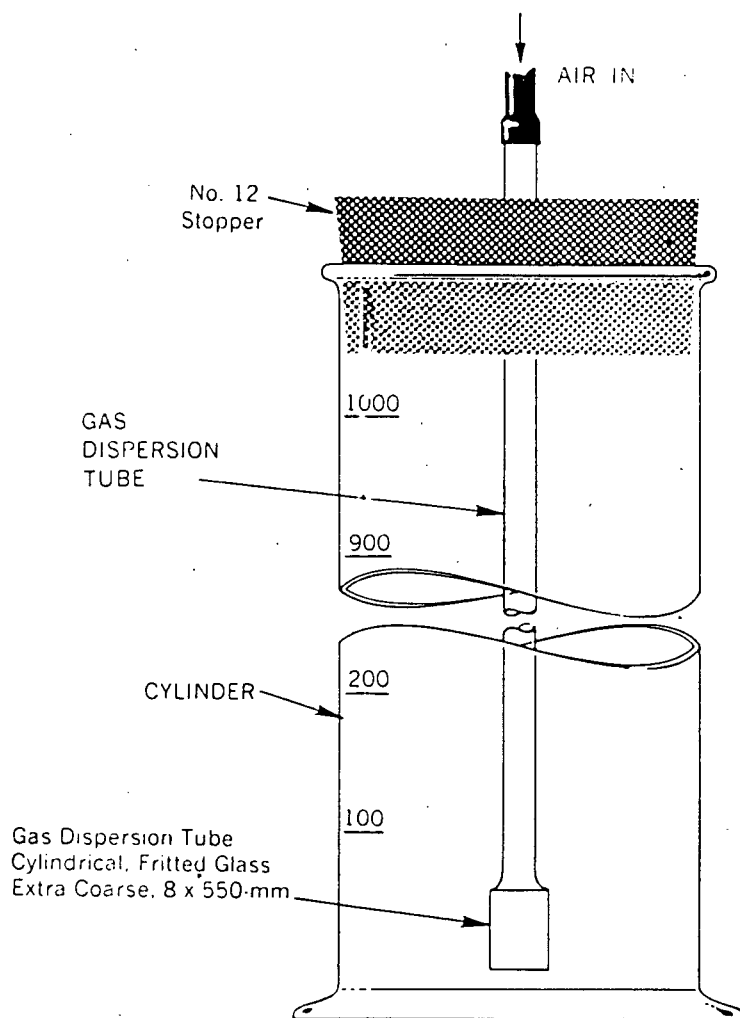


Figure 6.2 Schematic diagram of the foam testing apparatus.

## CHAPTER 7

### MODEL DEVELOPMENT

A theoretical model was developed in order to predict the rate of DEA degradation inside the heat transfer tube. The model consists of two major parts :

1. Heat exchanger model,
2. Kinetic model.

#### 7.1 HEAT EXCHANGER MODEL

A successive summation method was used for the heat exchanger calculation. The heat exchanger tube length was divided into small segments and each segment was treated as an individual heat exchanger unit. Transport properties were evaluated at the bulk solution temperature of each segment. This approach minimises the error associated with evaluating the transport properties at the average bulk solution temperature for the entire heat exchanger and thus allows the prediction of a more accurate temperature profile.

##### 7.1.1 Temperature profile determination

In order to determine the temperature profile, it was necessary to calculate the overall heat transfer co-efficient.

The inside film co-efficient was calculated by the following equation [72] :

$$h_i = 0.023 \left( \frac{T_k}{D_i} \right) (Re_c)^{0.8} (Pr_c)^{1/3} \left( \frac{\mu}{\mu_w} \right)^{0.14} \quad [7.1]$$

The corresponding outside film co-efficient was calculated by the following equation [73]:

$$h_o = 0.17 \left( \frac{T_k}{D_o} \right) (Re_o)^{0.67} (Pr_o)^{0.37} \left( \frac{D_b}{D_t} \right)^{0.1} \left( \frac{d_o}{D_t} \right)^{0.5} \left( \frac{\mu}{\mu_w} \right)^m \quad [7.2]$$

where

$$m = 0.714 \mu^{-0.21}$$

and the outside Reynolds number is defined as :

$$Re_o = \frac{D_b^2 \times RPS \times \rho_o}{\mu_o}$$

where

$D_b$  = blade diameter (m)

$D_t$  = tank diameter (m)

RPS = stirrer speed

$\rho_o$  = density of the heat transfer fluid (kg/m<sup>3</sup>)

$\mu_o$  = viscosity of the heat transfer fluid (pa.s).

The overall heat transfer coefficient (based on the inside diameter) for a straight tube, was calculated from [72]:

$$U_i = \frac{1}{(1/h_i) + (1/h_o)(D_i/D_o) + (x_m/T_{km})(D_i/D_{lm})} \quad [7.3]$$

Since the present experimental work involved a coiled heat transfer tube, the overall heat transfer coefficient for the coiled tube had to be found. This was done by means of the following equation [74] :

$$U_c = U_i (1 + 3.5(D_i/D_c)) \quad [7.4]$$

The heat exchanger tube was assumed to consist of "n" of small heat exchanger segments of length "x". Each segment was considered as an individual heat exchanger unit. Heat transfer calculations were then performed on successive heat exchanger segments.

The schematic diagram of the temperature profile across any small heat exchanger segment is shown in Figure 7.1

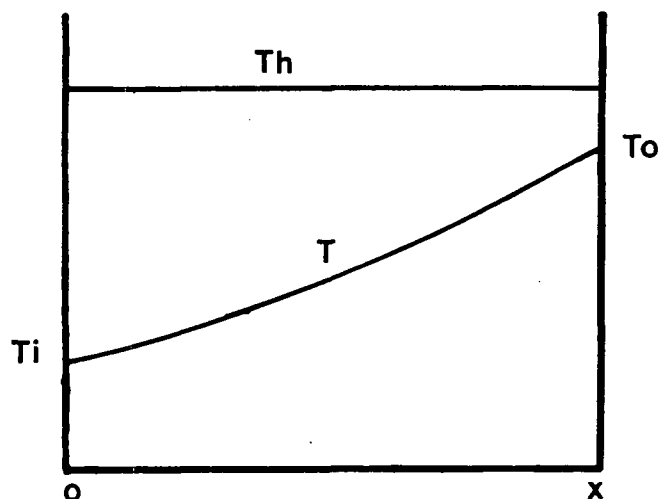


Figure 7.1 Schematic diagram of the temperature profile across a segment of the heat exchanger tube.

The heat balance for a small heat exchanger segment of length "x", may be written as :

$$W C_p dT = U_c dA (T_h - T) \quad [7.5]$$

Where

$W$  = Mass flow rate of the DEA solution,

$C_p$  = specific heat of the DEA solution,

$dT$  = temperature difference of the DEA solution,

$T_h$  = hot fluid temperature,

$T$  = bulk solution temperature,

$dA$  = elemental heat transfer area,

$U_c$  = overall heat transfer coefficient.



We can write  $dA = \pi D_i dx$ , so that Equation 7.5 becomes :

$$W C_p dT = U_c \pi D_i dx (T_h - T) \quad [7.6]$$

Assuming that  $U_c$  and  $C_p$  are constant and integrating gives,

$$\int \frac{dT}{(T_h - T)} = \int \frac{U_c \pi D_i dx}{W C_p}$$

$$\text{or} \quad \ln (T_h - T) = - \left\{ \frac{U_c \pi D_i x}{W C_p} \right\} + IC$$

where,  $IC$  denotes the integration constant.

$$\text{At, } x = 0, \quad \ln (T_h - T_i) = IC$$

where,  $T_i$  denotes the inlet temperature.

$$\text{Hence} \quad \ln (T_h - T) = - \left\{ \frac{U_c \pi D_i x}{W C_p} \right\} + \ln (T_h - T_i)$$

$$\text{or, } T = T_h - (T_h - T_i) \exp - \left\{ \frac{U_c \pi D_i x}{W C_p} \right\} \quad [7.7]$$

The bulk solution temperature in each individual segment can therefore be found provided  $T_h$  and  $T_i$  are known.

Since the temperature of the DEA solution at the inlet of the heat exchanger tube is known along with other pertinent information, the outlet temperature of the first segment can be calculated easily. The outlet temperature,  $T_o$ , of the first segment then becomes the inlet temperature,  $T_i$ , of the second segment and so forth. The following equation relates the outlet temperature of a segment to the inlet temperature of the following segment :

$$T_{i_j} = T_{o_{j-1}} ; 1 < j \leq n \quad [7.8]$$

where  $T_i$  - inlet temperature

$T_o$  - outlet temperature

$n$  - number of segments.

The outlet temperature of the last segment represents the exit temperature of the DEA solution leaving the heat transfer tube.

The calculations of the outside and inside wall temperatures require an analysis of individual heat transfer resistances. Figure 7.2 shows the temperature profile across the heat exchanger tube wall.

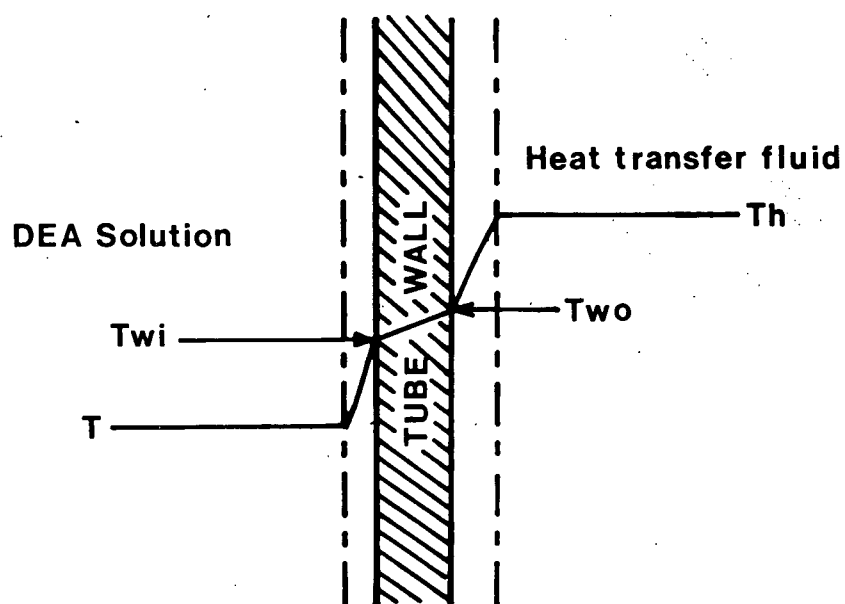


Figure 7.2 Schematic diagram of temperature profile across the metal tube wall.

Considering the individual resistances and temperature drops across each of the resistances, the following equation can be written :

$$\frac{T_h - T}{(1/U_c)} = \frac{T_h - T_{wo}}{(1/h_o)(D_i/D_o)} = \frac{T_{wo} - T_{wi}}{(x_m/T_{km})(D_i/D_{lm})} = \frac{T_{wi} - T}{(1/h_i)} \quad [7.9]$$

From equation 7.8 it follows that

$$T_h - T_{wo} = (1/h_o)(D_i/D_o)(T_h - T) U_c$$

or

$$T_{wo} = T_h - (T_h - T)(1/h_o)(D_i/D_o) U_c \quad [7.10]$$

Similarly,

$$T_{wo} - T_{wi} = (x_m/T_{km})(D_i/D_{lm})(T_h - T) U_c$$

or

$$T_{wi} = T_{wo} - (T_h - T)(x_m/T_{km})(D_i/D_{lm}) U_c \quad [7.11]$$

From equation 7.10 and 7.11, both the outside and inside wall temperatures can be calculated provided  $U, h, T$  etc. are known. However, to determine  $U, h$  and  $T$ , we need to know the outside and inside wall temperatures  $T_{wo}$  and  $T_{wi}$ . The latter were found by a trial and error method; a computer program was written for this purpose (see Appendix A).

### 7.1.2 DEA transport properties

Transport properties of DEA solutions are required to calculate the heat transfer co-efficients. Data on the physical properties of DEA solutions have been published in graphical form [26,75]. Since a computer-based successive summation method was used to perform the heat exchanger calculation, it was preferable to predict the properties by means of equations.

The following simple equations were therefore developed to predict the density, viscosity, thermal conductivity and specific heat of aqueous DEA solutions:

$$\rho = 998.0 - 0.00403 T^2 + C(3.4 - 0.00025 T^{1.45}) - C^{1.19} \quad [7.12]$$

$$\ln \mu = (0.067666 C - 6.820867)/(1 - 0.004395 C) \\ - (T(0.014066 + 0.000105 C)/(1 - 0.004965)) \quad [7.13]$$

$$k = (0.4675 - 0.0062 C^{0.8538}) T^{0.08} \quad [7.14]$$

$$C_p = 4.176 + 0.00046 T - 0.001837 C + 0.000054 C T \quad [7.15]$$

where  $\rho$  = density (kg/m<sup>3</sup>)

$\mu$  = viscosity (Pa.s)

$k$  = thermal conductivity (W/m°C)

$C_p$  = specific heat (J/g°C)

$T$  = temperature (°C)

$C$  = DEA concentration (wt%)

In all cases the percentage difference between the published and predicted values is less than 5% and in most cases it is less than 2% for temperatures between 20 and 100 °C and concentrations between 0 and 100 wt%.

### 7.1.3 Heat transfer fluid properties

The only information on the properties of Shell Thermia Oil-C was provided by Shell Canada [76]. Using the limited information provided, its properties were evaluated as follows:

#### Density

Density at 15°C was given as 874.6 kg/m<sup>3</sup> [76]. The following equation was developed from Figure 16-11 of G.P.S.A. Engineering Data Book [77] using density at 15°C.

$$\rho_o = 1000 ( 0.886662 - 0.000750 T ) \quad [7.16]$$

where  $\rho_o$  = density of the heat transfer fluid (kg/m<sup>3</sup>)

T = temperature (°C)

Density was determined experimentally and compared with the values predicted by equation 7.15. The comparison is shown in Table 7.1. The accuracy was found to be within  $\pm 1\%$ .

Table 7.1 Density of Shell Thermia Oil-C

Temp (C)	Density (kg/m <sup>3</sup> )	
	Measured	Predicted
15	874.6	875.4
20	872.0	871.7
40	852.5	856.7
100	808.5	811.7
140	780.0	781.7
160	764.8	766.7
200	732.5	736.7

### Viscosity

ASTM viscosity charts [78], can be used to obtain viscosities of petroleum oils at any temperature provided the viscosities at two different temperatures are known. The viscosities of Shell Thermia Oil-C were determined experimentally for different temperatures and the experimental procedure is described in Chapter 6. The following equation was then obtained for the viscosity determination :

$$\ln(\mu_o) = -(2.2177 + 0.0188 T) \quad [7.17]$$

where  $\mu_o$  = viscosity of the heat transfer fluid (Pa.s)

T = temperature ( $^{\circ}\text{C}$ )

Table 7.2 provides a comparison between viscosities determined experimentally and those predicted by equation 7.17. The accuracy is within  $\pm 10\%$ .

Table 7.2 Viscosity of Shell Thermia Oil-C

Temp(C)	Viscosity (pa.s)	
	Measured	Predicted
40	0.0514	0.0514
100	0.0154	0.0167
150	0.0070	0.0065
200	0.0025	0.0026



### Thermal conductivity

No data on the thermal conductivity were provided by Shell Canada; but it was recommended to use the following U.S. Bureau of Standards equation [79] :

$$Tk = [0.821 - 0.000244]/d \quad [7.18]$$

Where; Tk = thermal conductivity (BTU/ft<sup>2</sup>/hr/°F/inch),

T = temperature (°F),

d = specific gravity 60/60°F

The thermal conductivity can then be converted to S.I. units (W/m°C) simply by multiplying by a conversion factor of 0.1441314. Within the specific gravity range of 0.740 and 1.00 and at temperatures between -17.8 to 426 °C the accuracy is claimed to be ±10%.

### Specific heat

Specific heat data were also unavailable. The following U.S. Bureau of Standards equation [79] was used to calculate the specific heat :

$$Cp = [0.388 + 0.00045 T]/d^{0.5} \quad [7.19]$$

Where; Cp = specific heat (BTU/lb/°F),

T = temperature (°F),

d = specific gravity.

The specific heat thus obtained can then be converted to S.I. units (J/kg°C) by multiplying by a conversion factor of 4184. The stated accuracy is within ±4%.

#### 7.1.4 Thermal conductivity of stainless steel

Thermal conductivity of stainless steel is not strongly dependent on temperature between 150 and 250°C, the present experimental range. However, in order to perform the heat transfer calculations and especially to predict the tube wall temperature, the following equation was developed by fitting the data from the Metals Reference Book [80]. :

$$k_m = 15.60 + 0.006289 T \quad [7.20]$$

where  $k_m$  = thermal conductivity of 316 stainless steel (W/m°C)

$T$  = metal temperature (°C)

The accuracy is within ±0.5%.

### 7.1.5 Pressure drop determination

The Colebrook equation was used to calculate friction factors [81] :

$$\frac{1}{\sqrt{f}} = -4.0 \log \left( \frac{\epsilon}{D_i} + \frac{4.67}{Re \sqrt{f}} \right) + 2.28 \quad [7.21]$$

The solution of equation 7.21 requires an initial estimate of the friction factor " f " followed by a trial and error solution.

The initial friction factor was estimated by the following equation [81] :

$$f = 0.04 (Re)^{-0.16} \quad [7.22]$$

The initial surface roughness factor "  $\epsilon$  " was determined as 0.012 mm from pressure drop measurements of water flowing through a 0.5 m long section of the heat exchanger tube.

After calculating the friction factor " f ", the pressure drop for the straight pipe was calculated by [81]:

$$\Delta P_{st} = 2 \rho v^2 f L/D \quad [7.23]$$

The pressure drop in the coiled tube was determined from :

$$\Delta P_c = \Delta P_{st} + (1 + 3.5(D_i/D_c)) \quad [7.24]$$

This equation was chosen by analogy with equation 7.4 which relates heat transfer coefficient of a coiled tube to that of straight tube (see Equation 7.4) [74].

#### 7.1.6 Film thickness determination

The heat transfer film thickness "  $\delta L$  " was calculated by equating the conductive and convective terms in the heat flow equation :

$$dQ = k \, dA \, dT / \delta L = h \, dA \, dT$$

Hence,  $\delta L = k/h$  [7.25]

From equation 7.1 and neglecting the viscosity ratio term, the following equation can be derived to give the film thickness "  $\delta L$  " as a function of fluid transport properties, tube diameter and mass flow rate of the solution.

$$\delta L = \frac{k}{h} = \frac{43.478 \, d^{1.8}}{\left(\frac{4 \, W}{\pi \, \mu}\right)^{0.8} \left(\frac{C_p \, \mu}{T_k}\right)^{0.333}} \quad [7.26]$$

### 7.1.7 Heat exchanger model performance

The performance of the heat exchanger model may be evaluated by comparing the experimental outlet temperatures with those predicted by the model for various runs. Similarly, initial pressure drop measurements can also be compared.

The predicted outlet temperatures were found to be extremely close to the measured ones. This is surprising, considering the fact that a number of correlations were included in the model. Probably the errors associated with these correlations cancelled one another to some extent.

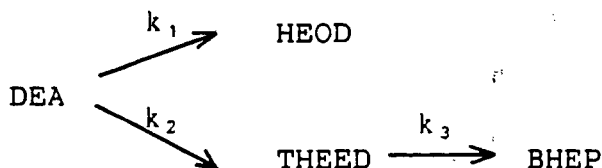
Initial pressure drop predictions were also in good agreement with the experimental results. This is probably due to the fact that the initial surface roughness was determined experimentally (albeit using water at ambient temperature). Table 7.3 shows the comparisons of outlet temperatures and initial pressure drops for various runs.

Table 7.3 Comparison of outlet temperature and initial pressure drop data for different runs.

Run No.	Outlet temp.(C)		Initial $\Delta P$ (kPa)	
	Expt.	Model	Expt.	Model
1	190	192	690	718
2	170	174	1207	1237
3	195	200	552	572
4	165	171	552	1339
5	165	171	552	574
6	140	141	552	581
7	195	200	552	572
8	195	200	552	572
9	195	200	552	602
10	195	200	552	548

## 7.2 KINETIC MODEL

Kennard's [51] simplified model for DEA degradation may be written as follows :



Kennard reported that the degradation rate is unaffected by  $\text{CO}_2$  partial pressures provided the  $\text{CO}_2$  concentration in the DEA solution exceeds  $0.2 \text{ gCO}_2/\text{g DEA}$ . He also reported the dependency of the degradation rate on the initial DEA concentration and plotted pseudo first order rate constants  $k_1$  and  $k_2$  as a function of temperature and DEA concentration. He found  $k_3$  to be independent of the DEA concentration but dependent on the temperature. Consequently, he did not include the effect of  $\text{CO}_2$  partial pressure in his model. However, under industrial conditions (especially in reboilers), the  $\text{CO}_2$  loading may be much lower than  $0.2 \text{ gCO}_2/\text{gDEA}$ . Therefore, the need to include a term which takes into account the  $\text{CO}_2$  partial pressure as well as DEA concentration is clear.

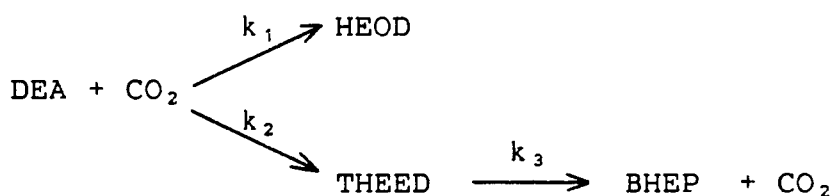
Both  $\text{CO}_2$  partial pressure and DEA concentration determine the solubility of  $\text{CO}_2$  in DEA solutions at a given temperature. Hence the  $\text{CO}_2$  solubility is a parameter which should be able to take into account the variation in  $\text{CO}_2$  partial pressure as well

as DEA concentration. It was therefore decided to include a  $\text{CO}_2$  solubility term in the rate equations. Kennard [51] reported that DEA degradation changes with DEA concentration. He identified three regions :

1. 0 - 10 wt% DEA, where the main degradation route is ionic.
2. 10 - 30 wt% DEA, where the degradation route is a combination of molecular and ionic routes.
3. 30 - 100 wt% DEA, where the main degradation route is molecular.

Recognising that it was impractical to develop a single equation for predicting the rate constants for a DEA concentration range of 0 - 100 wt%, it was decided to develop an equation for the intermediate range of 20 to 40 wt% which is of greatest industrial importance.

Kennard's model [51] was modified as follows :



The following equations represent the above kinetic model :

$$\frac{d[\text{DEA}]}{dt} = -k_1[\text{DEA}][\text{CO}_2] - k_2[\text{DEA}][\text{CO}_2] \quad [7.27]$$

$$\frac{d[\text{HEOD}]}{dt} = k_1[\text{DEA}][\text{CO}_2] \quad [7.28]$$



$$\frac{d[\text{THEED}]}{dt} = k_2[\text{DEA}][\text{CO}_2] - k_3[\text{THEED}] \quad [7.29]$$

$$\frac{d[\text{BHEP}]}{dt} = k_3[\text{THEED}] \quad [7.30]$$

Assuming  $\frac{d[\text{CO}_2]}{dt} = 0$ , integration of equation 7.27 yields,

$$[\text{DEA}] = [\text{DEA}]_0 \exp\{-(k_1+k_2)[\text{CO}_2]t\} \quad [7.31]$$

Equation 7.28 on substitution and integration yields,

$$\begin{aligned} \frac{d[\text{HEOD}]}{dt} &= k_1[\text{CO}_2][\text{DEA}]_0 \exp\{-(k_1+k_2)[\text{CO}_2]t\} \\ [\text{HEOD}] &= [\text{DEA}]_0 \frac{k_1}{(k_1+k_2)} (1 - \exp\{-(k_1+k_2)[\text{CO}_2]t\}) \\ &\quad + [\text{HEOD}]_0 \end{aligned} \quad [7.23]$$

Equation 7.29 can be written as follows :

$$\begin{aligned} \frac{d[\text{THEED}]}{dt} &= k_2[\text{CO}_2][\text{DEA}]_0 \exp\{-(k_1+k_2)[\text{CO}_2]t\} - k_3[\text{THEED}] \\ \text{or } \frac{d[\text{THEED}]}{dt} + k_3[\text{THEED}] &= k_2[\text{CO}_2][\text{DEA}]_0 \exp\{-(k_1+k_2)[\text{CO}_2]t\} \end{aligned} \quad [7.34]$$

The above equation is a first order linear differential equation and can be solved by multiplying by an integration factor  $\exp\{k_3t\}$

$$\begin{aligned} [\text{THEED}] \exp\{k_3t\} &= \int k_2[\text{CO}_2][\text{DEA}]_0 \exp\{(k_3-(k_1+k_2)[\text{CO}_2])t\} dt \\ &= \left( \frac{k_2[\text{CO}_2][\text{DEA}]_0}{k_3-(k_1+k_2)[\text{CO}_2]} \right) \exp\{(k_3-(k_1+k_2)[\text{CO}_2])t\} + \text{IC1} \end{aligned} \quad [7.35]$$

where IC1 denotes integration constant.

At  $t=0$ ,  $[\text{THEED}] = [\text{THEED}]_0$

$$[\text{THEED}]_0 = \frac{k_2[\text{CO}_2][\text{DEA}]_0}{k_3 - (k_1 + k_2)[\text{CO}_2]} + \text{IC1}$$

$$\text{Therefore, IC1} = [\text{THEED}]_0 - \frac{k_2[\text{CO}_2][\text{DEA}]_0}{k_3 - (k_1 + k_2)[\text{CO}_2]}$$

Equation 7.35 can then be written as :

$$\begin{aligned} [\text{THEED}] = & \left( \frac{k_2[\text{CO}_2][\text{DEA}]_0}{k_3 - (k_1 + k_2)[\text{CO}_2]} \right) (\exp\{-(k_1 + k_2)[\text{CO}_2]t\} - \exp\{-k_3t\}) \\ & + [\text{THEED}]_0 \exp\{-k_3t\} \quad [7.36] \end{aligned}$$

Equation 7.30 can then be solved as follows :

$$\begin{aligned} \frac{d[\text{BHEP}]}{dt} &= k_3[\text{THEED}] \\ &= \frac{k_2k_3[\text{CO}_2][\text{DEA}]_0}{k_3 - (k_1 + k_2)[\text{CO}_2]} (\exp\{-(k_1 + k_2)[\text{CO}_2]t\} - \exp\{-k_3t\}) \\ &\quad + [\text{THEED}]_0 \exp\{-k_3t\} \\ [\text{BHEP}] &= \int \frac{k_2k_3[\text{CO}_2][\text{DEA}]_0}{k_3 - (k_1 + k_2)[\text{CO}_2]} (\exp\{-(k_1 + k_2)[\text{CO}_2]t\} - \exp\{-k_3t\}) dt \\ &\quad + \int [\text{THEED}]_0 \exp\{-k_3t\} dt \\ [\text{BHEP}] &= \frac{k_2k_3[\text{CO}_2][\text{DEA}]_0}{k_3 - (k_1 + k_2)[\text{CO}_2]} \left( -\frac{\exp\{-(k_1 + k_2)[\text{CO}_2]t\}}{(k_1 + k_2)[\text{CO}_2]} \right. \\ &\quad \left. + \frac{1}{k_3} \exp\{-k_3t\} \right) - \frac{1}{k_3} [\text{THEED}]_0 \exp\{-k_3t\} + \text{IC2} \end{aligned}$$

where IC2 denotes integration constant.

At  $t=0$ ,  $[BHEP]=[BHEP]_0$

$$[BHEP]_0 = \frac{k_2 k_3 [CO_2] [DEA]_0}{k_3 - (k_1 + k_2) [CO_2]} \left( - \frac{k_3 - (k_1 + k_2) [CO_2]}{k_3 (k_1 + k_2) [CO_2]} \right) - \frac{[THEED]}{k_3} + IC2$$

$$IC2 = \frac{k_2 [DEA]_0}{(k_1 + k_2)} + \frac{[THEED]_0}{k_3} + [BHEP]_0$$

$$[BHEP] = \frac{k_2 k_3 [CO_2] [DEA]_0}{k_3 - (k_1 + k_2) [CO_2]} \left( - \frac{\exp\{-(k_1 + k_2) [CO_2] t\}}{(k_1 + k_2) [CO_2]} + \frac{\exp\{-k_3 t\}}{k_3} \right) + \frac{k_2 [DEA]_0}{(k_1 + k_2)} + \frac{[THEED]_0}{k_3} (1 - \exp\{-k_3 t\}) + [BHEP]_0 \quad [7.37]$$

### 7.2.1 Determination of rate constants

In order to determine the rate constants,  $CO_2$  solubility data were needed. In the absence of any reliable solubility model, the limited data of Lee et al. [82] were used. In some cases, interpolation was needed. This kind of approach is not very desirable for accurate prediction of rate constants but it was unavoidable. New values of  $k_1$  and  $k_2$  were generated from Kennard's [51] rate constants (identified by an asterisk) as follows:

$$k_1 = k_1^* / [CO_2]$$

$$k_2 = k_2^* / [CO_2]$$

The values of  $k_1$  and  $k_2$  were calculated for various temperatures. Values of  $k_3$  were obtained from Kennard's thesis.

It should be noted that most of Kennard's rate data were obtained at CO<sub>2</sub> partial pressures of 4137 kPa and thus there is some uncertainty when the CO<sub>2</sub> partial pressure is different. The following equations for predicting  $k_1$ ,  $k_2$  and  $k_3$  as a function of temperature were then obtained by least square fitting:

$$\ln(k_1) = 11.924 - 6421/T \quad [7.38]$$

$$\ln(k_2) = 8.450 - 5580/T \quad [7.39]$$

$$\ln(k_3) = 39.813 - 15160/T \quad [7.40]$$

where  $T$  denotes the absolute temperature in degrees Kelvin. Bulk solution temperature was used for the calculation of the rate constants.

Attempts were made to develop an empirical model for the prediction of CO<sub>2</sub> solubility in aqueous DEA solutions. However, mainly due to the lack of adequate data, it was not successful. It was therefore decided to use the CO<sub>2</sub> solubility under the initial saturation conditions in the autoclave. It then became possible to predict the rate of DEA degradation fairly accurately, covering the temperature range of 60 to 200 °C, CO<sub>2</sub> partial pressure range of 1379 to 4137 kPa and DEA concentration range of 20 to 40 wt%.

### 7.2.2 Determination of tube inlet conditions and residence time

For the computer calculations the inlet conditions as well as the residence time in the heat transfer tube need to be known.

Knowing the volume of the heat transfer tube and solution flow rate the time required to process one heat transfer tube volume equivalent DEA solution can be determined. This time is the residence time for a single pass,  $rt$ . The time required for all the DEA solution to pass through the heat exchanger tube once is denoted by  $tsp$ . The total no. of passes  $N$  can then be determined as follows:

$$N = t/tsp$$

The total residence time of the DEA solution in the heat transfer tube is then given by:

$$RT = rt \times N$$

The concentration changes for a single pass are very low. In addition, the quantity of DEA solution in the heat transfer tube is small compared to the total DEA solution inventory inside the autoclave. Therefore, the concentration change as a result of mixing of partially degraded DEA solution from the heat transfer tube with the DEA solution in the autoclave is very small. Consequently, it was assumed that all the DEA solution passes through the heat transfer tube before mixing occurs in the autoclave and the next pass begins. This approximation is not expected to affect the accuracy of the computer predictions significantly.

## CHAPTER 8

RESULTS AND DISCUSSION OF DEGRADATION EXPERIMENTS8.1 COMPARISON OF THE EXPERIMENTAL DATA WITH MODEL PREDICTION

The comparisons of experimental data with those predicted by the model are given in Table 8.1 to Table 8.10. The model predictions will also be compared with the experimental data in graphical form later in the chapter. As can be seen, the agreement between the predictions and the experimental values are quite good but not perfect. The reasons for the differences are not fully known but may be attributed to the following factors:

- \* Inaccuracies in the rate constants,
- \* The simplification involved in the reaction scheme,
- \* Inaccuracies in the CO<sub>2</sub> solubility data,
- \* Inaccuracies in the experimental measurements, especially the low BHEP concentrations.

TABLE 8.1

RUN NO.1 : 30WT% DEA, TIN=60C, TOUT=190C, TOUTC=192.4C  
 FLOW RATE=0.0124 L/s, DELP=690 kPa, CALDP=717.9 kPa  
 CO<sub>2</sub> PARTIAL PRESSURE = 4137 kPa, TH=250C

TIME hr	CONCENTRATION (MOLES/L)							
	DEA		HEOD		THEED		BHEP	
	EXP	CALC	EXP	CALC	EXP	CALC	EXP	CALC
00.0	3.00	3.00	-	-	-	-	-	-
24.0	2.92	2.91	0.05	0.06	-	0.01	-	-
48.0	2.83	2.82	0.11	0.12	-	0.03	-	-
72.0	2.73	2.72	0.16	0.18	0.05	0.04	-	-
96.0	2.64	2.63	0.22	0.24	0.06	0.05	-	0.01
120.0	2.56	2.54	0.30	0.30	0.07	0.06	-	0.01
144.0	2.50	2.45	0.35	0.36	0.09	0.08	-	0.01
168.0	2.41	2.35	0.40	0.42	0.11	0.09	0.05	0.01
192.0	2.27	2.26	0.47	0.49	0.13	0.10	0.05	0.01

TABLE 8.2

RUN NO.2 : 30WT% DEA, TIN=60C, TOUT=170C, TOUTC=173.7C  
 FLOW RATE=0.0165 L/s, DELP=1207 kPa, CALDP=1237 kPa  
 CO<sub>2</sub> PARTIAL PRESSURE = 4137 kPa TH=250C

TIME hr	CONCENTRATION (MOLES/L)							
	DEA		HEOD		THEED		BHEP	
	EXP	CALC	EXP	CALC	EXP	CALC	EXP	CALC
00.0	3.00	3.00	-	-	-	-	-	-
24.0	2.94	2.93	-	0.03	-	0.01	-	-
48.0	2.87	2.87	0.06	0.07	-	0.02	-	-
72.0	2.81	2.80	0.10	0.10	-	0.02	-	0.01
96.0	2.76	2.74	0.12	0.14	0.02	0.03	0.01	0.01
120.0	2.69	2.67	0.16	0.17	0.04	0.04	0.02	0.02
144.0	2.63	2.61	0.19	0.20	0.04	0.05	0.02	0.02
168.0	2.55	2.54	0.22	0.24	0.05	0.06	0.03	0.02
192.0	2.50	2.48	0.26	0.27	0.06	0.07	0.03	0.03

TABLE 8.3

RUN NO.3 : 30WT% DEA, TIN=60C, TOUT=195C, TOUTC=200C  
 FLOW RATE=0.0110 l/s, DELP=552 kPa, CALDP=571.9 kPa  
 CO<sub>2</sub> PARTIAL PRESSURE = 4137 kPa, TH=250 C

TIME hr	CONCENTRATION (MOLES/L)							
	DEA		HEOD		THEED		BHEP	
	EXP	CALC	EXP	CALC	EXP	CALC	EXP	CALC
00.0	3.00	3.00	-	-	-	-	-	-
24.0	2.89	2.89	0.05	0.08	-	0.02	-	-
48.0	2.75	2.78	0.14	0.15	-	0.03	-	-
72.0	2.68	2.67	0.20	0.23	-	0.05	-	0.01
96.0	2.57	2.57	0.28	0.30	0.05	0.06	-	0.01
120.0	2.46	2.46	0.35	0.38	0.05	0.08	-	0.01
144.0	2.35	2.35	0.44	0.46	0.07	0.10	-	0.02
168.0	2.25	2.24	0.52	0.53	0.08	0.11	0.02	0.02
192.0	2.13	2.13	0.58	0.61	0.10	0.12	0.02	0.02

TABLE 8.4

RUN NO.4 : 30WT% DEA, TIN=60C, TOUT=165C, TOUTC=170.9C  
 FLOW RATE=0.0172 L/s, DELP=1.31 MPa, CALDP=1.34 MPa  
 CO<sub>2</sub> PARTIAL PRESSURE = 4137 kPa, TH=250C

TIME hr	CONCENTRATION (MOLES/L)							
	DEA		HEOD		THEED		BHEP	
	EXP	CALC	EXP	CALC	EXP	CALC	EXP	CALC
00.0	3.00	3.00	-	-	-	-	-	-
24.0	2.94	2.94	-	0.03	-	0.01	-	-
48.0	2.88	2.87	0.06	0.06	-	0.02	-	-
72.0	2.84	2.81	0.10	0.09	-	0.02	-	0.01
96.0	2.78	2.75	0.12	0.13	0.02	0.03	0.01	0.01
120.0	2.72	2.69	0.15	0.16	0.04	0.04	0.02	0.01
144.0	2.64	2.62	0.18	0.19	0.04	0.05	0.02	0.02
168.0	2.57	2.56	0.21	0.22	0.05	0.05	0.03	0.02
192.0	2.51	2.50	0.26	0.25	0.06	0.06	0.04	0.02



TABLE 8.5

RUN NO.5 : 30WT% DEA, TIN=60C, TOUT=165C, TOUTC=171.5C  
 FLOW RATE=0.0110 L/s, DELP=552 kPa, CALDP=573.2kPa  
 CO<sub>2</sub> PARTIAL PRESSURE = 4137 kPa, TH=225C

TIME hr	CONCENTRATION (MOLES/L)							
	DEA		HEOD		THEED		BHEP	
	EXP	CALC	EXP	CALC	EXP	CALC	EXP	CALC
00.0	3.00	3.00	-	-	-	-	-	-
24.0	2.95	2.94	-	0.04	-	0.01	-	-
48.0	2.90	2.88	0.07	0.07	-	0.02	-	-
72.0	2.84	2.81	0.11	0.11	-	0.03	-	-
96.0	2.79	2.75	0.12	0.15	0.02	0.03	0.01	-
120.0	2.74	2.69	0.16	0.19	0.04	0.04	0.02	0.01
144.0	2.67	2.63	0.21	0.22	0.04	0.05	0.02	0.01
168.0	2.61	2.57	0.24	0.26	0.05	0.06	0.03	0.01
192.0	2.54	2.50	0.28	0.30	0.06	0.07	0.03	0.01

TABLE 8.6

RUN NO.6 : 30WT% DEA, TIN=60C, TOUT=140C, TOUTC=142.1C  
 FLOW RATE=0.0110 L/s, DELP=552 kPa, CALDP=581 kPa  
 CO<sub>2</sub> PARTIAL PRESSURE= 4137 kPa, TH=190C

TIME hr	CONCENTRATION (MOLES/L)							
	DEA		HEOD		THEED		BHEP	
	EXP	CALC	EXP	CALC	EXP	CALC	EXP	CALC
00.0	3.00	3.00	-	-	-	-	-	-
24.0	2.98	2.97	-	0.01	-	-	-	-
48.0	2.94	2.93	-	0.03	-	0.01	-	-
72.0	2.92	2.90	0.05	0.04	-	0.01	-	-
96.0	2.87	2.86	0.05	0.06	-	0.15	-	-
120.0	2.82	2.83	0.05	0.07	0.02	0.02	0.02	-
144.0	2.80	2.79	0.06	0.08	0.02	0.02	0.03	-
168.0	2.77	2.76	0.07	0.10	0.04	0.03	0.04	0.01
192.0	2.72	2.72	0.09	0.11	0.04	0.03	0.04	0.01

TABLE 8.7

RUN NO.7 : 30WT% DEA, TIN=60C, TOUT=195C, TOUTC=200 C  
 FLOW RATE=0.0110 L/s, DELP=552 kPa, CALDP=572 kPa  
 CO<sub>2</sub> PARTIAL PRESSURE = 2758 kPa, TH=250C

TIME hr	CONCENTRATION (MOLES/L)							
	DEA		HEOD		THEED		BHEP	
	EXP	CALC	EXP	CALC	EXP	CALC	EXP	CALC
00.0	3.00	3.00	-	-	-	-	-	-
24.0	2.91	2.91	0.05	0.07	-	0.01	-	-
48.0	2.82	2.80	0.15	0.14	-	0.03	-	-
72.0	2.71	2.69	0.20	0.21	-	0.04	-	0.01
96.0	2.60	2.59	0.30	0.29	0.05	0.06	-	0.01
120.0	2.50	2.49	0.35	0.36	0.06	0.07	0.01	0.01
144.0	2.40	2.39	0.45	0.43	0.08	0.09	0.02	0.01
168.0	2.30	2.29	0.50	0.50	0.10	0.10	0.03	0.01
192.0	2.20	2.18	0.58	0.57	0.10	0.11	0.03	0.01

TABLE 8.8

RUN NO.8 : 30WT% DEA, TIN=60C, TOUT=195C, TOUTC=200 C  
 FLOW RATE=0.0110 L/s, DELP=552 kPa, CALDP= 572 kPa  
 CO<sub>2</sub> PARTIAL PRESSURE =1379 kPa , TH=250C

TIME hr	CONCENTRATION (MOLES/L)							
	DEA		HEOD		THEED		BHEP	
	EXP	CALC	EXP	CALC	EXP	CALC	EXP	CALC
00.0	3.00	3.00	-	-	-	-	-	-
24.0	2.94	2.91	-	0.07	-	0.01	-	-
48.0	2.83	2.81	0.10	0.13	-	0.03	-	-
72.0	2.74	2.72	0.16	0.19	-	0.04	-	0.01
96.0	2.64	2.63	0.25	0.26	0.05	0.05	-	0.01
120.0	2.56	2.53	0.30	0.32	0.05	0.07	-	0.01
144.0	2.47	2.44	0.40	0.39	0.07	0.08	-	0.01
168.0	2.38	2.35	0.46	0.45	0.10	0.09	0.01	0.02
192.0	2.28	2.25	0.50	0.52	0.10	0.10	0.01	0.02

TABLE 8.9

RUN NO.9 : 40WT% DEA, TIN=60C, TOUT=195C, TOUTC=200 C  
 FLOW RATE=0.0110 L/s, DELP=552 kPa, CALDP= 602 kPa  
 CO<sub>2</sub> PARTIAL PRESSURE = 4137 kPa , TH=250C

TIME hr	CONCENTRATION (MOLES/L)							
	DEA		HEOD		THEED		BHEP	
	EXP	CALC	EXP	CALC	EXP	CALC	EXP	CALC
00.0	4.00	4.00	-	-	-	-	-	-
24.0	3.84	3.84	0.10	0.12	-	0.02	-	-
48.0	2.66	3.68	0.20	0.24	0.05	0.05	-	-
72.0	2.52	3.52	0.34	0.36	0.07	0.07	-	0.01
96.0	2.36	3.35	0.50	0.48	0.10	0.10	0.01	0.01
120.0	2.21	3.19	0.60	0.60	0.12	0.12	0.02	0.01
144.0	2.10	3.03	0.70	0.72	0.16	0.15	0.03	0.02
168.0	2.89	2.87	0.80	0.83	0.20	0.17	0.03	0.02
192.0	2.72	2.71	0.92	0.95	0.20	0.19	0.04	0.02

TABLE 8.10

RUN NO.10 : 20WT% DEA, TIN=60C, TOUT=195C, TOUTC=200 C  
 FLOW RATE=0.0110 L/s, DELP=552 kPa, CALDP= 572 kPa  
 CO<sub>2</sub> PARTIAL PRESSURE = 4137 kPa , TH=250C

TIME hr	CONCENTRATION (MOLES/L)							
	DEA		HEOD		THEED		BHEP	
	EXP	CALC	EXP	CALC	EXP	CALC	EXP	CALC
00.0	2.00	2.00	-	-	-	-	-	-
24.0	1.94	1.94	-	0.04	-	0.01	-	-
48.0	1.89	1.88	0.06	0.08	0.01	0.02	-	0.01
72.0	1.82	1.81	0.10	0.11	0.02	0.02	-	0.01
96.0	1.76	1.75	0.15	0.15	0.02	0.03	-	0.02
120.0	1.70	1.69	0.20	0.19	0.03	0.04	-	0.02
144.0	1.64	1.63	0.22	0.23	0.05	0.05	-	0.02
168.0	1.57	1.57	0.25	0.26	0.05	0.05	0.01	0.03
192.0	1.52	1.50	0.28	0.30	0.06	0.06	0.01	0.03

## 8.2 EFFECTS OF OPERATING VARIABLES ON DEGRADATION

The effects of temperature, solution concentration, CO<sub>2</sub> partial pressure and especially of solution flow rate on DEA degradation were studied.

### 8.2.1 Effect of flow rate

In order to examine the effect of flow rate on DEA degradation, two sets of experiments were carried out. In first set, the flow rate was varied while keeping the temperature of the heating fluid constant. The temperature of the DEA solution leaving the heat transfer coil was allowed to vary. The results are plotted in Figure 8.1. As might be expected, lower flow rates resulted in higher degradation rates. The increase in DEA degradation can be attributed to the combined effect of the residence time for single pass in the tube and the solution temperature. Since the degradation rate increases rapidly with temperature, the temperature in the outlet section can be assumed to exert the predominating influence.

In order to elucidate the effect of flow rate only, a second set of experiments was carried out.

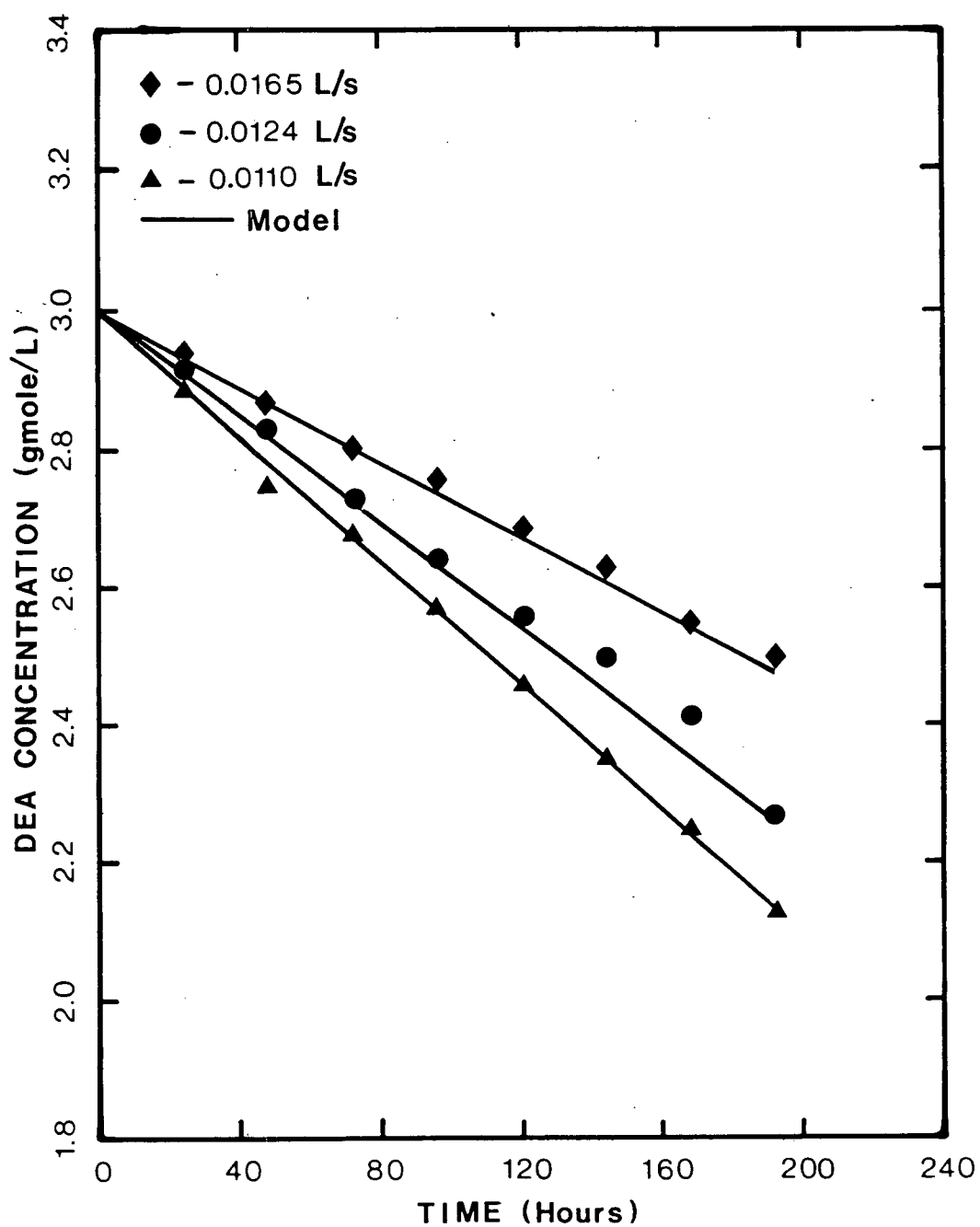


Figure 8.1 DEA concentration as a function of time and flow rate. (30 wt% DEA, inlet temp. 60°C, heating oil temp. 250 °C, CO<sub>2</sub> partial pressure 4.14 MPa)

The flow rates were varied while the outlet temperature was kept constant by regulating the hot fluid temperature. Two flow rates were chosen, one at 0.0172 L/s (5.3 m/s) and the other at 0.011 L/s (3.4 m/s). The temperature profiles resulting from the two flow rates are shown in Figure 8.2. As can be seen, they are almost identical. DEA concentrations as a function of time are plotted in Figure 8.3. DEA degradation remains almost the same for both flow rates. The model predictions of the concentration profiles for the two flow rates are plotted in Figure 8.4. As can be seen, for a single pass, the degradation rate is higher at lower flow rates (0.011 L/s). Although the degradation rate for a single pass at the lower flow rate is higher, the overall degradation rates for a given period (and when the fluids are recirculated) are almost the same for both flow rates. This is due to the "total residence time", which is the same in both cases.

The effect of residence time can be explained by considering two flow rates  $W_1$  and  $W_2$  ( $W_1 < W_2$ ) and defining :

$W_1$  = lower flow rate

$W_2$  = higher flow rate

$N_1$  = total no. of passes at flow rate  $W_1$

$N_2$  = total no. of passes at flow rate  $W_2$

$RT_1$  = total residence time at flow rate  $W_1$

$RT_2$  = total residence time at flow rate  $W_2$

$rt_1$  = residence time for single pass at flow rate  $W_1$

$rt_2$  = residence time for single pass at flow rate  $W_2$

The residence time for a single pass  $tr_1$ , at the lower flow rate  $W_1$ , is higher than the residence time  $tr_2$ , at the higher flow rate  $W_2$ . However, for a given time  $T$ , the number of passes  $N_1$  through the tube is lower than  $N_2$  of the higher flow rate.

We can write :

$$RT_1 = rt_1 \times N_1, \text{ and } RT_2 = rt_2 \times N_2$$

If  $rt_1 \times N_1 = rt_2 \times N_2$ , then the total residence time is the same for both flow rates  $W_1$  and  $W_2$ . This is the case for flow rates of 0.011 L/s (3.4 m/s) and 0.0172 L/s (5.3 m/s).

Based on hydrodynamic considerations, one more factor has to be examined. This is the so-called "boundary film", i.e. the layer adjacent to the heat exchanger tube wall. The film thickness decreases with increasing flow rate. A large film thickness means that a higher proportion of the liquid is in contact with the surface of the heat exchanger and, consequently, results in higher rates of degradation. Film thicknesses as predicted by the theoretical model are shown in Figure 8.5. Film thicknesses are very thin because of the small diameter tube and higher Reynolds number used in the experiments. Therefore, the degradation rate could be predicted accurately using the bulk solution temperature. However in industrial heat exchangers, the film thicknesses may be large and therefore, metal wall temperature may have to be used for calculating the rate constants.

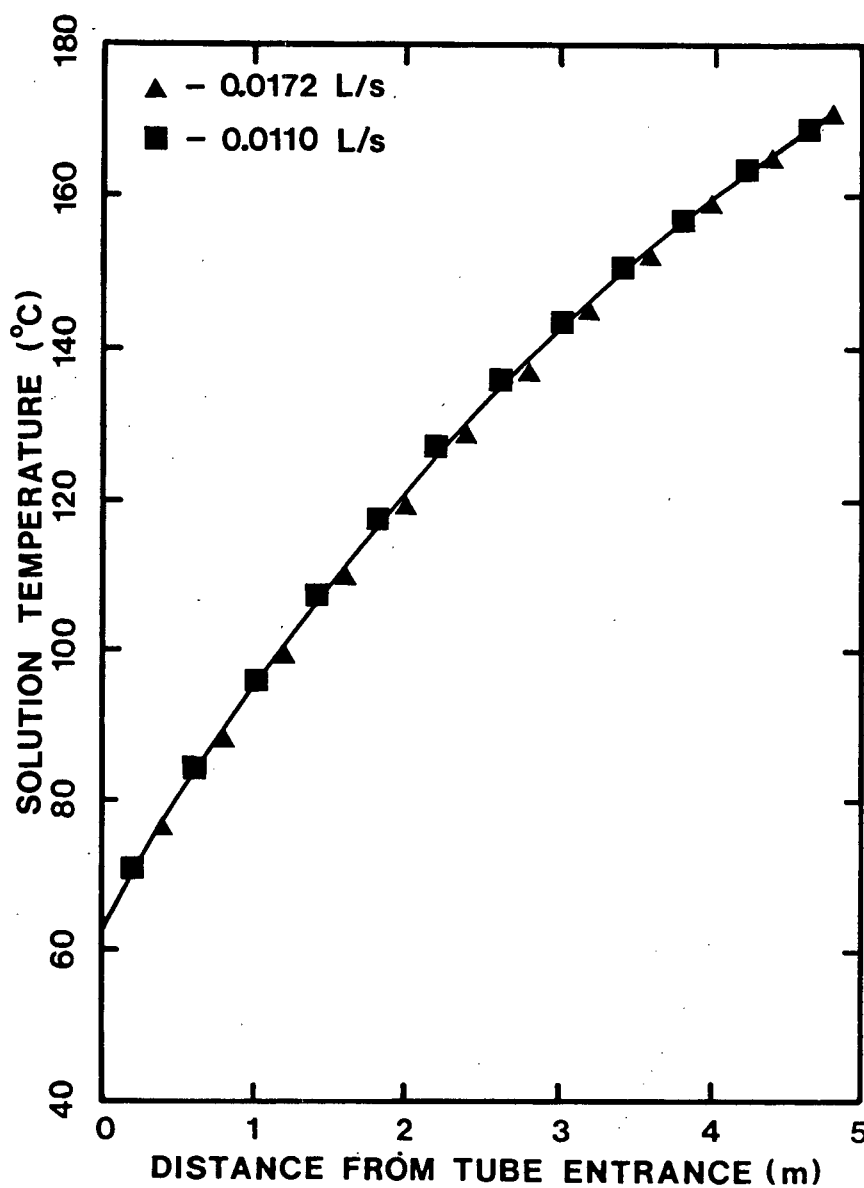


Figure 8.2 Temperature of the DEA solution as a function of the distance from the tube entrance and flow rate. (30 wt% DEA, inlet temp. 60°C, outlet temp. 170°C, CO<sub>2</sub> partial pressure 4.14 MPa)



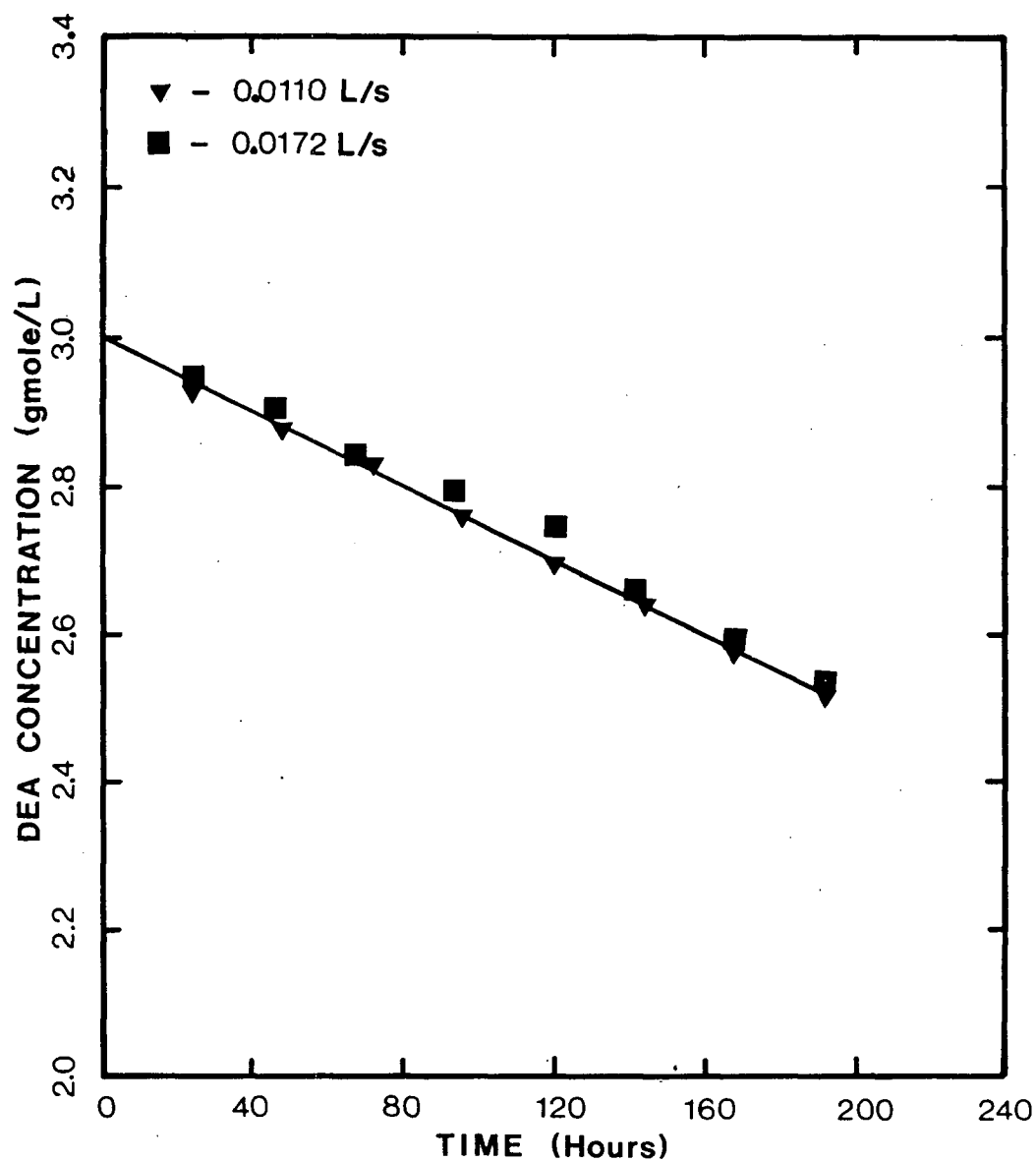


Figure 8.3 DEA concentration as a function of time and flow rate. (30 wt% DEA, inlet temp. 60°C, outlet temp. 170°C, CO<sub>2</sub> partial pressure 4.14 MPa)

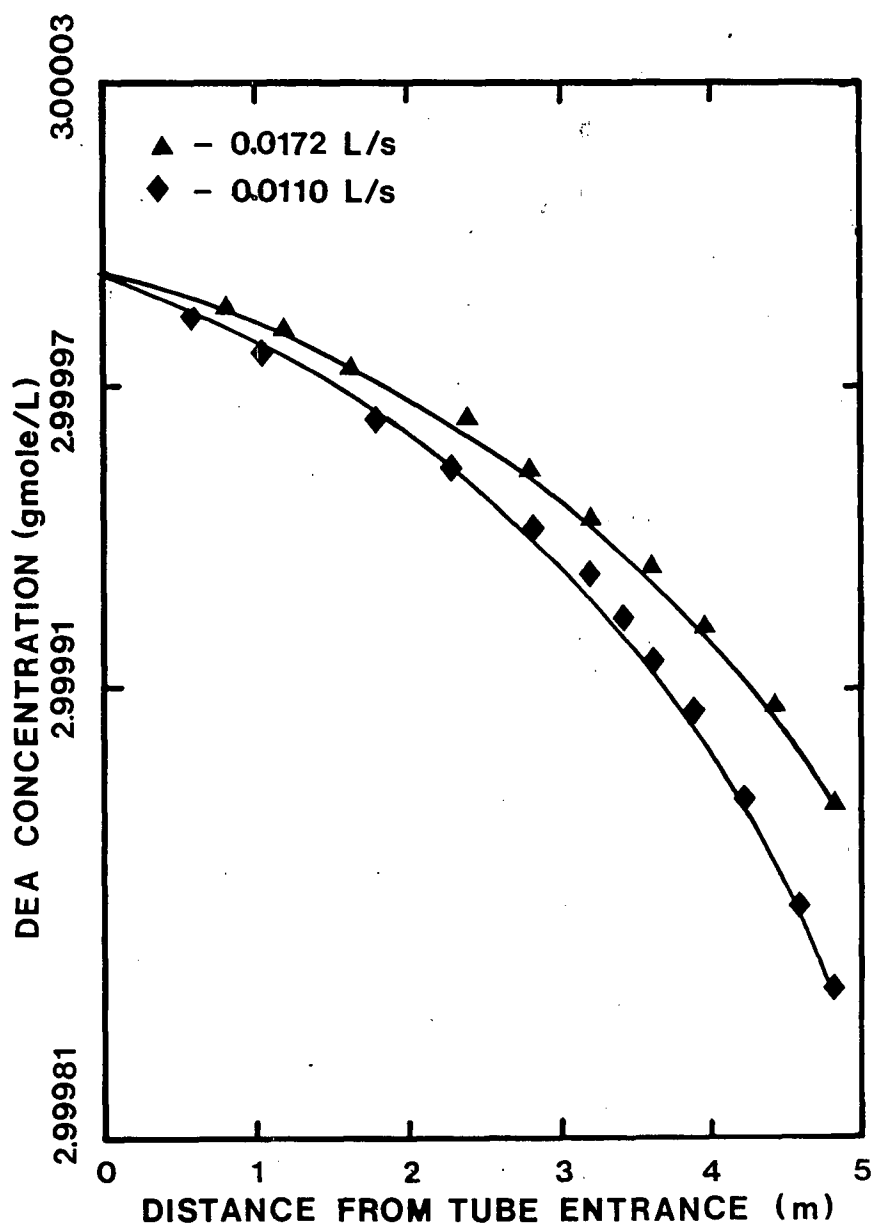


Figure 8.4 Model prediction of DEA concentration as a function of time and flow rate (single pass). (30 wt% DEA, inlet temp. 60°C, outlet temp. 170°C, CO<sub>2</sub> partial pressure 4.14 MPa)

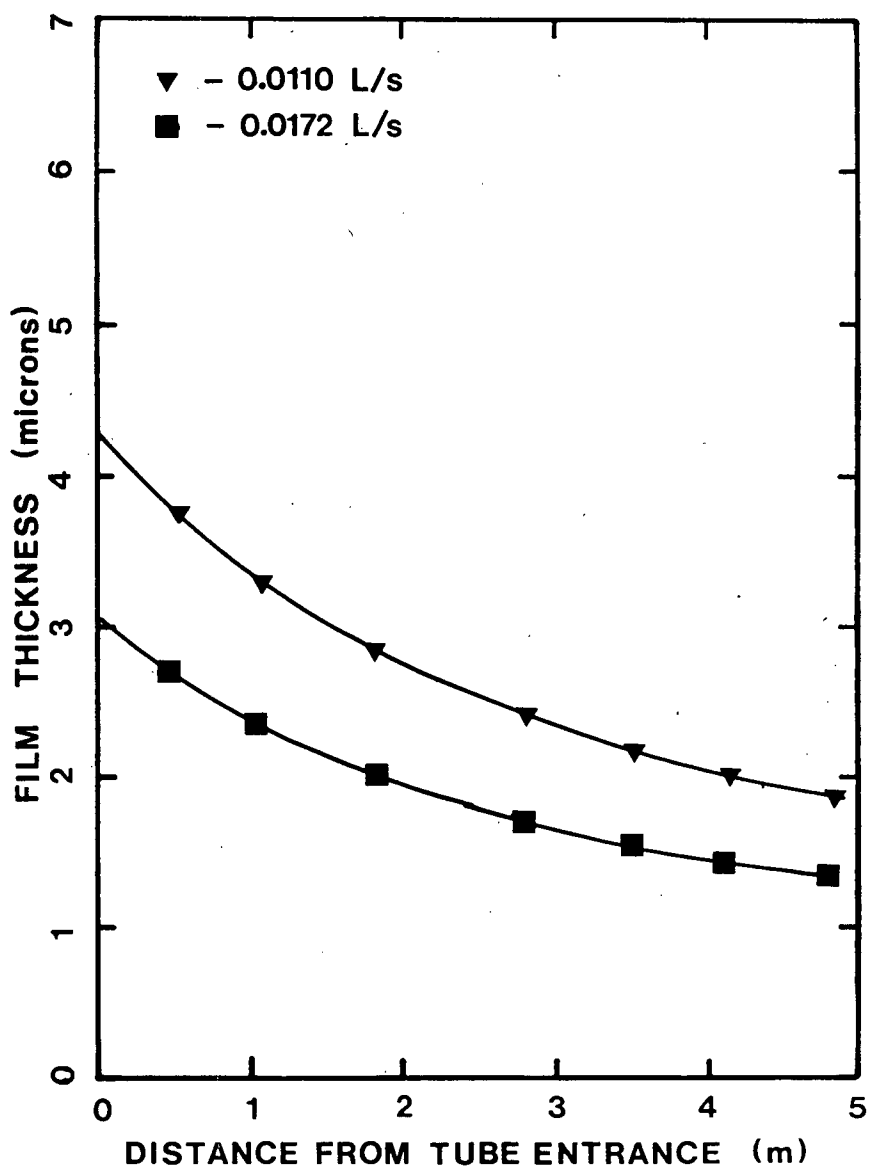


Figure 8.5 Model prediction of the film thickness as a function of the distance from the tube entrance and flow rate. (30 wt% DEA, inlet temp. 60°C, outlet temp. 170°C, CO<sub>2</sub> partial pressure 4.14 Mpa)

### 8.1.2 Effect of temperature

The rate of DEA degradation is known to be strongly dependent on temperature. DEA concentrations are plotted in Figure 8.6. as a function of time for three different heat transfer fluid temperatures. The flow rate was kept constant and the heat transfer tube outlet temperature was allowed to vary with the temperature of heat transfer fluid. As can be seen from Figure 8.6, the DEA concentration falls with increasing temperature. This is consistent with previous findings.

### 8.2.2 Effect of solution concentration

Three experiments were carried out with 20, 30 and 40 wt% DEA solutions at a constant flow rate of 0.011 L/s. These concentrations were chosen to reflect typical industrial conditions. Figure 8.7 shows the DEA concentration as a function of time for these experiments. It is clear from this figure that the degradation rate increases with the solution concentration. Since the temperature of the solution varied along the heat transfer tube, it was not possible to calculate the rate of degradation accurately. However for comparison purposes, average values of degradation rates were calculated using initial and final DEA concentrations and are presented in Table 8.11.

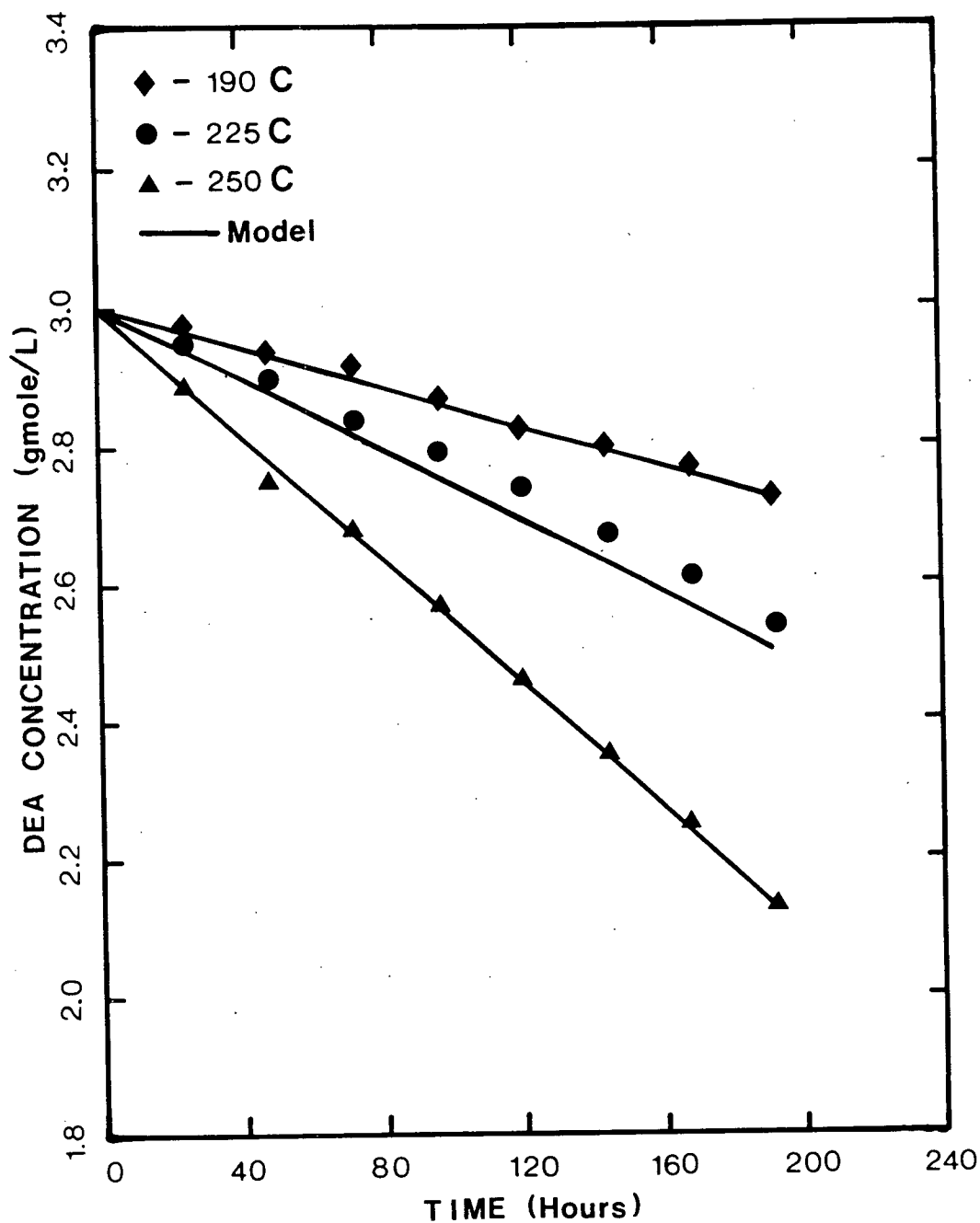


Figure 8.6 DEA concentration as a function of time, and heating fluid temperature. (30 wt% DEA, flow rate 0.011 L/s, inlet temp. 60°C, cO<sub>2</sub> partial pressure 4.14 Mpa)

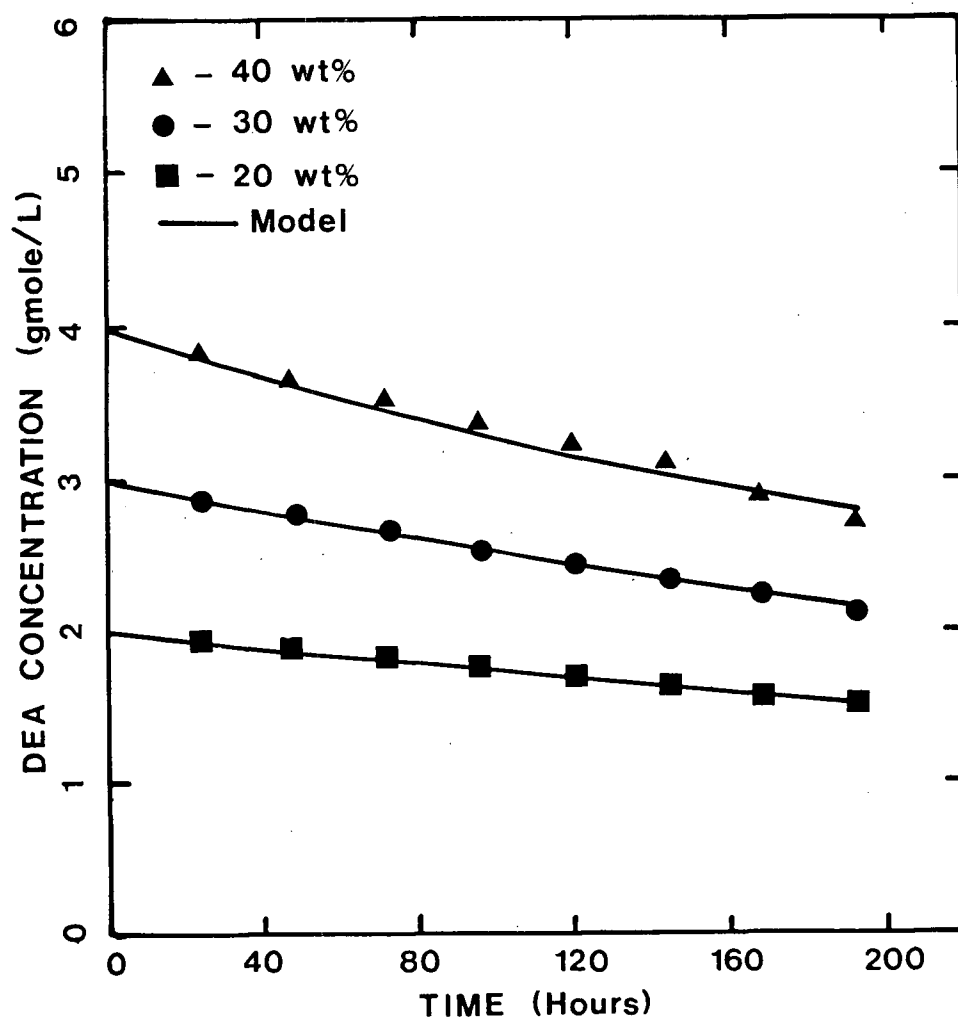


Figure 8.7 DEA concentration as a function of time and initial DEA concentration. (Inlet temp. 60°C, outlet temp. 195°C, heating fluid temp. 250°C, flow rate 0.011 L/s, CO<sub>2</sub> partial pressure 4.14 MPa)

Table 8.11 Average degradation rates. (Inlet temp. 60 C, outlet temp. 195 C, heating fluid temp. 250 C, flow rate 0.011 L/s)

Solution conc.	Degradation rate
wt%	moles/(L hr)
20	0.0025
30	0.0045
40	0.0065

The increase in degradation rate may be explained in terms of higher solution strength and CO<sub>2</sub> dissolved in the DEA solution. The higher the DEA concentration, the higher the alkalinity and consequently the quantity of CO<sub>2</sub> dissolved in the DEA solution. For example, at 100°C and a CO<sub>2</sub> partial pressure of 690 kPa, the CO<sub>2</sub> concentration in 3.5 N (30 wt%) DEA is 1.883 N (0.538 mole CO<sub>2</sub>/mole DEA) as compared to 1.290 N (0.490 mole CO<sub>2</sub>/mole DEA) of 2 N (20 wt%) DEA [82]. At higher solution concentrations, more CO<sub>2</sub> is dissolved in the solution and this causes the degradation rate to rise.

#### 8.2.4 Effect of CO<sub>2</sub> partial pressure

Experiments using 30 wt% DEA at 4137, 2758, and 1379 kPa of CO<sub>2</sub> partial pressures were carried out in order to study their effect on degradation. The DEA concentrations for these three runs are plotted in Figure 8.8 as a function of time.

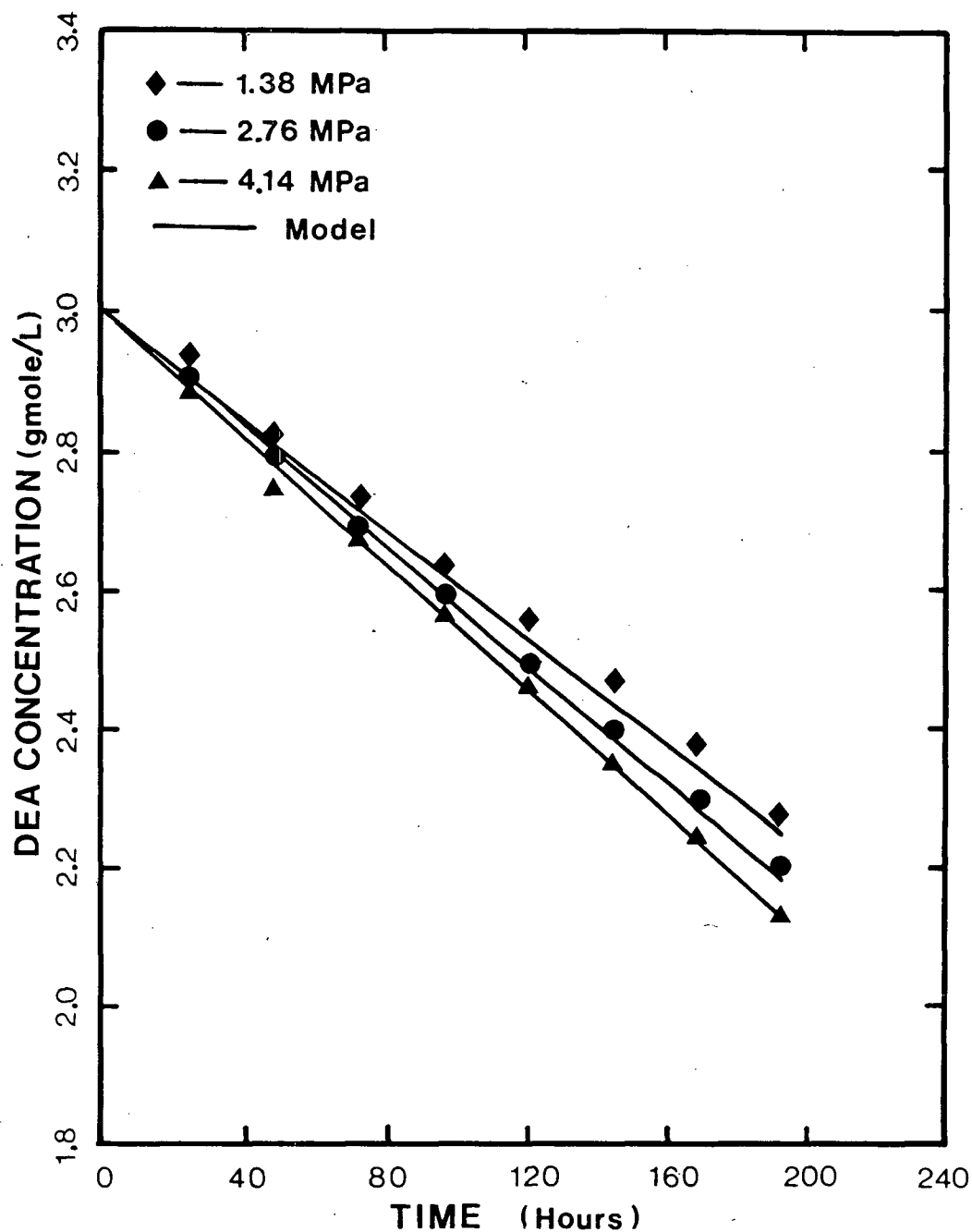


Figure 8.8 DEA concentration as a function of time and CO<sub>2</sub> partial pressure. (30 wt% DEA, inlet temp. 60°C, outlet temp. 195°C, heating fluid temp. 250°C, flow rate 0.011 L/s)



As expected, the degradation rate was found to increase with  $\text{CO}_2$  partial pressure. Again this increase can be attributed to the increase in dissolved  $\text{CO}_2$  in the DEA solutions at higher  $\text{CO}_2$  partial pressures.

### 8.3 EFFECT OF DEGRADATION ON SOLUTION VISCOSITY

The accumulation of degradation products increases the viscosity of DEA solutions. The viscosity changes of typical runs are shown in Figure 8.9. Although the viscosity increase is not very significant (4 to 12% of the initial solution viscosity), if left unattended, it might have some very serious consequences on plant performance such as unsatisfactory operation or higher power consumption by the DEA solution pumps. It also decreases the heat transfer coefficient of the heat exchangers. Furthermore mass transfer co-efficients decrease with viscosity. Therefore, viscosity increases will likely result in poor performance of the  $\text{CO}_2$  absorber in industrial facilities.

### 8.4 EFFECT OF DEGRADATION ON SOLUTION FOAMING

In order to determine whether degradation has any effect on solution foaming, foaming tests as described in Chapter 6 were carried out. The results are presented in Table 8.12.

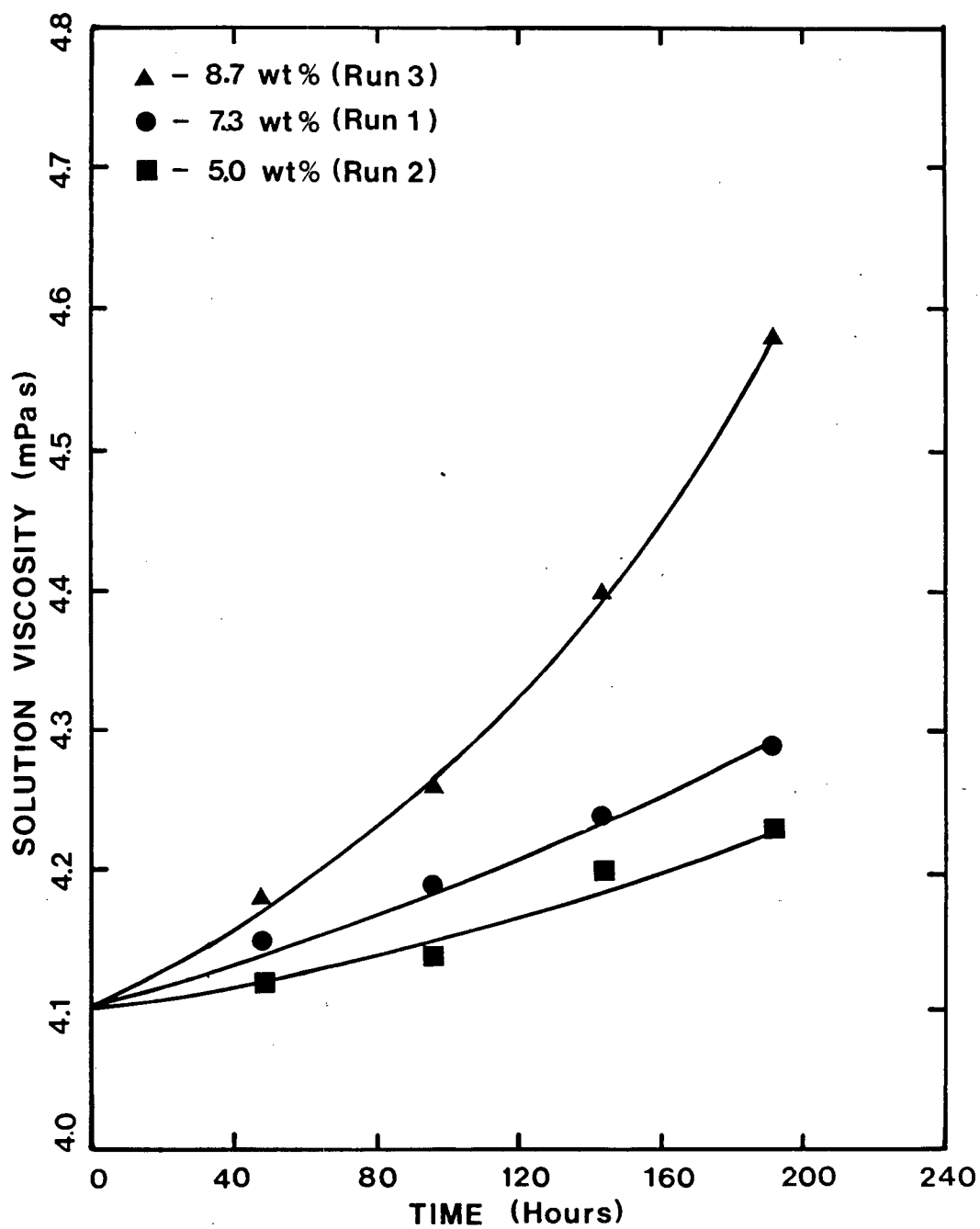


Figure 8.9 Solution viscosity as a function of time and degradation product concentration.

Table 8.12 Results of foaming tests with 30 wt% DEA

Sample description	Foam height mL	Foam breakdown time (s)
0.0 wt% degraded DEA	40	5
5.0 wt% degraded DEA	50	30
7.3 wt% degraded DEA	80	70
8.7 wt% degraded DEA	100	100

As can be seen from the results, accumulation of degradation products increases the foaming tendency of the solution. However, it was not possible to determine which degradation compound(s) are primarily responsible for foaming

#### 8.5 EFFECT OF DEGRADATION ON SOLUTION pH

When DEA degrades, the concentration of DEA in the solution decreases and the concentration of degradation products increases. The alkalinity of the two principal degradation compounds (BHEP and THEED) is lower than that of DEA and is equivalent to TEA [41]. Therefore, as DEA degrades, the pH of the solution decreases. Furthermore, formation of other degradation compounds is also partly responsible for the decrease in pH of the DEA solution. Hall and Barron [53]

presented industrial data showing a gradual reduction in solution pH with the formation of heat stable salts. These heat stable salts are formed as a result of neutralization of carboxylic acids with DEA [45] thereby reducing the basicity of the solution.

These findings are confirmed by the experimental results obtained from degradation experiments in which the solution pH was measured as a function of time. (see, for example, Figure 8.10) The initial sharp drop in pH can be attributed to the absorption of  $\text{CO}_2$ . The gradual decrease thereafter represents the loss of basicity due to the loss of DEA accompanied by the formation of less basic degradation products BHEP and THEED.

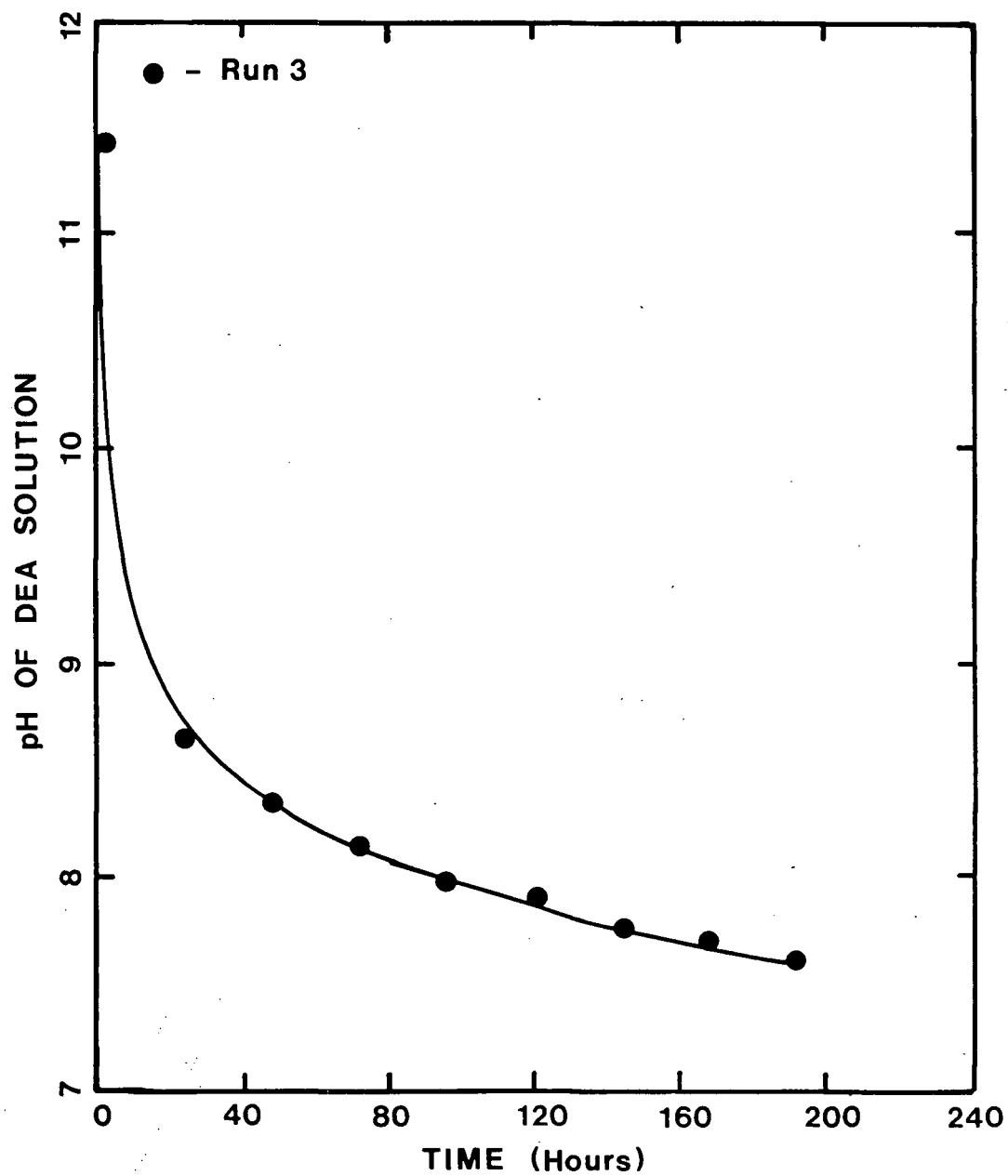


Figure 8.10 Typical pH change of partially degraded DEA solution as a function of time.  
(30 wt% DEA, inlet temp. 60C, outlet temp. 195C, heating fluid temp. 250C, flow rate 0.011 L/s)

## 8.6 HEAT EXCHANGER FOULING

Heat exchanger fouling creates a resistance to flow which results in increased pressure drops. Therefore pressure drop measurements can provide information on fouling. In order to study the effect of solution degradation on fouling of heat exchangers, the pressure drop across the heat exchanger coil was recorded for each run.

### 8.6.1 Effect of temperature

The temperature of the hot heat transfer fluid seems to influence the fouling rate. In three different runs performed at the same flow rate (0.011 L/s), the hot fluid temperature was varied and the outlet temperature was allowed to change accordingly. Figure 8.11 shows the pressure drop as a function of time for these three runs. As can be seen from Figure 8.11, the fouling rate rises with increasing temperature and reaches a constant value in each case. All these runs were carried out in the turbulent region, where viscous forces play a minor role. Therefore, in spite of slight viscosity increases as a result of solution degradation, the increase in pressure drop can be attributed mostly to fouling.

Fouling may increase the pressure drop by reducing the effective tube diameter due to scale formation and also by increasing the surface roughness of the tube.

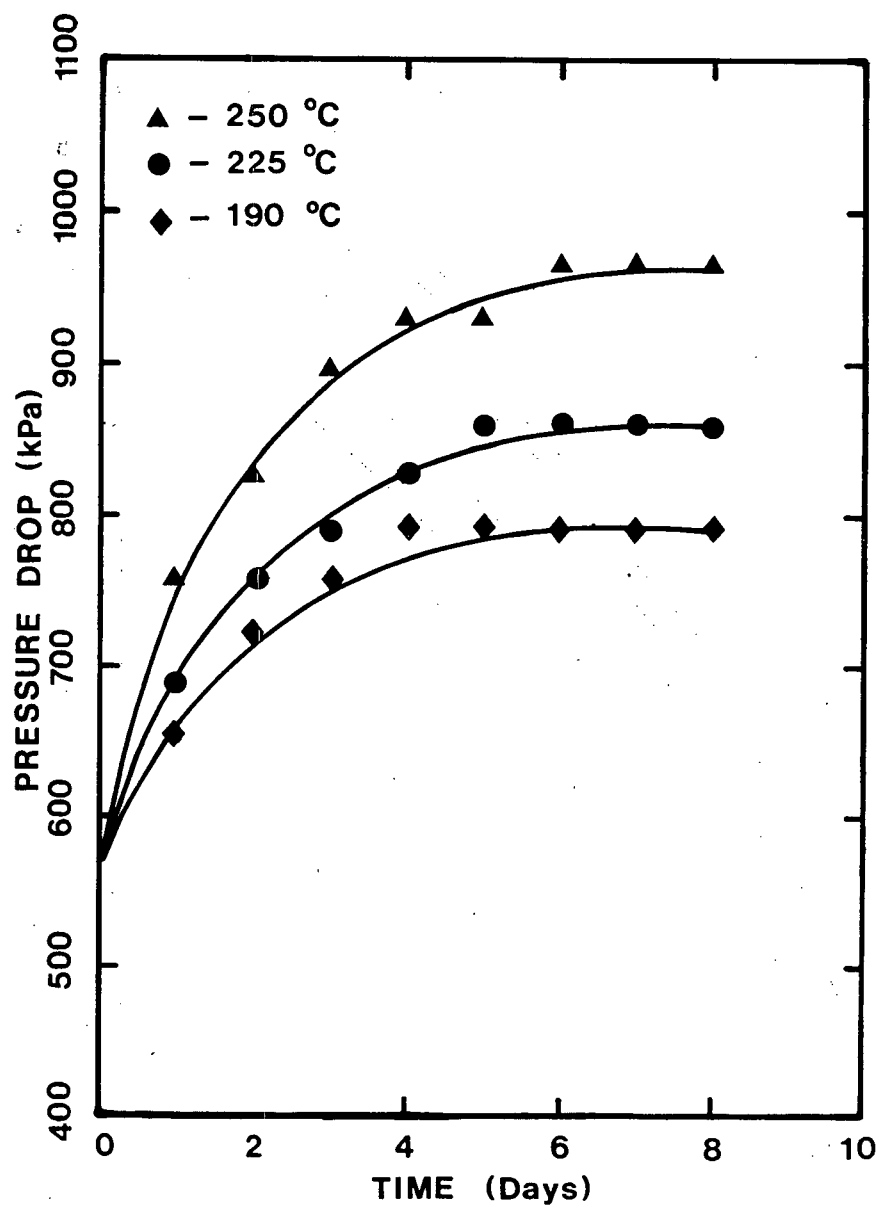


Figure 8.11 Pressure drop as a function of time and heating fluid temperature. (30 wt% DEA, inlet temp. 60°C, heating fluid temp. 250°C, flow rate 0.011 L/s, CO<sub>2</sub> partial pressure 4.14 MPa)

Electron micrographic photos of the surfaces of an uncontaminated and a contaminated tube section are shown Figure 8.12. Figure 8.13 show the electron micrographic photos of a cross section of the contaminated tube and a magnified view (400 x), of the fouling scale.

#### 8.6.2 Electron microprobe analysis

Electron microprobe analysis of the fouled heat exchanger surface revealed the presence of aluminum in the fouling scale. However, the source of aluminum could not be determined. It should be noted that no aluminum was used in the flow circuit. Electron microprobe plots of the contaminated and uncontaminated surfaces are shown in Figure 8.14.

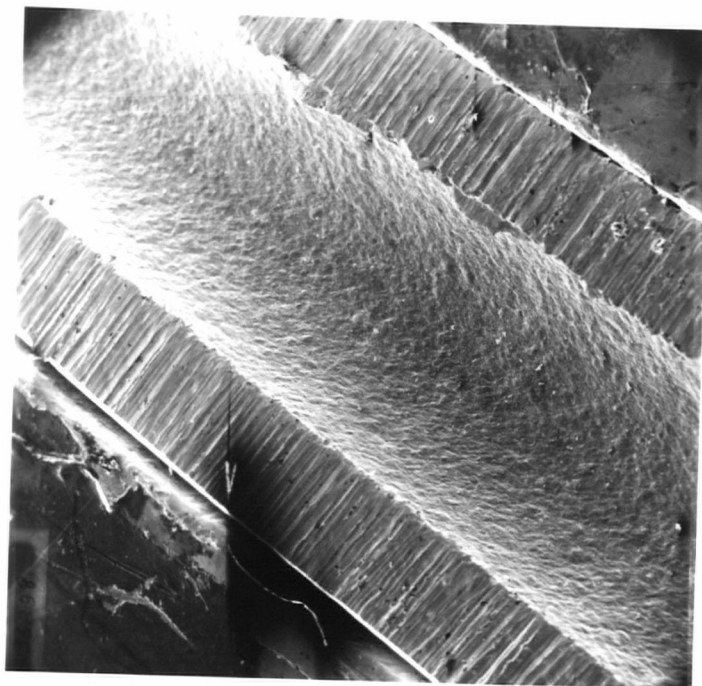
#### 8.6.3 Apparent deposit thickness

Apparent deposit thickness was calculated from the pressure drop data. It was assumed that the increase in the pressure drop was only due to the decrease in the effective tube diameter as a result of scale formation. Deposit thicknesses are plotted in Figure 8.15 as a function of time.

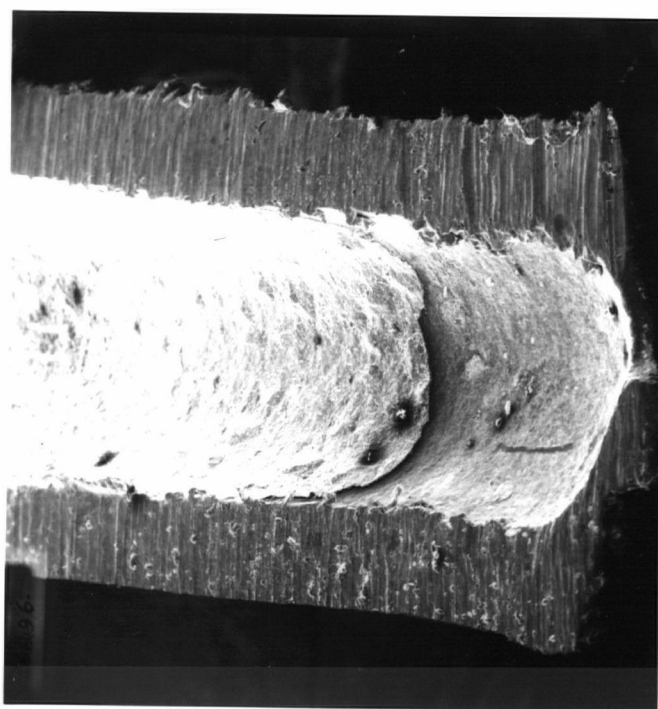


## 8.7 EXPERIMENT WITH A NEW TUBE

Run 1 (30 wt% DEA, inlet temp. 60°C, outlet temp. 190°C, flow rate 0.0124 L/s, heating fluid temp. 250°C and CO<sub>2</sub> partial pressure 4137 kPa) was repeated using a new uncontaminated tube of same dimension (4.80 m long, 3.175 mm OD, 2.032 mm ID and a turning radius of 0.4064 m). Degradation as well as pressure drop data matched accurately with the previous results.



a) Uncontaminated



b) Contaminated

Figure 8.12 Electron micrographic photos of the uncontaminated and contaminated surfaces of the heat exchanger tube. (20 x)

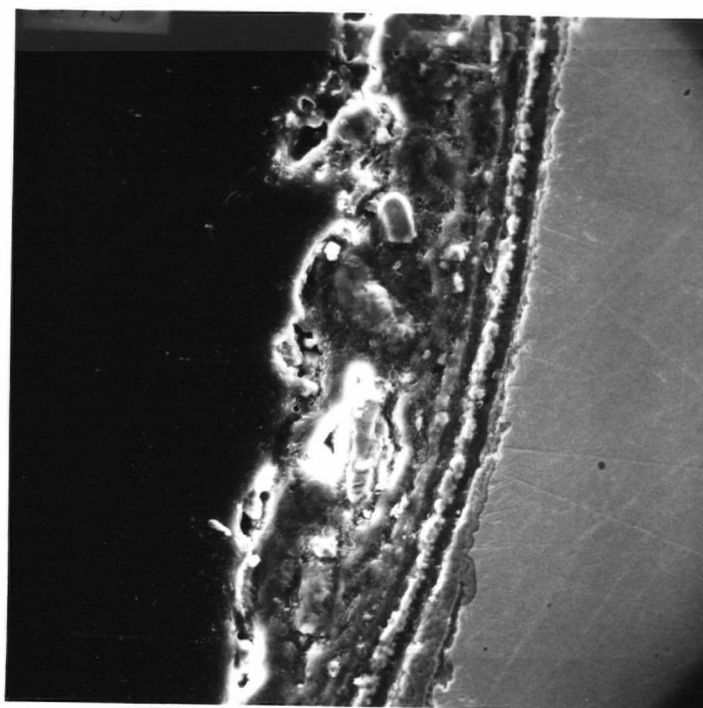
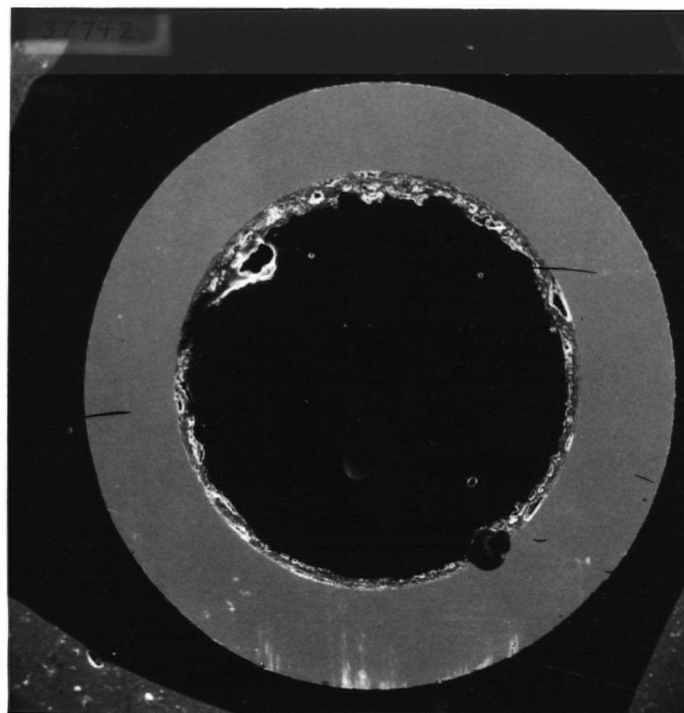


Figure 8.13 Electron micrographic photos of the fouled surface of the heat exchanger tube (20 x) and a magnified view (400 x) of the same surface

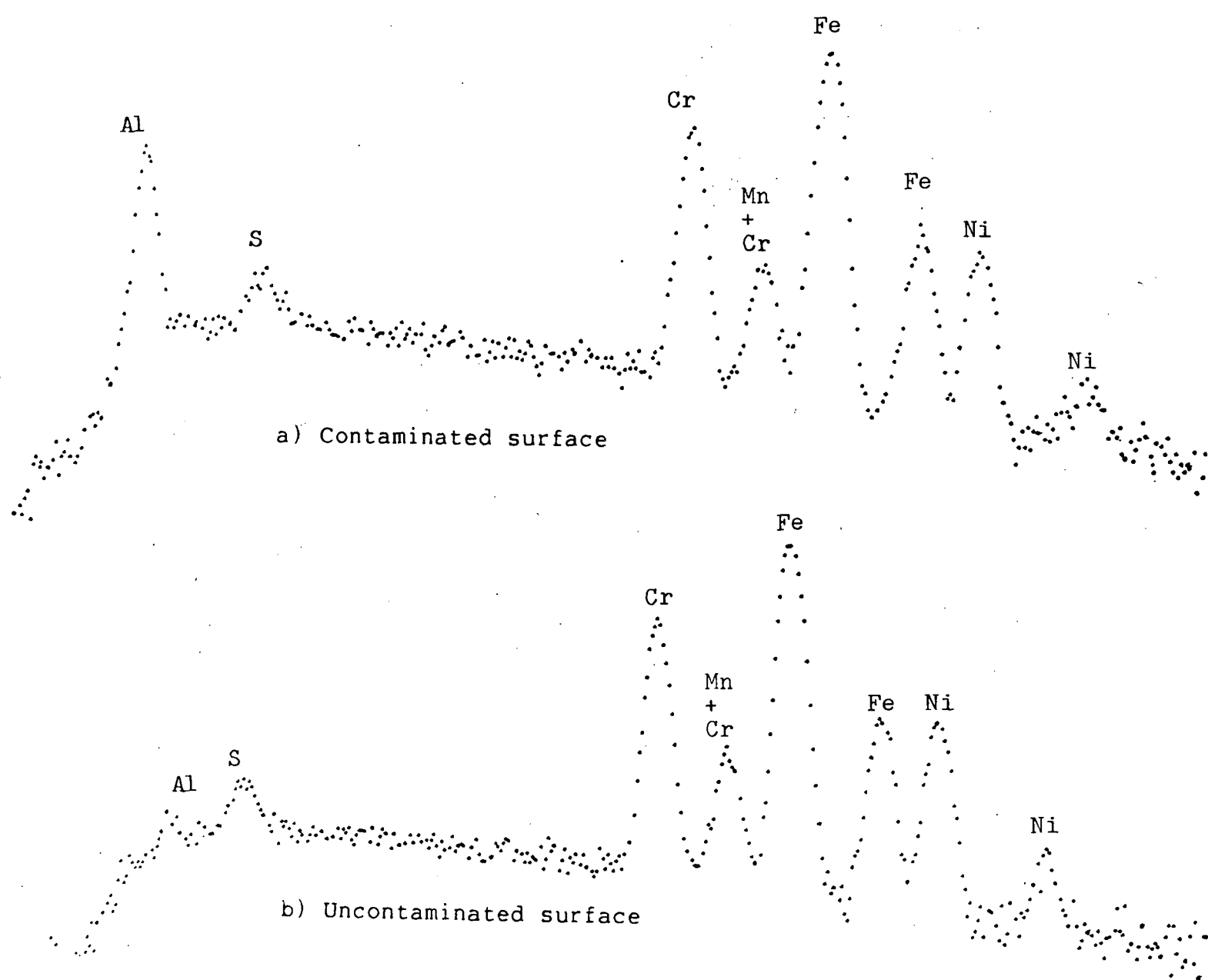


Figure 8.14 Electron microprobe plots of the contaminated and uncontaminated surfaces of the heat exchanger tube.

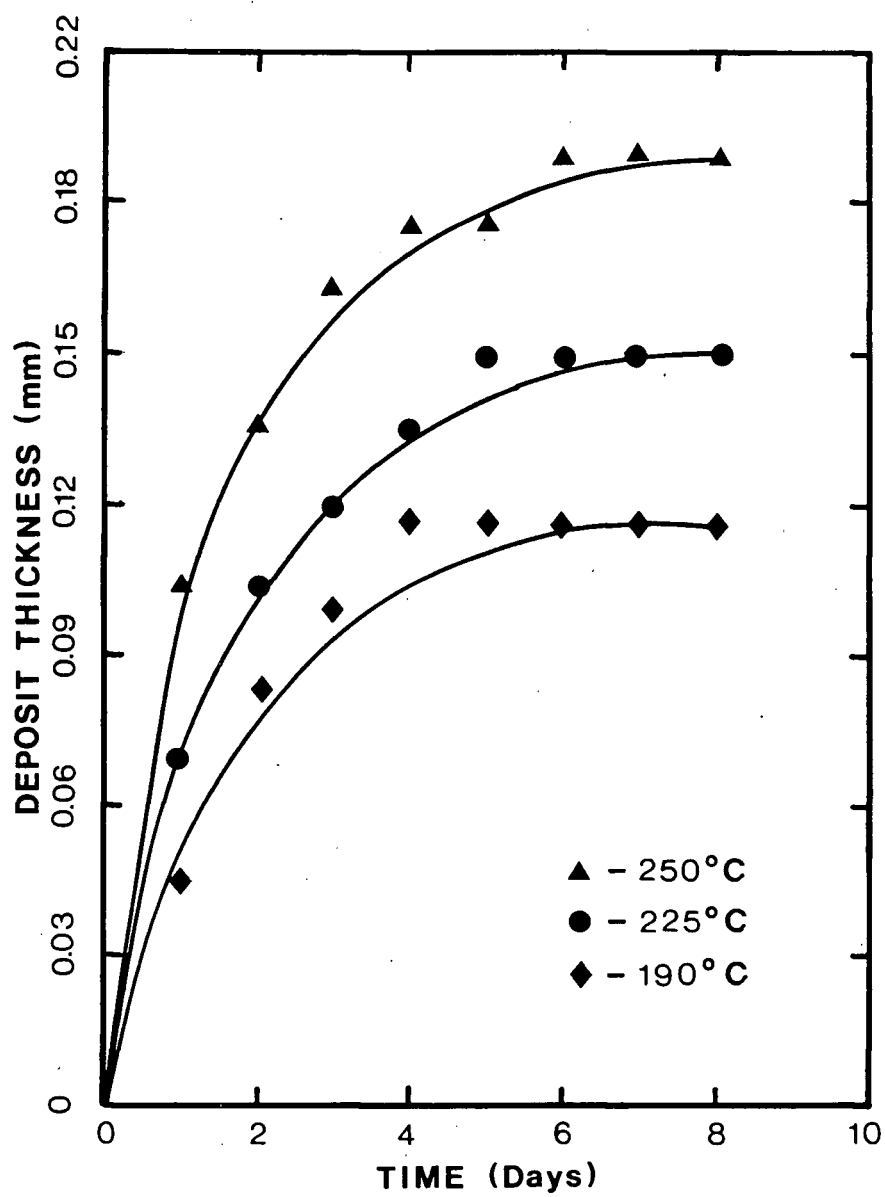


Figure 8.15 Apparent deposit thickness as a function of time and heating fluid temperature.  
(30 wt% DEA, inlet temp. 60°C, flow rate 0.011 L/s)

## CHAPTER 9

RESULTS AND DISCUSSION OF CORROSION STUDIES9.1 CORROSION RATE IN UNDEGRADED DEA SOLUTIONS

The corrosion rate of carbon steel in the un-degraded solution, as determined by potentiodynamic test (see Figure 9.1), was 0.06 mm/year (2.46 mpy), This is quite close to the corrosion rate of 0.05 mm/year (2 mpy) obtained by Blanc et al. [45] in one of their tests using the Fe-H<sub>2</sub>S-DEA system. The corrosion rates are practically the same. It should be noted that CO<sub>2</sub> was not used in their corrosion tests. Since H<sub>2</sub>S is known to inhibit DEA degradation [43], their DEA solution, which was saturated only with H<sub>2</sub>S, did not degrade noticeably.

9.2 CORROSION RATES IN DEGRADED DEA SOLUTIONS

A degraded sample of DEA solution containing about 8.7 % degradation products yielded a corrosion rate of 0.4 mm/year (16.1 mpy), about 6.5 times higher than that of un-degraded solution. This indicates that degraded DEA solutions containing HEOD, THEED and BHEP are, in fact, corrosive towards carbon steel and thereby contradicts earlier claims [45].

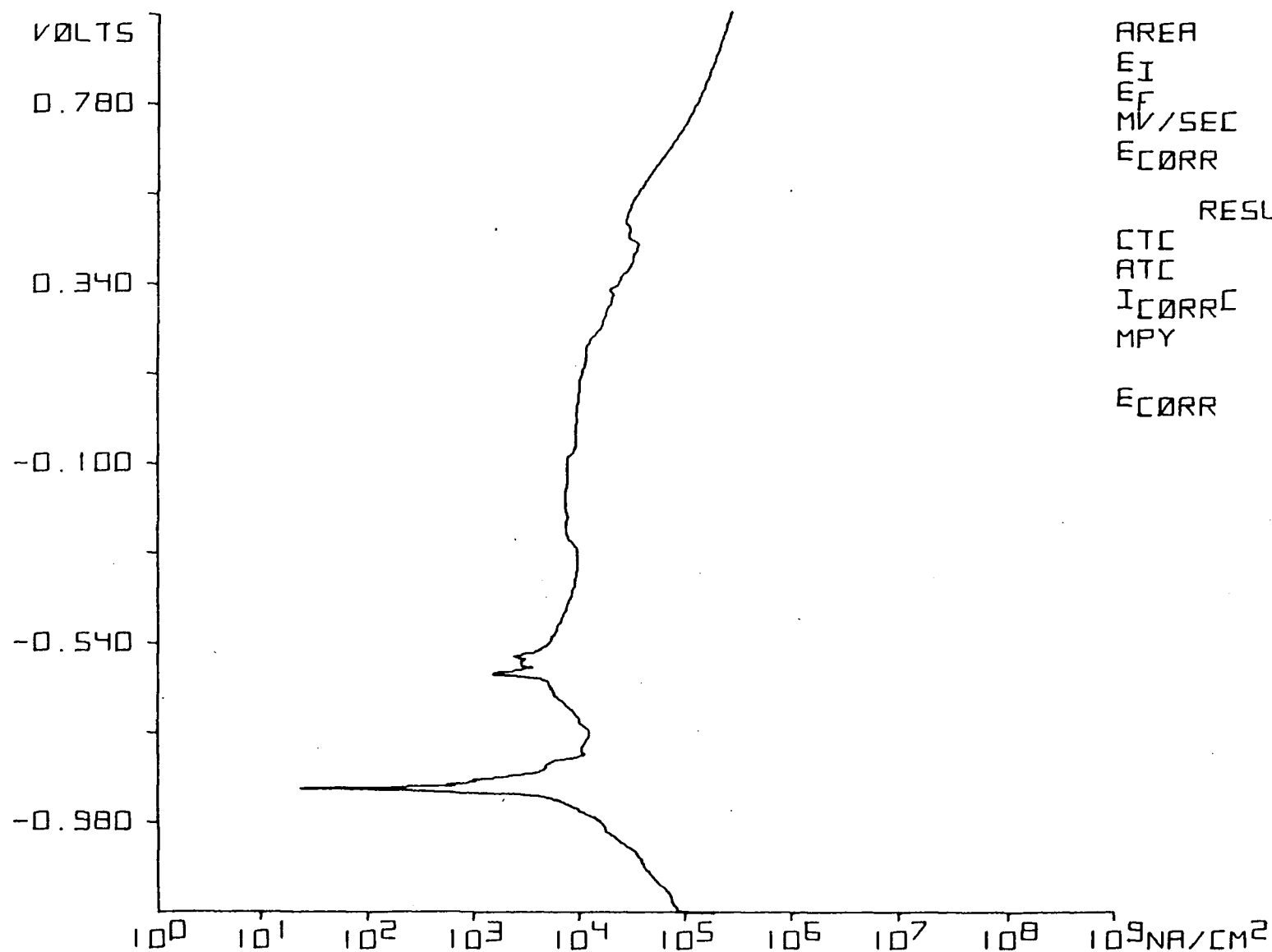
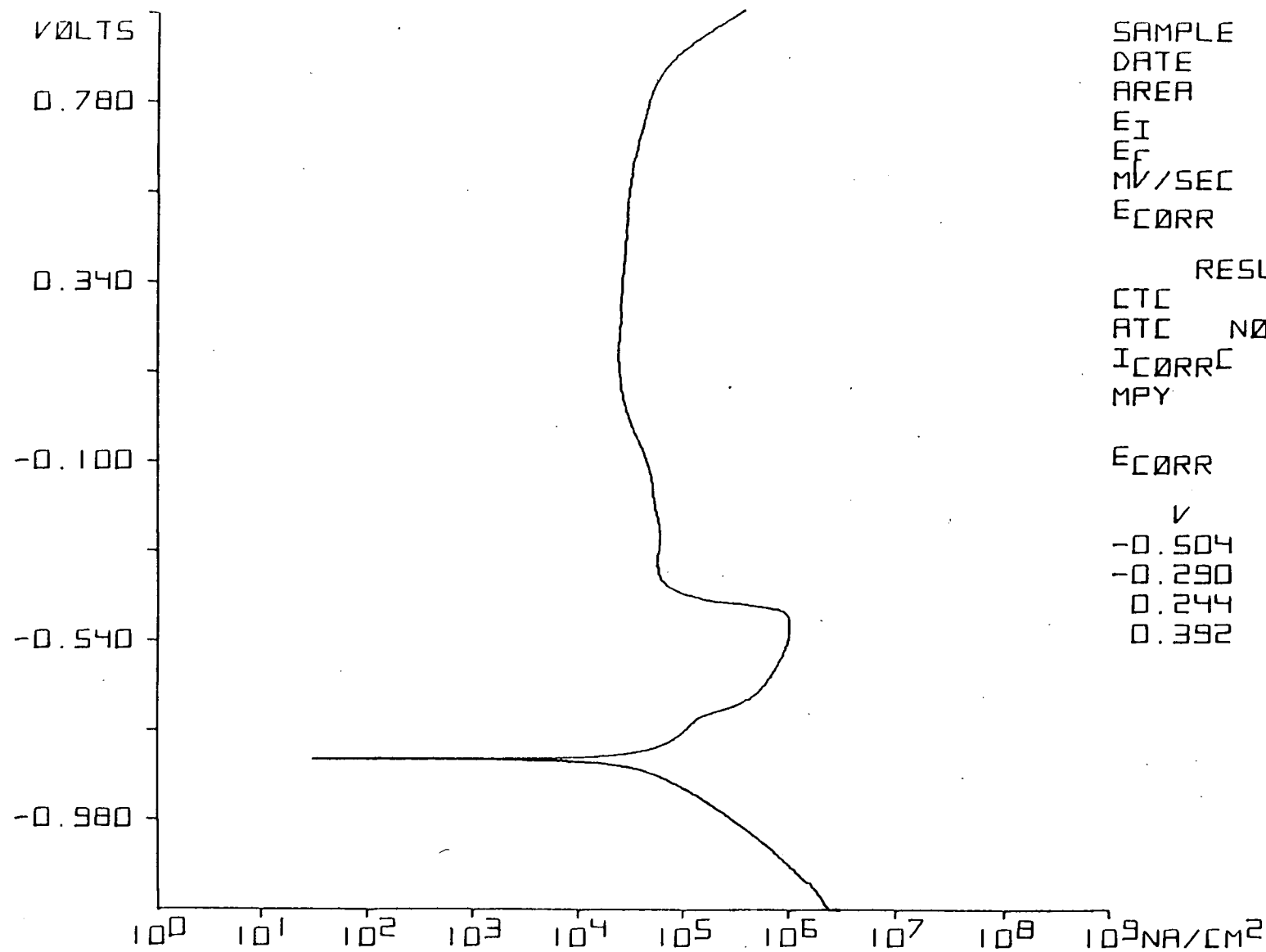


Figure 9.1 Potentiodynamic anodic polarization curve of 30 wt% undegraded DEA solution. (temp. 25 C)



SAMPLE 2  
 DATE 02.01  
 AREA 6.441  
 E<sub>I</sub> -1.200  
 E<sub>F</sub> 1.000  
 MV/SEC 1.000  
 E<sub>CORR</sub> -0.780

RESULTS  
 CTC 0.177  
 ATC NOT FOUND  
 I<sub>CORR</sub> 3.490E4  
 MPY 1.610E1  
 E<sub>CORR</sub> -0.832

V	NA/CM <sup>2</sup>
-0.504	9.984E5
-0.290	5.811E4
0.244	2.458E4
0.392	2.670E4

Figure 9.2 Potentiodynamic anodic polarization curve of 30 wt% partially degraded DEA solution containing 8.7 wt% degradation products. (Temp. 25C)



### 9.3 EFFECT OF CO<sub>2</sub> DISSOLVED IN DEA SOLUTIONS ON CORROSION

DEA solutions in the absence of CO<sub>2</sub> are not corrosive. However, when they are saturated with CO<sub>2</sub>, they become corrosive. This can be concluded from Table 9.1 by comparing the corrosion rates obtained with 40 wt% DEA solutions which are either free of or initially saturated with CO<sub>2</sub> at atmospheric pressure and 100 °C.

Table 9.1 Effect of CO<sub>2</sub> on corrosion rates

Sample	Corrosion rates	
	mm/year	mils/year
40 wt% DEA	0.003	0.1
40 wt% DEA + CO <sub>2</sub>	1.840	72.32

#### 9.4 EFFECT OF SOLUTION CONCENTRATION

When DEA contains  $\text{CO}_2$ , the corrosion rate increases with the DEA concentration. Weight loss results conducted at various DEA concentrations are presented in Table 9.2. They clearly indicate that the corrosion rate increases with DEA concentration.

Table 9.2 Effect of DEA concentration on corrosion rates

Sample	Corrosion rates	
	mm/year	mils/year
30 wt% DEA + $\text{CO}_2$	1.60	63.1
40 wt% DEA + $\text{CO}_2$	1.840	72.32
60 wt% DEA + $\text{CO}_2$	2.070	81.60

#### 9.5 EFFECT OF SOLUTION pH ON CORROSION

Pourbaix potential-pH diagram for Fe- $\text{H}_2\text{O}$  system [60] can provide qualitative information on the effect of pH on corrosion. As seen from Figure 2.2, there exist two distinct regions of corrosion, one at pH greater than 13 and the other at pH lower than 9. At intermediate pH values, the corrosion rate would be minimal due to the formation of metal oxide on the surface.

Therefore, any decrease in solution pH, tends to lead the system gradually towards the corrosion region and therefore increases the corrosion rate. As discussed in Chapter 8, the pH of DEA solutions initially decrease rapidly as a result of CO<sub>2</sub> absorption and thereafter drop gradually due to the formation of degradation products. Therefore, solutions are expected to become more corrosive as degradation occurs.

#### 9.6 EFFECT OF INDIVIDUAL DEGRADATION PRODUCTS

After noticing the corrosive nature of degraded DEA samples, it was desirable to identify which degradation products are primarily responsible for corrosion of carbon steel. Weight loss tests were carried out with different aqueous solutions containing HEOD and BHEP separately as well as with mixtures of DEA plus HEOD and DEA plus BHEP. Table 9.3 summarizes the results of these weight loss tests.

Table 9.3 Effect of individual degradation compound on corrosion

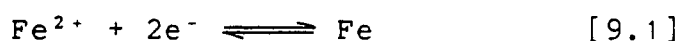
Sample	Corrosion rates	
	mm/year	mils/year
15 wt% DEA + CO <sub>2</sub>	0.13	5.1
15 wt% BHEP + CO <sub>2</sub>	0.16	6.3
15 wt% HEOD + CO <sub>2</sub>	1.95	76.6
30 wt% DEA + CO <sub>2</sub>	1.60	63.1
30 wt% DEA + 5 wt% BHEP + CO <sub>2</sub>	1.57	62.0
30 wt% DEA + 5 wt% HEOD + CO <sub>2</sub>	1.91	75.0

The corrosion rate in the solution containing DEA and BHEP, is slightly lower than that of DEA alone. This indicates the non-corrosive nature of BHEP in DEA solutions and is in agreement with the findings of Blanc et al. [45]. However, BHEP solutions (on a constant weight basis) are more corrosive than DEA on its own. This can be seen by comparing the weight loss data for 15 wt% DEA and 15 wt % BHEP solutions, respectively. This is also in agreement with the findings of Hakka et al. [41].

The corrosion rates in the solution containing DEA plus HEOD were higher than those containing DEA alone and DEA plus BHEP. This indicates the corrosive nature of HEOD.

## 9.7 EFFECT OF METAL COMPLEXING

Aqueous DEA solutions can be regarded as mixtures of ionised species in equilibria, consisting mainly of  $H^+$ ,  $OH^-$ ,  $HCO_3^-$ ,  $R_2NCOO^-$ , as well as  $CO_2$  and  $R_2NH^+$  [51]. Among the above mentioned species,  $OH^-$ ,  $HCO_3^-$ ,  $R_2NCOO^-$  and  $R_2NH^+$  are capable of forming metal complexes with carbon steel. Major DEA degradation products, HEOD and THEED are also likely to form metal complexes. Other contaminants, such as hydrazine, cyanides, sulphides, etc., if present, may also act as complex forming ligands. Comeaux [57] reported the formation of iron chelates with polyamines such as ethylenediamine, N-(Hydroxyethyl)-Ethylenediamine etc. (A chelate is a complexing agent which attaches to a metal ion at more than one point). Hall and Barron [53] reported the presence of iron chelates, which tie up iron, in industrial DEA solutions. Considering the presence of all these species with complex forming abilities in degraded DEA solutions, it is very likely that metal complexes of one kind or another are produced with the metal ions in the solution. The main effect of complexing is the reduction of the potential of the metal-ion/metal equilibrium represented by the following reaction :



The reduction in this equilibrium potential enlarges the corrosion regions in the potential-pH diagram.

Formation of metal complexes stabilises metal ions in the solution, and therefore, results in an increase in the solubility of the metal. It may also promote breakdown of passive films; the extent of the breakdown depends on the concentration of the complexes in solution.

## 9.8 PASSIVITY

An examination of polarization curves for both the undegraded and the degraded samples (see, Figure 9.1 and 9.2, respectively), indicates that although regions of passivity do exist over a wide potential range, they are not quite stable. Particularly in the case of undegraded DEA (see Figure 9.1), the film seem to be very unstable. More important is that the corrosion current in the passive region is very close to the critical corrosion current and consequently does not provide adequate protection. Therefore, the idea of maintaining lower solution velocities, in order to protect the protective passive film on the metal surface is questionable. However, there are other factors, such as acid gas break out, to be considered in this respect.

## 9.9 PITTING

The pitting potential of undegraded DEA solutions was not found to be very distinct (see Figure 9.1). However, in the case of degraded DEA solutions, the pitting potential is clearly visible. This seems to indicate that degraded DEA solutions might induce pitting corrosion under certain conditions. Electron micrographic photos of the test coupons used in different corrosion tests, in fact show pitting very clearly (see Figures 9.3 to 9.6 respectively). Pitting is most severe in the case of the test coupon immersed in HEOD. Intragranular corrosion is also evident. A 2000 x magnification of a pit area is shown in Figure 9.7.



Figure 9.3 Electron micrographic photo of an uncorroded AISI 1020 carbon steel test coupon. (400x)



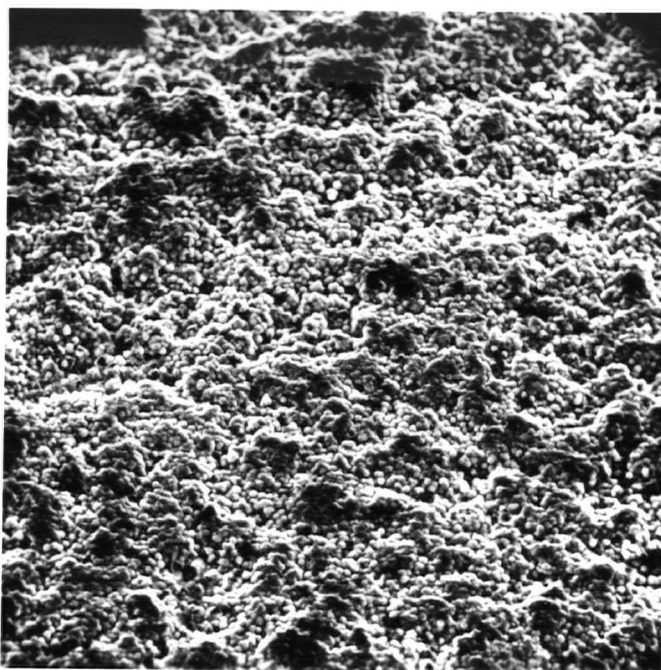


Figure 9.4 Electron micrographic photo of AISI 1020 carbon steel test coupon after 120 hr immersion in 15 wt% DEA solution at 100 C. (400x)

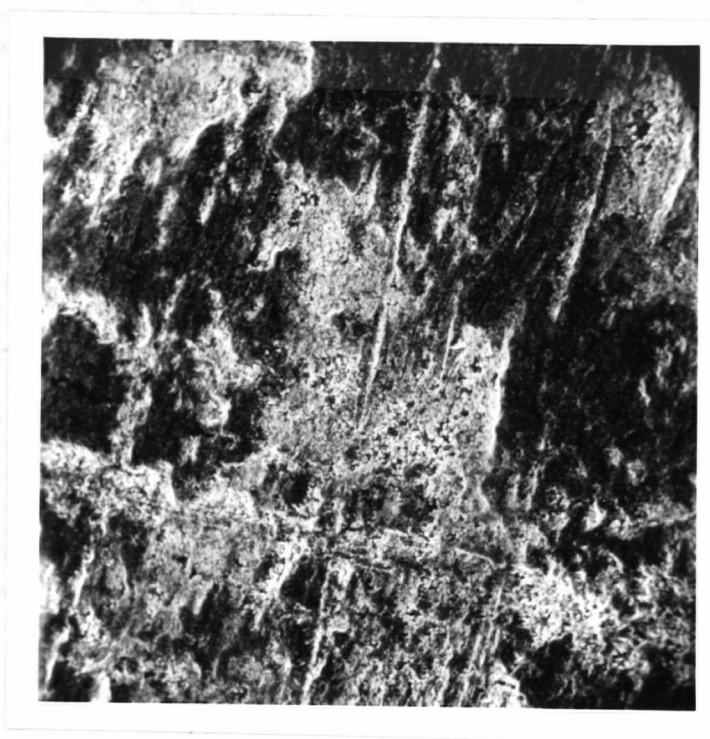


Figure 9.5 Electron micrographic photo of AISI 1020 carbon steel test coupon after 120 hr. immersion in 15 wt% BHEP solution at 100 C. (400x)



Figure 9.6 Electron micrographic photo of AISI 1020 carbon steel test coupon after 120 hr. immersion in 15 wt% HEOD solution at 100 C. (400x)

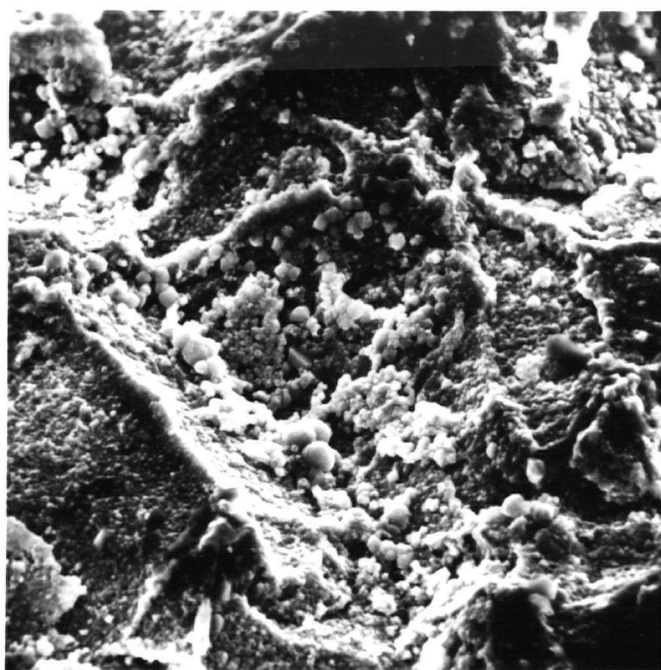


Figure 9.7 Electron micrographic photo of a pit area of AISI 1020 carbon steel test coupon after 120 hr. immersion in 15 wt% HEOD solution at 100 C. (2000x)

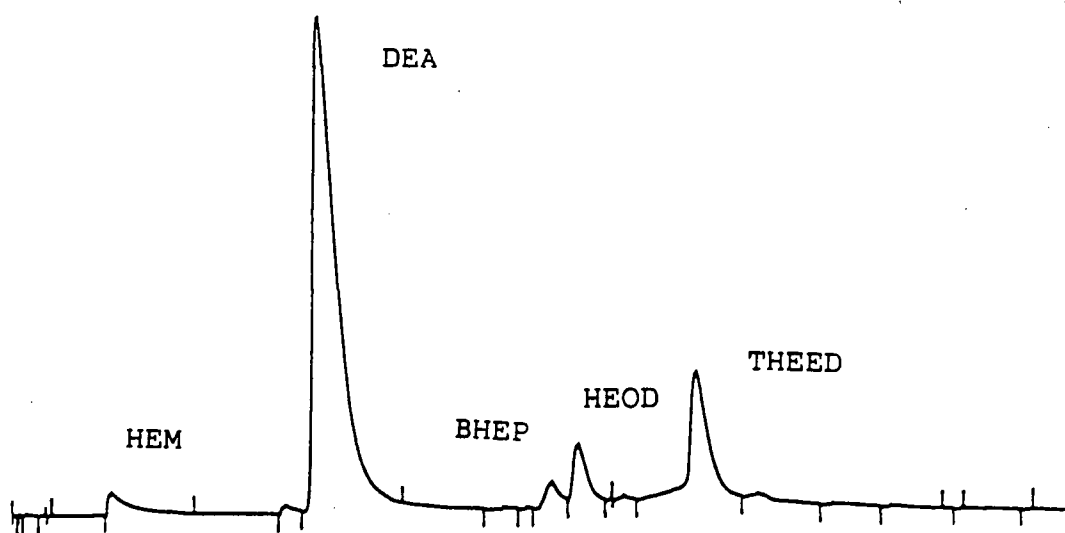
## CHAPTER 10

PURIFICATION OF DEGRADED DEA SOLUTIONS

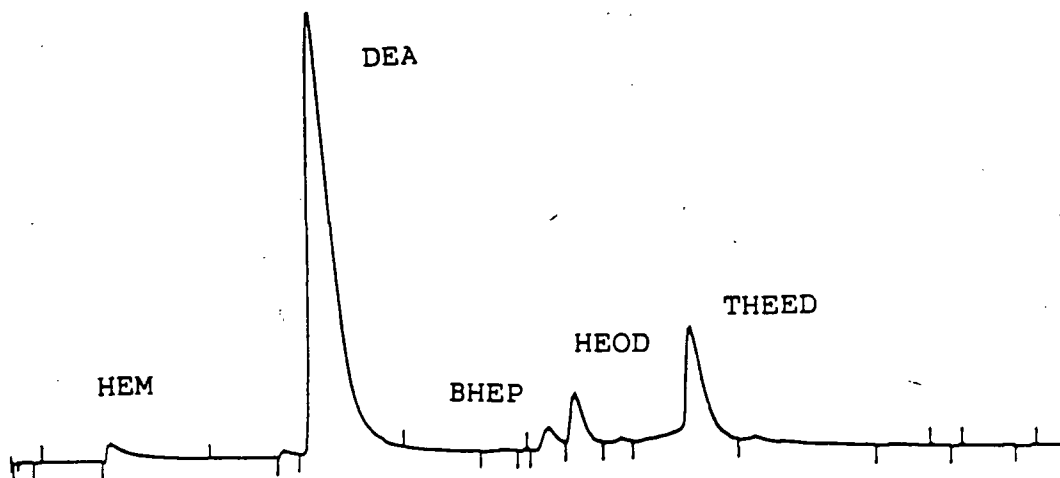
Unlike MEA, degraded DEA solutions can not be purified by distillation at atmospheric pressure. The reason for this is that DEA and its degradation products have similar vapor pressures.

10.1 USE OF CARBON FILTERS

Activated carbon filters are widely used to purify degraded DEA solutions. They can remove suspended solids, heavy hydrocarbons and probably some of the heat stable salts [51]. Although their successful operation has been reported by several authors [12,15,16], Meisen and Kennard's limited laboratory tests indicated that activated carbon filters do not remove any major DEA degradation compounds. Chromatograms of DEA samples taken upstream and downstream of activated carbon filters in a gas treating plant located in Alberta are shown in Figure 10.1. These chromatograms also confirm that none of the major DEA degradation products were removed by the activated carbon filter.



a) Sample taken upstream of filter



b) Sample taken downstream of filter

Figure 10.1 Chromatograms of partially degraded DEA samples taken upstream and downstream of an activated carbon filter located in a gas plant in Alberta.

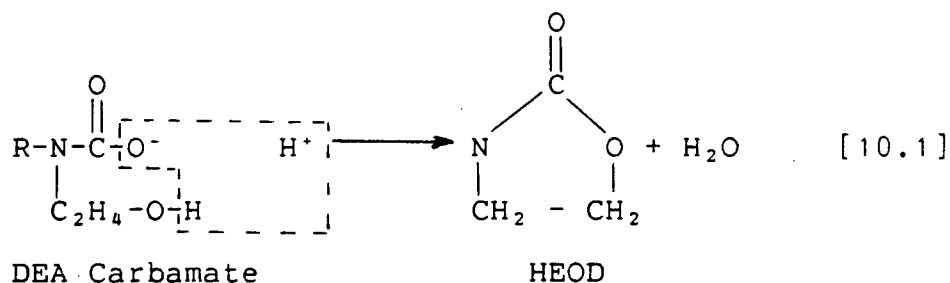
## 10.2 USE OF CHEMICALS

Scheirman [15] reported the use of soda ash ( $\text{Na}_2\text{CO}_3$ ) for the removal of heat stable salts. He also suggested the possible use of sodium hydroxide ( $\text{NaOH}$ ) and potassium compounds instead of soda ash. Hall and Barron [53] reported the use of both activated carbon filters and  $\text{NaOH}$  in the Ram River Gas Plant. They presented data indicating a reduction in the heat stable salt content as a result of these treatments.

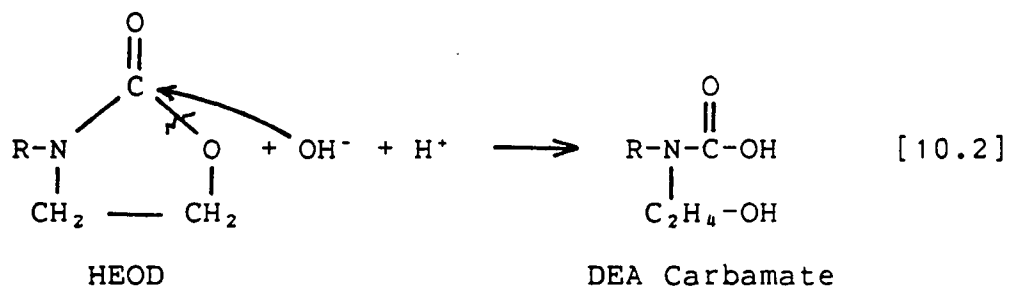
Since corrosion tests indicated that BHEP is not corrosive, present efforts were directed towards the removal of HEOD and THEED.

## 10.3 REMOVAL OF HEOD

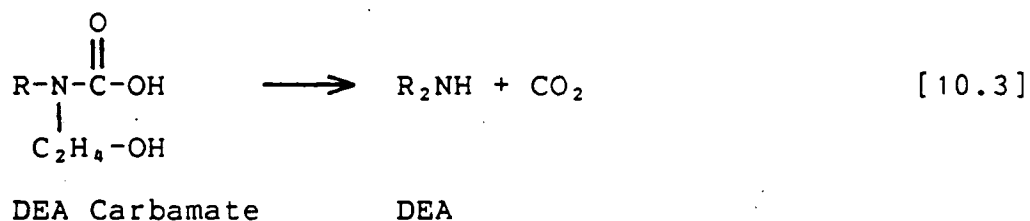
According to Kennard [51], HEOD is formed by the dehydration of DEA carbamate.



Kennard [51] suggested that NaOH addition to HEOD solutions can convert most of the HEOD to DEA. This is due to the fact that the HEOD ring is unstable and the electron deficient carbonyl atom of the ring is easily attacked by  $\text{OH}^-$ .



When NaOH is added, HEOD is converted back to DEA carbamate and DEA can be regenerated by driving off  $\text{CO}_2$  from the carbamate upon applying heat.







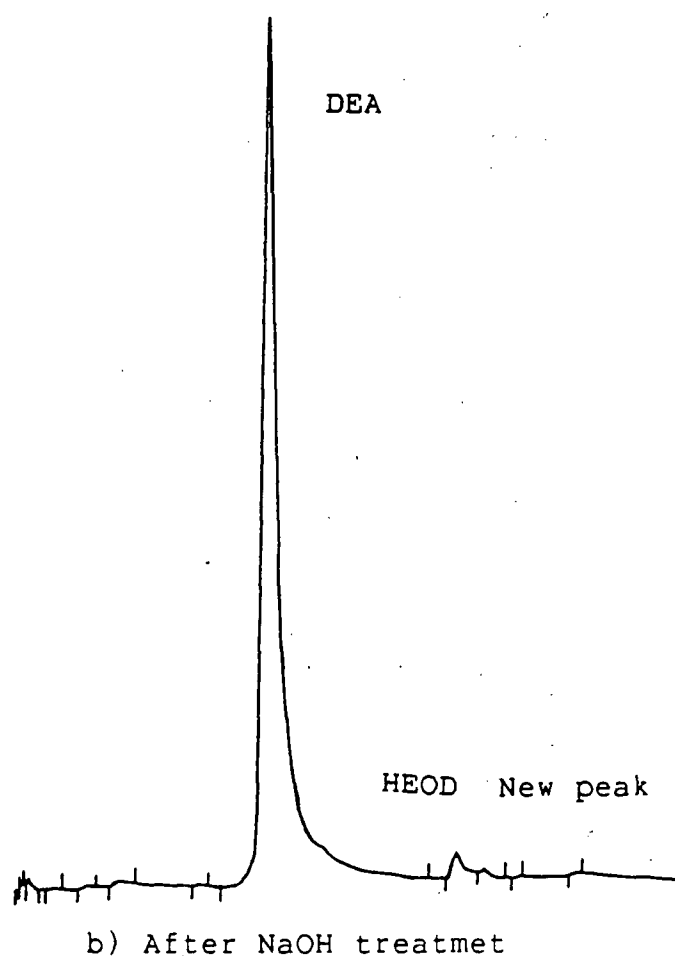
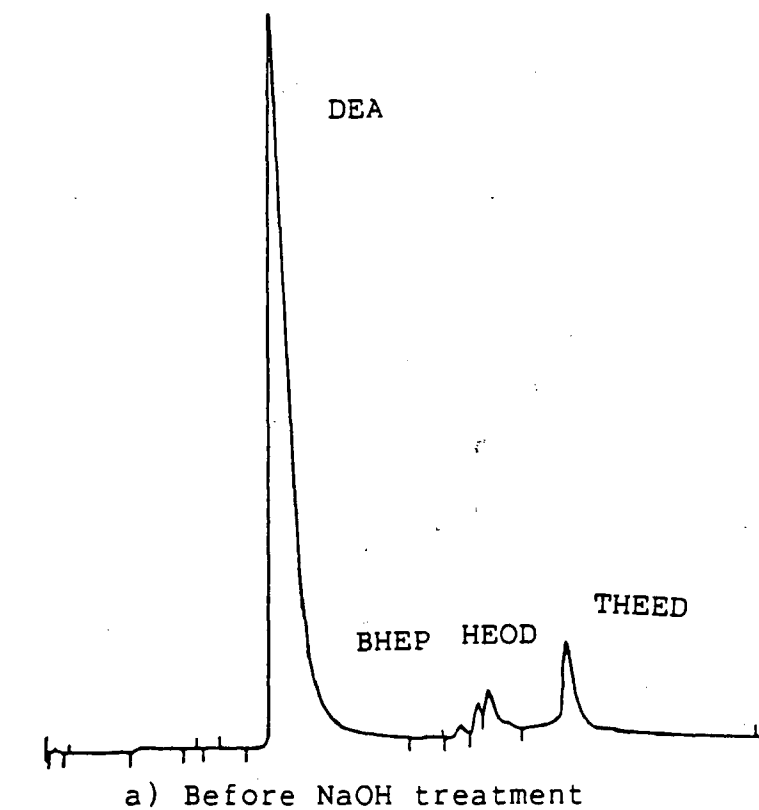
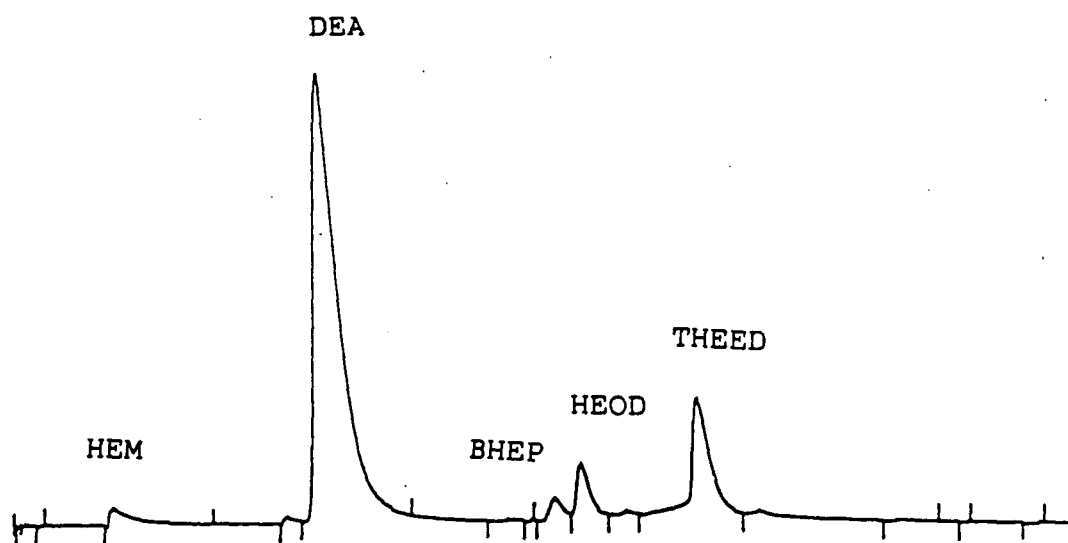
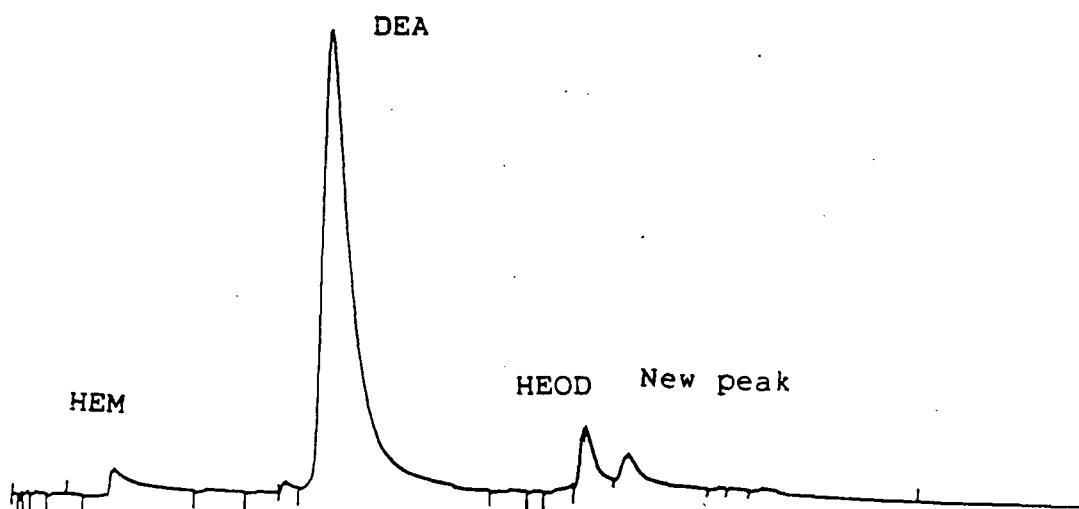


Figure 10.2 Chromatograms of a partially degraded DEA sample of run 3 before and after NaOH treatment.



a) Before NaOH treatment



b) After NaOH treatment

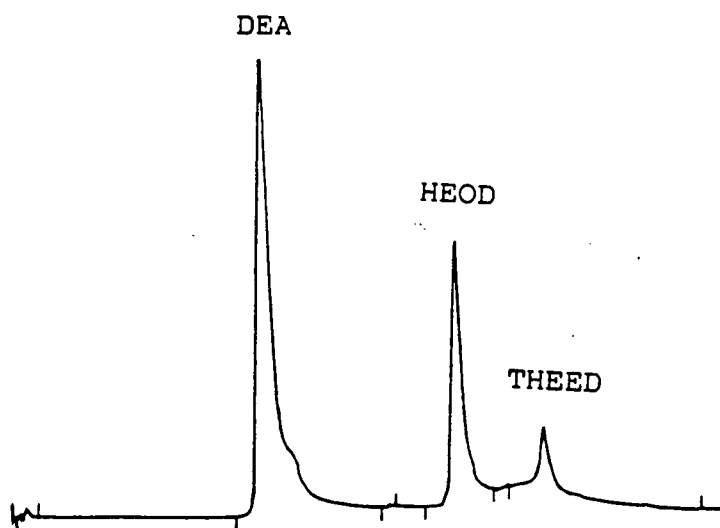
Figure 10.3 Chromatograms of a degraded from a gas processing plant before and after NaOH treatment.

Once again, THEED was removed completely, HEOD was removed partially and a new peak appeared.

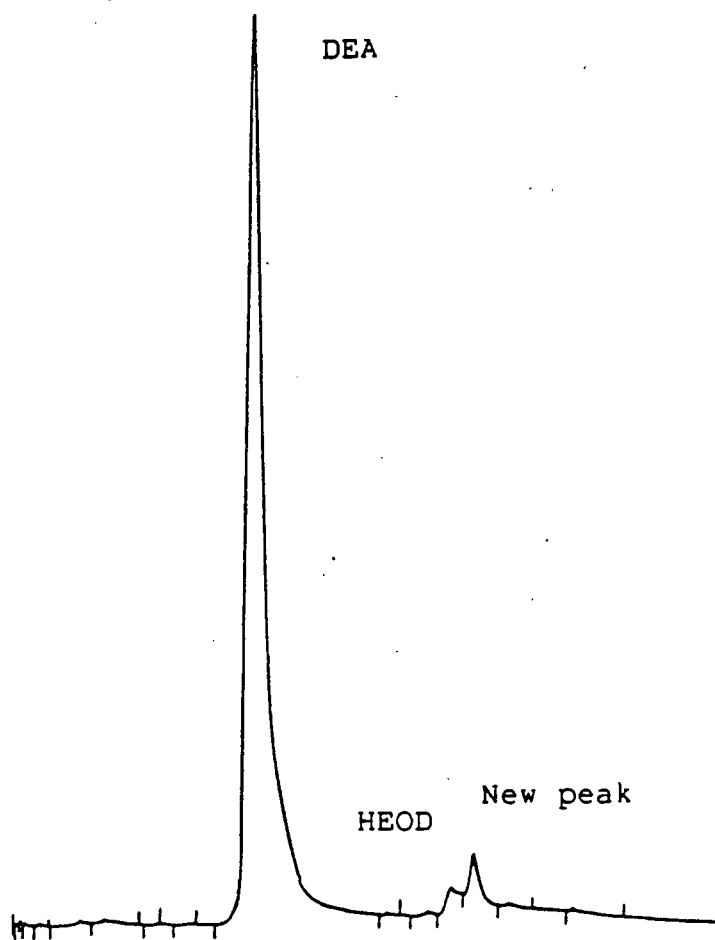
This partial removal of HEOD was somewhat surprising and may have been due to the presence of N-(hydroxyethyl)ethyleneamine ("HEM"), which was not present in the laboratory sample.

#### 10.6 NaOH TREATMENT OF A MIXTURE OF DEA, HEOD AND THEED

Because of the inability to remove HEOD completely from the laboratory and especially from the industrial sample, it was decided to prepare a 20 mL mixture of 30 wt%, 12 wt% and 8 wt% of DEA, HEOD and THEED, respectively, in the laboratory in the absence of other contaminants. 2 mL of 1 N NaOH was then added to the solution and the mixture was heated at 80°C for 2 min. The appropriate chromatograms are shown in Figure 10.4. This time, almost complete removal of HEOD was achieved. THEED removal was complete and the new peak appeared again. Consequently, the HEOD removal efficiency by NaOH treatment appears to depend on the presence of other contaminants.



a) Before NaOH treatment

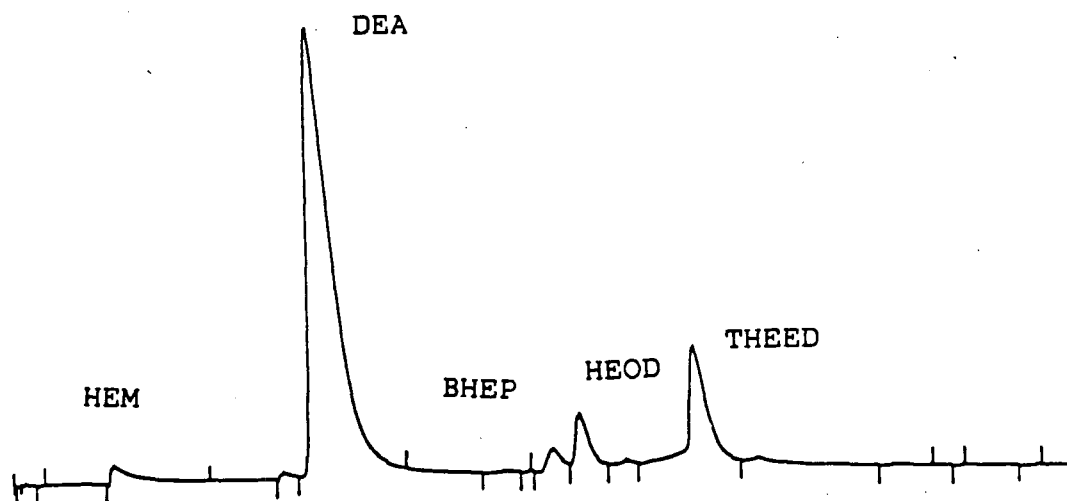


b) After NaOH treatment

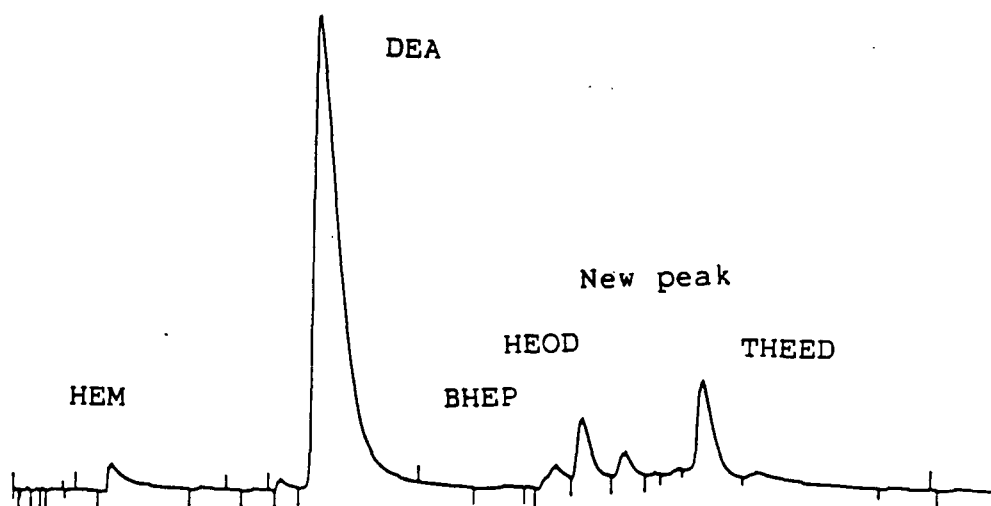
Figure 10.4 Chromatograms of laboratory made mixture of 30 wt % DEA, 12 wt% HEOD and 8 wt% THEED before and after NaOH treatment.

### 10.7 SODA ASH TREATMENT

Soda ash ( $\text{Na}_2\text{CO}_3$ ) is occasionally used for the removal of degradation compounds, especially the heat stable salts from degraded DEA solutions. In order to assess the effect of  $\text{Na}_2\text{CO}_3$  addition upon the removal of major degradation compounds,  $\text{Na}_2\text{CO}_3$  was added to an industrial DEA solution sample and the mixture was heated at 80 C for about 2 min. The chromatograms of the sample before and after  $\text{Na}_2\text{CO}_3$  treatment are shown in Figure 10.5. As can be seen, none of the major degradation compounds was removed. On the contrary, another peak appears which has the same retention time as the "new" peak mentioned above.



a) Before soda ash treatment



b) After soda ash treatment

Figure 10.5 Chromatograms of a degraded DEA sample from a gas processing plant before and after soda ash treatment.

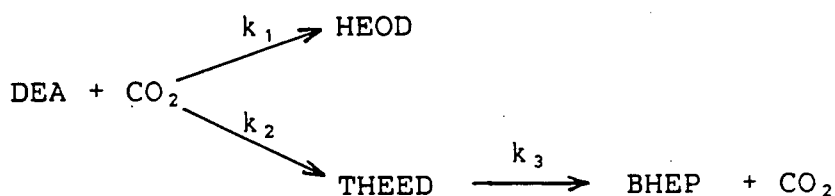
## CHAPTER 11

CONCLUSION AND RECOMMENDATIONS11.1 CONCLUSIONS:

1. Degradation of DEA in heat exchangers mainly depends on temperature, CO<sub>2</sub> partial pressure and DEA concentration.
2. Accumulation of DEA degradation compounds, increases the solution viscosity.
3. DEA degradation results in severe fouling of process equipment.
4. DEA degradation also increases the foaming tendency of the solution.
5. Skin temperature and not the bulk solution temperature largely determines the DEA degradation rate.
6. Solution flow rate can be used as an operating variable in minimising skin temperature. Higher solution flow rate can minimise the rate of degradation by decreasing the film thickness of the solution adjacent to the metal wall.



7. Kennard's simplified kinetic model was not able to predict DEA degradation under variable  $\text{CO}_2$  partial pressures. His model provides different rate constants for three different concentration ranges. In order to predict the DEA degradation rate under variable  $\text{CO}_2$  partial pressure and DEA concentrations, Kennard's model was modified as follows:



The pseudo rate constants  $k_1$ ,  $k_2$  and  $k_3$  can be calculated as a function of temperature by using the following equations:

$$\ln(k_1) = 11.924 - 6451/T(K)$$

$$\ln(k_2) = 8.450 - 5580/T(K)$$

$$\ln(k_3) = 39.813 - 15160/T(K)$$

Using the above model, it was possible to predict the rate of DEA degradation for the temperature range of 60 to 200 °C, the  $\text{CO}_2$  partial pressure range of 1379 to 4137 kPa, and DEA solution concentration range of 20 to 40 wt%.

8. HEOD, one of the major DEA degradation products was found to be corrosive towards mild steel.
9. HEOD, THEED and some other minor degradation compounds can be converted back to DEA by adding NaOH and applying heat.
10. The HEOD removal efficiency by NaOH apparently depends on the presence of other degradation compounds.
11. Industrially used activated carbon filters are not able to remove any major DEA degradation products.
12.  $\text{Na}_2\text{CO}_3$  treatment is not able to remove BHEP, HEOD or THEED from degraded DEA solutions.

## 11.2 RECOMMENDATIONS :

### a) The effect of temperature :

Temperature is the most important operating variable to be controlled in order to minimise DEA degradation. Elevated temperatures, especially high metal skin temperatures and local hot spots, should be avoided throughout the plant. In designing heat exchangers for amine treating plants, consideration should be given to metal skin temperature. This can be done by selecting individual heat transfer resistances such that heat transfer requirements are met without creating high metal skin temperature. Metal skin temperatures should preferably be limited to 120°C and be monitored carefully. At least two thermocouples, one at the inlet and the other at the outlet should be attached to the heat transfer surface for this purpose. If the metal skin temperature increases due to any process upset during plant operation, it should be brought under control either by increasing the solution flow rate or by decreasing the temperature of the heating medium. However, increasing the flow rate would provide a swifter and better temperature control than lowering temperature of the heating medium.

b) Effect of dissolved  $\text{CO}_2$  :

$\text{CO}_2$  catalyses DEA degradation reactions. In the absence of  $\text{CO}_2$ , DEA degradation is not appreciable. Since, the highest temperature is experienced by DEA in the regenerator reboiler, all the dissolved  $\text{CO}_2$  should be stripped out of the solution in the regenerator trays. The reboiler should serve only to provide the necessary steam for regeneration, but not to strip dissolved  $\text{CO}_2$  in the reboiler. If the DEA solution entering the reboiler contains very little dissolved  $\text{CO}_2$ , then degradation in the reboiler would be minimal. In order to see whether the regenerator is stripping out almost all the dissolved  $\text{CO}_2$ , the efficiency of the stripping operation should be checked. This can be done by analysing lean DEA samples leaving the regenerator and DEA samples entering the reboiler for dissolved  $\text{CO}_2$ . The  $\text{CO}_2$  concentrations in both samples should be the same. If the  $\text{CO}_2$  content of the DEA solution entering the reboiler is found to be higher than that of the lean DEA solution, steps should be taken to increase the stripping efficiency of the regenerator. This should be done by increasing the reflux rate, not by increasing the temperature.

### c) Corrosion control :

Solution pH has a strong effect on corrosion of mild steel. Therefore the pH of the rich DEA solution leaving the CO<sub>2</sub> absorber should be monitored, preferably with an on-line pH meter. The solution pH should not be allowed to go below 9. Corrosive degradation compounds such as HEOD should be removed from the solution and formation of organic acids should be minimised by preventing oxygen from coming in contact with the DEA solution.

### d) Solution Purification :

Both activated carbon filter and NaOH injection may be employed as means of solution purification. The activated carbon filter removes suspended particles. NaOH injection serves two purposes: it removes HEOD and THEED to some extent and it also helps maintain the solution pH above 9. As a result of NaOH addition sodium salts would gradually build up inside the system. A reclaimer might be used to separate these salts from the DEA solution if the salt build up becomes excessive.

DEA solutions should be routinely analysed for degradation products and NaOH, slightly above stoichiometric requirement for the removal of HEOD, THEED and other organic acids (if present), should be added.

### 11.3 RECOMMENDATIONS FOR FURTHER WORK:

#### a) Kinetic Model :

The kinetic model developed in this thesis needs some improvement. The following is recommended for this purpose :

- $\text{CO}_2$  concentration in the DEA solution is an important parameter in the model. A theoretical thermodynamic model for the prediction of solubility in DEA solution needs to be developed and incorporated with the kinetic model.
- Kinetic data at lower  $\text{CO}_2$  partial pressure and temperature range of 40 C to 120 C should be obtained from batchwise experiments. This, combined with  $\text{CO}_2$  solubility data, can then be used to calculate the pseudo-rate constants.
- Potentiodynamic corrosion studies should be carried out in order to identify other corrosive degradation compounds and to study the corrosion mechanisms in DEA solution.

#### b) Purification of DEA solution :

- Although NaOH addition can aid in the regeneration of DEA from some of the degradation compounds, its excessive use might have some adverse affect on the stripping efficiency of the regenerator. Therefore, it is desireable to have some information on the effect of NaOH addition on vapor-liquid equilibria of DEA- $\text{CO}_2$  system under the regenerator conditions.

## NOMENCLATURE

A	Heat transfer surface area ( $\text{m}^2$ )
BHEP	N,N-Bis(hydroxyethyl) piperazine
BHEU	N,N-Bis(hydroxyethyl) urea
C	DEA concentration (wt%)
Cp	Specific heat of DEA solution ( $\text{J/g}^\circ\text{C}$ )
Cpo	Specific of heating fluid ( $\text{J/g}^\circ\text{C}$ )
d	Specific gravity
Db	Stirrer blade diameter (m)
Dc	Turning diameter of the heat transfer tube (m)
Di	Inside diameter of the heat transfer tube (m)
Dlm	Log mean diameter $(D_o - D_i) / \ln[D_o / D_i]$
Do	Outside diameter of the heat transfer tube (m)
Dt	Diameter of the tank containing heat transfer fluid (m)
DEA	Diethanolamine
Ecorr	Free corrosion potential (Volts)
f	Friction factor, equation 7.22
hi	Inside heat transfer coefficient ( $\text{J/m}^2\text{s}^\circ\text{C}$ )
HEED	N-(hydroxyethyl) ethylenediamine
HEI	N-(hydroxyethyl) imidazolidone
HEM	N-(hydroxyethyl) ethylenimine
HEOD	3-(hydroxyethyl)-2-oxazolidone
ho	Outside heat transfer coefficient ( $\text{J/m}^2\text{s}^\circ\text{C}$ )
Ia	Anodic current (Amps)
Ic	Cathodic current (Amps)
Icorr	Corrosion current (Amps)

k	Thermal conductivity of aqueous DEA solution (W/m°C)
$K_1, K_2, k_3$	Rate constants used in the kinetic model for the degradation of DEA (L/moles hr)
km	Thermal conductivity of the tube metal (W/m°C)
L	Length of the heat transfer tube (m)
MEA	Monoethanolamine
N	No. of passes through the heat transfer tube
OZD	Oxazolidone
P	Pressure (kPa)
Q	Heat duty (kJ/s)
R	-C <sub>2</sub> H <sub>4</sub> -OH
RPS	Revolutions per second
rt	Residence time for a single pass (hr)
RT	Total residence time (hr)
t	Time (hr)
T	Bulk solution temperature (°C)
TEA	Triethanolamine
THEED	N,N,N-Tris(hydroxyethyl) ethylenediamine
Ti	Heat transfer tube inlet temperature (°C)
Tk	Thermal conductivity of heating oil (W/m°C)
To	Heat transfer tube outlet temperature (°C)
Th	Heat transfer fluid temperature (°C)
tsp	Time required to pass total DEA inventory through the heat transfer tube in a single pass (hr)



Tw <sub>i</sub>	Inside wall temperature of the heat transfer tube (°C)
Tw <sub>o</sub>	Outside wall temperature of the heat transfer tube (°C)
U <sub>i</sub>	Overall heat transfer coefficient based on inside surface of the straight heat transfer tube (J/m <sup>2</sup> s°C)
U <sub>c</sub>	Overall heat transfer coefficient for the coiled heat transfer tube (J/m <sup>2</sup> s°C)
W	Mass flow rate (kg/s)
x	Length of a small segment of the heat transfer tube
x <sub>m</sub>	Heat transfer tube wall thickness (m)

#### DIMENSIONLESS GROUPS

Nu	Nusselt Number, $hD/k$
Pr	Prandtl Number, $C_p\mu/k$
Re	Reynolds Number, $\rho vD/\mu$

#### GREEK LETTERS

$\beta_a$	Anodic Tafel constant, equation 5.4
$\beta_c$	Cathodic Tafel constant, equation 5.3
$\epsilon$	Surface roughness factor of the heat transfer tube
$\phi$	Potential (Volts)
$\phi_{corr}$	Corrosion potential (Volts)
$\rho$	Density of DEA solution (kg/m <sup>3</sup> )
$\rho_o$	Density of the heating fluid (kg/m <sup>3</sup> )
$\mu$	Viscosity of DEA solution (Pa.s)

$\mu_w$       Viscosity of DEA solution at the wall temperature  
          (Pa.s)

$\mu_o$       Viscosity of the heating fluid (Pa.s)

$\mu_{ow}$      Viscosity of the heating fluid at the wall temperature  
          (Pa.s)

#### SUBSCRIPTS

i          Inside

o          Outside

REFERENCES

1. Bottoms, R.R., U.S. Patent 1,783,901 1930.
2. Bottoms, R.R., "Organic Bases for Gas Purification," Ind. Eng. Chem., 23 (5), 501, 1931.
3. Maddox, R.N., "Gas and Liquid Sweetening," 2nd. Edition, Campbell Petroleum Series, Norman, OK, 1977.
4. Dankwerts, P.V. and Sharma, M.M., " The Absorption of Carbon Dioxide into Solutions of Alkalies and Amines," The Chemical Engineer, CE244, October, 1966.
5. Swaim, C.D., "Gas Sweetening Processes of the 1960s," Hydrocarbon Processing, 49 (3), 127, 1970.
6. Jones, V.W. and Perry, C.R., "Fundamentals of Gas Treating," Proc. of Gas Cond. Conf., 23 (E), 1, 1973.
7. Younger, A.H., "Process for Sour Natural Gas Treating," Symp. on Sulphur recovery from hydrocarbon feedstocks, Vancouver, B.C., Sept. 1973.
8. Butwell, K.F., Kubek, D.J., and Sigmund, P.W., Union Carbide Publication "Primary vs. Secondary Amines," 1979.
9. Butwell, K.F., Kubek, D.J., and Sigmund, P.W., "Alkanolamine Treating," Hydrocarbon Processing, 62 (3), 108, 1982.
10. Wendt, C.J., Jr. and Dailey, L.W., "Gas Treating: SNPA Process," Hydrocarbon Processing, 46 (10), 155, 1967.

11. Moore, K.L., "Corrosion Problems in a Refinery Diethanolamine System," Corrosion, N.A.C.E., 16 (Oct), 111, 1960.
12. Polderman, L.D. and Steele, A.S., "Why Diethanolamine Break Down in Gas Treating Service," Oil and Gas Journal, 54 (July 30), 206, 1956.
13. Smith, R.F. and Younger, A.H., "Tips on DEA Treating," Hydrocarbon Processing, 51 (7), 98, 1972.
14. Nonhebel, G., "Gas Purification for Air Pollution Control, 2nd Edition, Newness-Butterworths, London, 1972.
15. Scheirman, W.L., "Filter DEA Treating Solution," Hydrocarbon Processing, 52 (8), 95, 1973.
16. Keaton, M.M. and Rourke, M.J., "Activated Carbon System Cuts Foaming and Amine Losses," Hydrocarbon Processing, 62 (8), 71, 1983.
17. Meisen, A. and Kennard, M.L., "DEA degradation Mechanism," Hydrocarbon Processing, 61 (10), 105, 1982.
18. Smith, R.F., and Younger, A.H., "Operating Experiences of Canadian Diethanolamine Plants," Proc. of Gas Cond. Conf., 22 (E), 1, 1972.
19. Beck, J.E., "Diethanolamine - An Enrgy Conserver," Proc. of Gas Cond. Conf., 25 (A), 1, 1975.
20. Butwell, K.F., and Perry, C.R., "Performance of Gas Purification Systems Utilizing DEA Solutions," Proc. of Gas Cond. Conf., 25 (B), 1, 1975.

21. Heisler, L., and Weiss, I.H., "Operating Experiences at Aderklaa with Alkanolamine Gas Treating Plants for Sour Natural Gas Sweetening," Proc. of Gas Cond. Conf., 25 (H), 1, 1975.
22. Katz, D.L., Cornell, D., Kobayashi, R., Poettman, F.H., Vary, J.A., Elenbaas, J.R., and Weinang, C.F., "Handbook of Natural Gas Engineering," McGraw-Hill Co., Inc., N.Y., 1960.
23. Kohl, A., and Riesenfeld, F., "Gas Purification," McGraw-Hill Book Co., N.Y., 1960.
24. Campbell, J.M., "Gas Conditioning and Processing," Vol.2, Campbell Petroleum Series, Norman, OK., 1976.
25. Astarita, G., Savage, D.W., and Bisio, A., "Gas Treating with Chemical Solvents," John-Wiley Interscience, N.Y., 1983.
26. Dow Chemical Company, "Gas Conditioning Fact Book," The Dow Chemical Co., Midland, Michigan, 1962.
27. Van Krevelen, D.W. and Hoftizer, P.J., Chem. Eng. Prog., 44 (7), 529, 1948.
28. Nunge, R. and Gill, W.N., "Gas-Liquid Kinetics: the Absorption of Carbon Dioxide in Diethanolamine," A.I.Ch.E. Journal, 9 (4), 529, 1963.
29. Sada, E., Kumazawa, H., and Butt, M.A., "Gas Absorption with Consecutive Chemical Reaction: Absorption of Carbon Dioxide into Aqueous Amine Solutions," Can. J. of Chem. Eng., 54 (5), 421, 1976.

30. Coldrey, P.W., and Harris, I.J., "Kinetics of Liquid Phase Reaction Between Carbon Dioxide and Diethanolamine," Can J. of Chemical Engg., 54 (6), 566, 1976.
31. Hikita, H., Asai, S., Ishikuma, H., and Houda, M., "The Kinetics of Reactions of Carbon Dioxide with Monoethanolamine, Diethanolamine and Triethanolamine by a Rapid Mixing Method," The Chem. Engg. Journal, 13, 7, 1977.
32. Dankwerts, P.V., "The Reaction of CO<sub>2</sub> with ethanolamines," Chem. Engg. Sci., 34 , 443, 1979.
33. Alvarez-Fuster, C., Midoux, N., Laurent, A., and Charpentier, J.C., Chem. Engg. Sci. 35 , 1717, 1980.
34. Donaldson, T.L. and Nguyen, Y.N., Ind. Engg. Chem. Fundls., 19, 260, 1980.
35. Alvarez-Fuster, C., Midoux, N., Laurent, A., and Charpentier, J.C., "Chemical Kinetics of the Reaction of CO<sub>2</sub> with Amines in Pseudo m-nth Order Conditions in Polar and Viscous Organic Solutions," Chem. Engg. Sci., 36 , 1513, 1981.
36. Ratkovics, F. and Horvath, I., Hungarian J. of Ind. Chem. 9 , 281, 1981.
37. Blanc, C., and Demarais, G., " The Reaction of CO<sub>2</sub> with Diethanolamine," Entropie, 17 (102), 53, 1981.
38. Mahajani, V.V., and Dankwerts, P.V., "Investigation of Carbon Dioxide Absorption by Absorbents Impregnated with Alkanolamines," Chem. Engg. Sci., 37 (6), 943, 1982.

39. Laddha, S.S., and Danckwerts, P.V., "Reaction of CO<sub>2</sub> with Ethanolamine: kinetics from Gas Absorption," Chem. Engg. Sci., 37 , 475, 1982.
40. Blauwhoff, P.M.M., Versteeg, G.F., and Van Swaaij, W.P.M., "A study on the Reaction Between CO<sub>2</sub> and Alkanolamines in Aqueous Solutions," Chem. Engg. Sci., 38 (9), 1411, 1983.
41. Hakka, L.E., Singh, K.P., Bata, G.L., Testart, A.G., and Andrejchyshyn, W.M., "Some Aspects of Diethanolamine Degradation in Gas Sweetening," Gas Processing/Canada, 61 (1), 32, 1968.
42. Choy, E.T., and Meisen, A., "Degradation of DEA Treating Solutions," Proc. Canadian Natural Gas Processors Association, Calgary, Nov. 1977.
43. Choy, E.T., "Degradation of DEA Treating Solutions," Masters Thesis, Univ. of B.C., 1978.
44. Kennard, M.L., and Meisen, A., Hydrocarbon Processing, 59 (4), 103, 1980.
45. Blanc, C., Grall, M., and Demarais, G., "The Part Played by Degradation Compounds in the Corrosion of Gas Sweetening Plants using DEA and MDEA," Proc. Gas Cond. Conf., 32, March, 1982.
46. Henry, M.S., and Grennert, M., Petroleum Refiner, 34 (6), 177, 1955.
47. Henry, M.S., and Grennert, M., "Detection and Measurement of Components in Diethanolamine Used for Hydrogen Sulphide Removal from Petroleum Refinery Gases," California Natural Gasoline Assoc. Proc., 28, 64, 1955.

48. Polderman, L.D., Dillon, C.P., and Steele, A.B., "Why MEA Solution Breaks Down in Gas Treating Service," Oil and Gas Journal, 54 (2), 180, 1955.
49. Berlie, E.M., and Estep, J.W., "Preventing MEA Degradation," Chem. Engg. Prog., 61 (4), 82, 1965.
50. Watermann, J., Kosseim, A.J., and Butwell, K.F., "DEA Retrofit at Montana Power Gas Sweetening Plant Ends Corrosion, Sludge Problems," Oil and Gas Journal, Feb. 6, 1984.
51. Kennard, M.L., "Degradation of Diethanolamine Solutions," Ph.D. Thesis, Univ. of B.C., 1983.
52. Fitzgerald, K.J., and Richardson, J.A., "How Gas Composition Affects Treating Process Selection," Hydrocarbon Processing, 45 (7), 125, 1966.
53. Hall, W.D., and Barron, J.G., "Solving Gas Treating Problems - A different Approach," Proc. of 31st Annual Gas Conditioning Conference, Norman, Oklahoma, March 2-4, 1981.
54. McMin, R.E., and Farmer, F., "An Integrated Sulphur Manufacturing System," Conf. on Sulphur Recovery Processes, Oklahoma State University, March 1969.
55. Lang, F.S. and Mason, J.F., Jr., "Corrosion in Amine Gas Treating Solutions," Corrosion, 14 (Feb), 65, 1958.
56. Gillis, G.A., Hawker, L.E., and Blake, R.J., "N-(2-Hydroxyethyl) Ethylenediamine, A Corrosive Contaminant in Monoethanolamine Gas Treating Solutions," Proc. of Gas Conditioning Conference, Norman, 1963.



57. Comeaux, R.V., "The Mechanism of MEA Corrosion," Proc. of American Petroleum Institute, Refining Division, 42 (III), 481, 1962.
58. Dingman, J.C., Allen, D.L., and Moore, T.F., "Minimize Corrosion in MEA Units," Hydrocarbon Processing, 45 (9), 285, 1966.
59. Hawkes, E.N., and Mago, B.F., "Stop MEA CO<sub>2</sub> Corrosion," Hydrocarbon Processing, 50 (8), 109, 1971.
60. Pourbaix, M. "Atlas of Electrochemical Equilibria in Aqueous Solutions," 2nd English Edition, NACE, Houston, 1974.
61. Ballard, D., "How to Operate an Amine Plant," Hydrocarbon Processing, 45 (4), 137, 1966.
62. Sheilan, M. and Smith, R.F., "Effect of Hydraulic Flow on Amine Plant Corrosion," Proc. of Gas Conditioning Conference, University of Oklahoma, Norman, Oklahoma, March 5-7, 1984.
63. Maddox, R.N., and Mains, G.J., "Data and Design for Amine treating," Proc. of Gas Processors Association Annual Meeting, New Orleans, 1984.
64. Chruttenden, B.D., "Chemical Reaction Fouling," Continuing Education Course Notes on The Fouling of Heat Exchangers, Inst. of Chemical Engineers and The Chemical Engineering Dept. of The Univ of Birmingham, March 19-20, 1981.
65. Watkinson, A.P., and Epstein, N., Proc. 4th Int. Heat Transfer Conf., Vol.1, Paper HE 1.6, Paris, 1970.

66. Shah, Y.T., Stuart, E.B., and Sheth, K.D., Ind. Engg. Chem., Prod. Res. and Dev., 15 (4), 518, 1976.
67. Gough, G.G., "The Analysis and Analytical Interpretation of Gas Conditioning Diethanolamine Solutions," Proc. Canadian Natural Gas Processors Association, Calgary, 1969.
68. Brydia, L.E., and Persinger, H.E., Anal. Chem., 39 (11), 1316, 1967.
69. Piekos, R., Kobyiczek, K., and Grzybowski, J., Anal. Chem., 47 (7), 1157, 1975.
70. Saha, N.C., Jain, S.K. and Dua, R.K., Chromatographia, 10 (7), 368, 1977.
71. Uhlig, H.H., "Corrosion and Corrosion Control," 3rd Printing, John Wiley and Sons, Inc., New York, 1965.
72. Kern, D.Q., "Process Heat Transfer," McGraw-Hill Book Co., New York, 1950.
73. Oldshue, J.Y., and Gretton, A.T., "Helical Coil Heat Transfer in Mixing Vessels," Chem. Eng. Prog., 50 (12), 615, December, 1954.
74. McAdams, W.H., "Heat Transmission," Third Edition, McGraw Hill Book Co., New York, 1954.
75. "Gas Treating Chemicals", Union Carbide Ethylene Oxide Derivative Division, Danbury, CT., 1980.
76. "Lube Report - T.I.P. 3.21.4.", Shell Canada.
77. G.P.S.A. Engineering Data Book, 9th Edition, Gas Processors Suppliers Association, Tulsa, OK., 1976.

78. Standards of Tubular Exchanger Manufacturers Association (TEMA) 6th Edition, TEMA, New York, 1978.
79. U.S. Bureau of Standards Miscellaneous Publications 97.
80. Smithells, C.J., "Metals Reference Book", Vol.III, 4th Edition, Butterworths, London, 1967.
81. Denn, M.N., "Process Fluid Mechanics", Prentice-Hall, Inc., Englewood Cliffs, New Jersey, 1980.
82. Lee, I.J., Otto, F.D. and Mather, A.E., "Solubility of Carbon Dioxide in Aqueous Diethanolamine Solutions at High Pressures," J. of Chemical Engineering Data, 17 (4), 465, 1972.

## APPENDIX - A

Listing of the computer program for the determination of temperature profile, pressure drop, film thickness and the DEA degradation rate in the heat exchanger tube.

```

C      PROGRAM TO PREDICT TEMPERATURE PROFILE, PRESSURE DROP,
C      FILM THICKNESS, DEA, HEOD, THEED AND BHEP CONCENTRATIONS
C      IN THE HEAT TRANSFER TUBE OF THE DEA DEGRADATION EXPT.
C
C      TH=TEMPERATURE OF THE HEATING MEDIUM (C)
C      TS=TEMPERATURE OF THE AUTOCLAVE (C)
C      TWIN=INSIDE WALL TEMPERATURE OF THE COIL (C)
C      TCL=TOTAL COIL LENGTH (M)
C      TLV=TOTAL LIQUID INVENTORY (CU.M)
C      TSPS=TIME FOR A SINGLE PASS THRU HEX. (SEC)
C      DEAL=QNTY. OF DEGRADED DEA IN 1 PASS
C      DEANP=DEA CONC. AFTER NP PASSES
C      HEONP=HEOD CONC. " "
C      THENP=THEED CONC. " "
C      TQTHR=TOTAL TIME (HR)
C      NPT=TOTAL NO. OF PASSES
C      NPHR=NO. OF PASSES PER HOUR
C      X =COIL LENGTH (M)
C      DEALT=LOSS OF DEA AT THE END OF EACH INCREMENT
C      HEODT=HEOD CONC. " " " "
C      THEEDT= THEED CONC. " " " "
C      DEACT=DEA CONC. " " " "
C      FFT=FRICITION FACTOR TOLERANCE
C      K=COLEBROOK CONST.
C      DELP=PRESSURE DROP (PA.)
REAL NPRO, NPRO, NPT, NPHR, NPNHR
DATA DOT, DB, RPH /0.7112, 0.1016, 8./
DATA VOLS /0.00001100/
DATA DI, DO, DC, XW /0.002032, 0.003175, 0.4064, 0.000715/
DATA TQTHR, TCL, TLV /200., 4.8, .0025/
DATA TINC, TEPS, XINC, FFT /1., .001, .1, 0.001/
CO2 = 3.200
DEAO = 30.00
DEAOT = DEAO
DEALT = DEAO
HEODT = 0.0
THEEDT = 0.0
BHEPT = 0.0
SUMDP = 0.0
REAL K, K1, K2, K3, LNK1, LNK2, LNK3
K = 0.000012
PI = 4. * ATAN(1.)
C      INITIAL WALL TEMPERATURE
TS = 60.0
T = 60.0
T1 = TS
TH = 250.0
TWOUT = TH
TWIN = TH - 10.0
TW = TWIN
X = 0.00
DX = 0.1
WRITE (6,10)
10 FORMAT (1X, 'LENGTH(m)', 2X, 'WALL T(C)', 2X, 'SOL.T(C)', 5X,
1 'RE', 6X, 'DEA CONC.', 6X, 'DELX*E5', //)

```

```

C
C   CALL SUBROUTINE THERM TO CALCULATE PROPERTIES OF SHELL THERMIA
C
C   CALL THERM(TH, CPO, TKO, RHOO, VISO)
C
C   CALL SUBROUTINE DPROP TO CALCULATE DEA PROPERTIES
C
C   CALL DPROP(TS, DEAO, RHOS, VISS, TKS, CPS)
C   CALL DPROP(T, DEAO, RHO, VIS, TK, CP)
C   GO TO 30
20 CALL DPROP(T, DEAO, RHO, VIS, TK, CP)
30 CALL DPROP(TWIN, DEAO, RHO, VIS, TK, CP)
C   CALL THERM(TWO, CPO, TKO, VISOW)
C
C   CALL SUBROUTINE SSPROP TO CALCULATE TH. COND. OF METAL WALL
C
C   CALL SSPROP(TW, TKM)
C
C   CALCULATE PROCESS SIDE HEAT TRANSFER COEFFICIENT
C
C   VOLT = VOLS * (RHOS/RHO)
C   WT = VOLS * RHOS
C   VELT = (4.*WT) / (RHO*PI*DI**2.)
C   G = (4.*WT) / (PI*DI**2.)
C   REC = (DI*G) / VIS
C   NPRC = (CP*VIS) / TK
C   HI = 0.023 * (TK/DI) * (REC**0.8) * (NPRC**0.333333) * (VIS/VISW)
C   1 ** 0.14
C   DELX = 43.5 * DI ** 1.8 / (((4.*WT)/(PI*VIS))**0.8*(NPRC**0.
C   1333333))
C   DELX = DELX * 100000.
C
C   CALCULATE THE OUTSIDE HEAT TRANSFER COEFFICIENT
C
C   REO = DB ** 2. * RPH * RHOO / VISO
C   NPRO = CPO * VISO / TKO
C   VISEX = 0.1 * (VISO*8.621E-05) ** (-0.21)
C   HO = 0.17 * (TKO/DO) * (REO**0.6667) * (NPRO**0.3333) * (DB/DO)
C   1 ** 0.1 * (DO/DO) ** .5 * (VISO/VISO) ** VISEX
C
C   CALCULATE LOG MEAN DIAMETER
C
C   DL = (DO - DI) / (ALOG(DO/DI))
C
C   CALCULATE THE OVERALL HEAT TRANSFER COEFFICIENT
C
C   U = 1. / ((1./HI) + ((1./HO)*(DI/DO)) + ((XW/TKM)*(DI/DL)))
C   UC = U * (1 + 3.5*(DI/DC))
C
C   CALCULATE THE BULK TEMPERATURE OF DEA SOLN.
C
C   T = TH - (TH - T1) * EXP((-UC*PI*DI*DX)/(WT*CP))

```

```

C
C      CALCULATE INSIDE WALL TEMPERATURE AND CHECK WITH ASSUMED VALUE
C
      TWOUT = TH - ((TH - T)*(1./HO)*(DI/DO)*UC)
      TWINC = TWOUT - ((TH - T)*(XW/TKM)*(DO/DL)*UC)
      IF ((TWINC - T) .LT. 0.0000001) GO TO 50
      IF (ABS(TWINC - TWIN) .LT. TEPS) GO TO 60
      IF (ABS(TWINC - TWIN) .GT. TEPS) GO TO 40
40    TWIN = TWINC
      TW = (TWIN + TWOUT) / 2.
      GO TO 20
50    TWIN = T
60    THR = XINC / VELT
      THR = THR / 3600.

C
C      PRESSURE DROP CALCULATION
C
C      ININIAL ESTIMATE OF FRICTION FACTOR
C
      FI = 0.04 * REC ** (-0.16)

C
C      CALCULATION OF FRICTION FACTOR BY COLEBROOK FORMULA
C
70    F = (1./((-4.0*ALOG10((K/DI) + (4.67/(REC*FI**0.5)))) + 2.28)) ** 2.
      IF (ABS(F - FI) .LT. FFT) GO TO 90
      IF (ABS(F - FI) .GT. FFT) GO TO 80
80    FI = F
      GO TO 70
90    DELP = (2.*RHO*VELT**2.*F*XINC) / DI
      DELP = DELP * (1. + 3.5*(DI/DC))
      DELP = DELP / 1000.
      SUMDP = SUMDP + DELP

C
C      CALL SUBROUTINE RATE TO CALCULATE CONC. PROFILE FOR 1 PASS
C
      CALL RATE(T, THR, DEAOT, CO2, DEAX, HEODX, THEEDX, THEEDT, BHEPX)
      DEALT = DEALT - DEAX
      HEODT = HEODT + HEODX
      THEEDT = THEEDX
      BHEPT = BHEPX
      DEAOT = DEAOT - DEALT
      WRITE (6,100) X, TWIN, T, REC, DEAX, DELX
100  FORMAT (1X, F5.2, 4X, F8.3, 4X, F8.3, 2X, F10.2, 3X, F8.4, 3X,
1    F10.4, /)
      X = X + 0.100
      IF (X .GE. TCL) GO TO 120
      IF (X .LT. TCL) GO TO 110
110  DEAOT = DEAX
      T1 = T
      GO TO 20

```

```

C
C      *CALCULATE TIME FOR TOTAL LIQUID VOL.TO PASS*
C
120 TSPS = TLV / VOLS
    WRITE (6,130) TSPS
130 FORMAT (1X, 'TSPS=', F12.6, //)
    TOTS = TOTHR * 3600.
    PSI = SUMDP / 6.894757
    WRITE (6,140) SUMDP, PSI
140 FORMAT (1X, 'TOTAL PRES. DROP,kPa=', F12.4, 2X, 'PSI=', F12.4, //)
    NPT = TOTS / TSPS
    WRITE (6,150) VOLS, TH
150 FORMAT (2X, 'VOL. FLOW RATE=', F10.7, 4X, 'HOT FLUID TEMP.=',
1      F8.2, //)
    WRITE (6,160) DEAO, CO2
160 FORMAT (1X, 'INITIAL DEA CONC. = ', F6.2, 4X, '[CO]L = ', F6.2, //
1      )

C
C      CALCULATE DEA,HEOD & THEED CONC. FOR NP PASSES
C
    WRITE (6,170)
170 FORMAT ('1', 2X, 'TIME(hr)', 4X, 'RT (sec)', 4X, 'DEA CONC.', 4X,
1      'HEOD CONC', 4X, 'THEED CONC.', 4X, 'BHEP CONC', //)
    HR = 0.
    NPHR = 3600. / TSPS
180 NPNHR = NPHR * HR
    RTS = THR * NPNHR * 3600.
    DEAL = DEAO - DEAX
    DEANP = DEAO - (DEAO - DEAX) * NPNHR
    HEONP = HEODT * NPNHR
    THENP = THEEDT * NPNHR
    BHENP = BHEPT * NPNHR
    WRITE (6,190) HR, RTS, DEANP, HEONP, THENP, BHENP
190 FORMAT (1X, F10.4, 1X, F10.4, 2X, F10.4, 3X, F10.4, 4X, F10.4, 4X,
1      F10.4, //)
    HR = HR + 24.
    IF (HR .GE. TOTHR) GO TO 200
    IF (HR .LT. TOTHR) GO TO 180
200 STOP
    END

C
C      SUBROUTINE DPROP TO CALCULATE DEA PROPERTIES
C
    SUBROUTINE DPROP(T, DEAO, RHO, VIS, TK, CP)
    RHO = 998.0 - 0.00403 * T ** 2 + DEAO * (3.4 - 0.00025*T**1.45) -
1    DEAO ** 1.19
    VIS1 = (0.067666*DEAO - 6.820867) / (1. - 0.004395*DEAO)
    VIS2 = T * ((0.014066 + 0.0000105*DEAO)/(1. - 0.004965*DEAO))
    VIS = EXP(VIS1 - VIS2)
    TK = (0.4675 - 0.0062*DEAO**0.8538) * T ** 0.08
    CP = 4.176 + 0.00046 * T - 0.01837 * DEAO + 0.000054 * DEAO * T
    CP = CP * 1000.
    RETURN
    END

```

```

SUBROUTINE RATE(T, THR, DEAO, CO2, DEAX, HEODX, THEEDX, THEEDT, BHEPX)
REAL K1, K2, K3, LNK1, LNK2, LNK3
DATA A1, A2 /11.924, -6.451/
DATA A3, A4 /8.45, -5.58/
DATA A5, A6 /20.640, -6.52/
LNK1 = A1 + A2 * (1000./(T + 273.))
K1 = EXP(LNK1)
LNK2 = A3 + A4 * (1000./(T + 273.))
K2 = EXP(LNK2)
LNK3 = A5 + A6 * (1000./(T + 273.))
K3 = EXP(LNK3)
A = EXP(-(K1 + K2)*CO2*THR)
B = K1 / (K1 + K2)
C = K2 * CO2 / (K3 - (K1 + K2)*CO2)
D = K2 / (K1 + K2)
D1=K2*K3*CO2*DEAO/(K3-(K1+K2)*CO2)
D2= 1./((K1+K2)*CO2)
D3= 1./K3
E = K3 / (K3 - (K1 + K2)*CO2)
F = ((K1 + K2)*CO2) / (K3 - (K1 + K2)*CO2)
G = EXP(-K3*THR)
C2= THEEDT*G
C3= (THEEDT/K3)*(1.-G)

```

C  
C  
C

CALCULATES DEA CONCENTRATION

```

DEAX = DEAO * A
HEODX = DEAO * B * (1. - A)
THEEDX = DEAO * C * (A - G) + C2
BHEPX = D1*((-A*D2)+(D3*G))-C3 + (DEAO*D) + BHEPT
RETURN
END

```

C  
C  
C

SUBROUTINE SSPROP CALCULATES TH. COND. OF METAL

```

SUBROUTINE SSPROP(TW, TKM)
TKM = 15.60 + 0.006289 * TW
RETURN
END

```

C  
C  
C

SUBROUTINE THERM CALCULATES THE PROPERTIES OF SHELL THERMIA

```

SUBROUTINE THERM(TH, CPO, TKO, RHOO, VISO)
CPO = (0.388 + 0.00045*(TH*(9./5.) + 32.)) / 0.9352
CPO = CPO * 4184
TKO = (0.821 - 0.000244*(TH*(9./5.) + 32.)) / 0.8742
TKO = TKO * 0.1441314
RHOO = 0.886662 - 0.000750 * TH
RHOO = RHOO * 1000.
VISO = -(2.2177 + 0.0188*TH)
VISO = EXP(VISO)
RETURN
END

```



PUBLICATIONS :

- Chakma,A. and Meisen,A., "Predicting Density, Viscosity, Thermal Conductivity and Specific Heat of Aqueous DEA Solutions", Hydrocarbon Processing, in press.
- Chakma,A. and Meisen,A., "Degradation of Aqueous DEA Solutions in Heat Transfer Tubes", to be presented at the 1984 Annual Meeting of A.I.Ch.E., San Francisco, Nov., 1984.
- Chakma,A. and Meisen,A., "Corrosivity of DEA Solutions and their Degradation Products", to be presented at the 34th Canadian Chemical Engineering Conference, Quebec City, Canada, Oct. 1984.